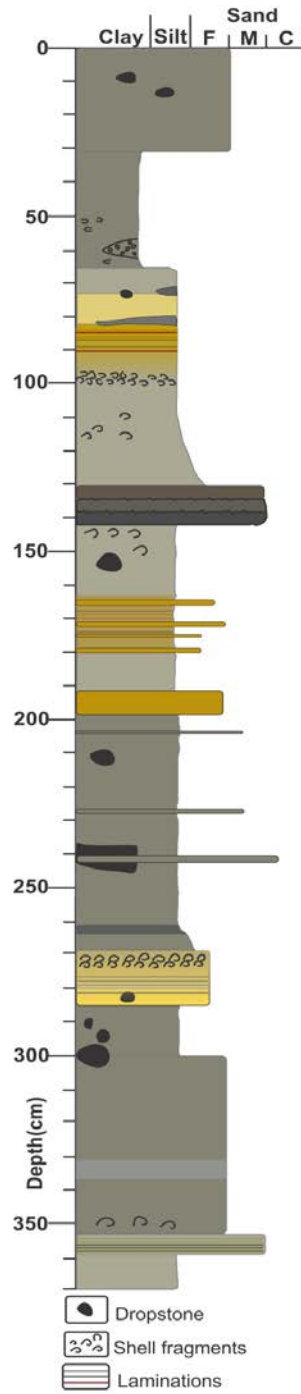
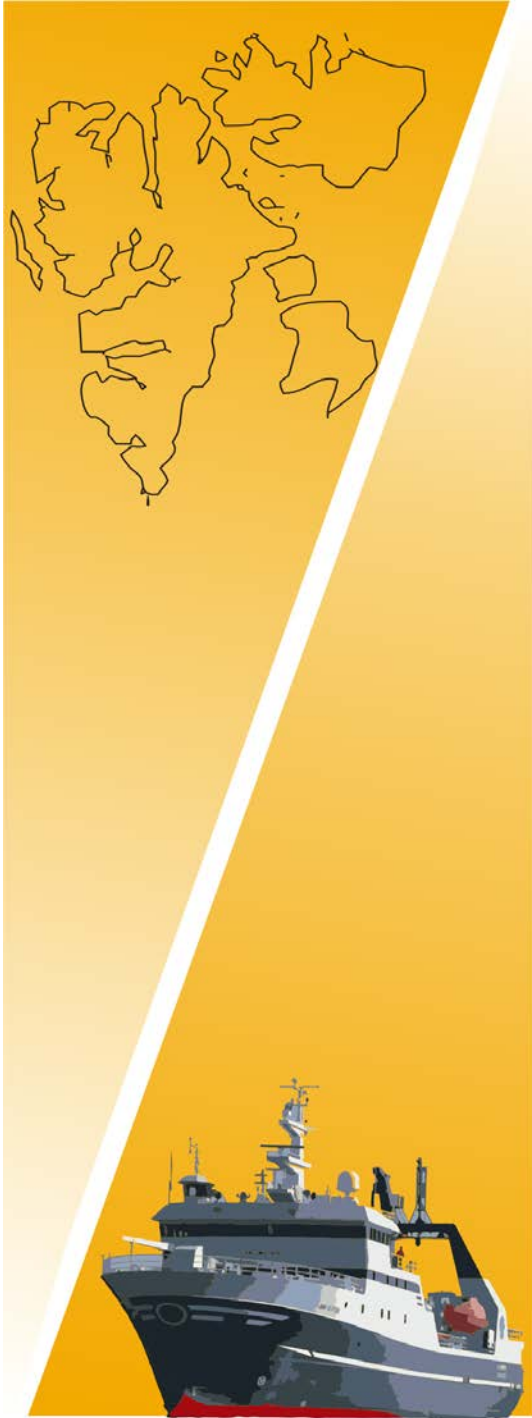


# Late Quaternary paleoceanography of the northern continental margin of Svalbard

—  
**Teena Chauhan**

*A dissertation for the degree of Philosophiae Doctor – June 2015*





Teena Chauhan

Late Quaternary paleoceanography of the  
northern continental margin of Svalbard





# Late Quaternary paleoceanography of the northern continental margin of Svalbard

**Teena Chauhan**

A dissertation submitted to the Faculty of Science and Technology,  
UiT The Arctic University of Norway  
for the degree of Philosophiae Doctor (PhD)



Department of Arctic Geology  
The University Centre in Svalbard (UNIS)

and



Department of Geology  
UiT The Arctic University of Norway

June 2015



The Thesis work was conducted at UNIS and affiliated with AMGG PhD Trainee School at UiT The Arctic University of Norway.

© 2015 Teena Chauhan (Section I)

This work is licensed under a Creative Commons Attribution-Noncommercial-Share Alike 3.0-License  
<http://creativecommons.org/licenses/by-nc-sa/3.0/>

© Section II re-printed with kind permission from Elsevier, Wiley and Springer

Supervised by: Assoc. Prof. Riko Noormets  
Department of Arctic Geology  
The University Centre in Svalbard (UNIS)  
Longyearbyen, Norway

Prof. Tine L. Rasmussen  
CAGE - Centre for Arctic Gas Hydrate, Environment and Climate  
Department of Geology  
UiT The Arctic University of Norway  
Tromsø, Norway

ISBN (online): xxx-xxx-xx

ISBN (print): xxx-xx-xxxx-xx

<http://hdl.handle.net/10037/xxxx>

Print: Tromsprodukt AS, Tromsø, Norway

Front cover illustration: Svalbard archipelago outline map, research vessel *Helmer Hanssen* of the UiT The Arctic University of Norway, lithological log of sediment core and scanning electron micrographs of planktic (*N. pachyderma*: top) and benthic foraminifera (*C. neoteretis*: middle and *E. excavatum*: bottom) from this study. Last page photo: Teena Chauhan

I know the cure for everything: Salt water....in one form or  
another: sweat, tears or the sea.

– *The Deluge at Norderney, Seven Gothic Tales, 1934*

-Karen Blixen  
(Isak Dinesen)



## ABSTRACT

This thesis presents new results from paleoceanographic studies based on sediment cores from the north-western and northern continental margin of Svalbard. Two sediment cores have been investigated to reconstruct the late Quaternary paleoceanographic variations, in particular, the variability of Atlantic Water inflow to the Arctic Ocean during the last interglacial-glacial-interglacial period. Additionally, the relationship between the natural variability of Atlantic Water and the evolution of the Svalbard-Barents Sea Ice Sheet (SBIS), sea-ice cover and ocean circulation, has been studied. For the first time studies of the variations in bottom current activity associated with Atlantic Water inflow and its influence on the depositional environment at the north-western and northern Svalbard margin were carried out.

The reconstruction of Atlantic Water variability is based on planktic and benthic foraminiferal assemblages, oxygen and carbon stable isotopes in planktic and benthic foraminifera, and ice-rafted debris (IRD) content. Paleo-bottom current strength and depositional environments have been elucidated on the basis of grain size analysis, mainly, sortable silt (10–63  $\mu\text{m}$ ) and organic carbon content.

The results suggest that the Atlantic Water inflow and freshwater production from the glacial melt in combination with changes in insolation have played major role in driving regional climate change. These climate forcing mechanisms have controlled the stability of the SBIS and sea-ice cover since Marine Isotope Stage (MIS) 5 at 128 ka. In general, the southern Yermak Plateau at the north-western Svalbard margin received relatively warmer Atlantic Water, which resulted in open water conditions and seasonal sea-ice cover whereas, the reduced influence of Atlantic Water at the upper continental slope, north of Nordaustlandet, led to expansion of near-perennial sea-ice cover. The interglacial/interstadial periods of MIS 5 were characterized by warmer conditions compared to interglacial/interstadial periods in MIS 3 and the cold period of the late Holocene due to varied intensity of insolation and the Atlantic Water inflow. MIS 4 was relatively colder than MIS 2, because of the weaker influence of saline Atlantic Water over fresh Polar Water. Differences in depositional environments and bottom current strength in MIS 4 and

MIS 2 at the north-western vs. northern Svalbard margin were caused mainly by the different topographic settings of these two areas. The onset of the last deglaciation at *c.* 19 ka was characterized by a distinct increase in freshwater flux from the retreating SBIS, melting of icebergs and sea-ice, and consequently weakening of ocean circulation and poor ventilation at the sea-floor. The freshwater layer at the surface facilitated the sea-ice expansion during the Younger Dryas cold period.

The study shows that the influence of climate forcing mechanisms varied temporally and spatially along the northern Svalbard margin, with significant effect on the local sedimentary and oceanographic environment. This emphasizes the importance of considering regional environmental parameters and feedback mechanisms in reconstructions of past climate.

The results of the Thesis are presented in three research papers.

## PREFACE

This dissertation is submitted in partial fulfilment of the requirements for the Degree of Philosophiae Doctor (PhD) in Geology. The PhD work has been supervised by Assoc. Prof. Riko Noormets from UNIS and Prof. Tine. L. Rasmussen from UiT The Arctic University of Norway. The 3 year PhD position for an Indian student at The University Centre in Svalbard (UNIS), Spitsbergen, Norway was financed by the Research Council of Norway as a part of cooperation between Norway and India (Norsk-Indisk forskningssamarbeid), in the field of glacial marine geology. The Norwegian Research School in Climate Dynamics (ResClim) partially funded laboratory work and supervisors arranged partial funding for six months.

The Thesis work was conducted at UNIS and affiliated with PhD Trainee School in Arctic Marine Geology and Geophysics (AMGG). The Department of Geology at UiT The Arctic University of Norway hosts the trainee school. At the beginning of the PhD study, the candidate participated in an obligatory Arctic safety course at UNIS. To obtain PhD education equivalent to 30 credit points, the candidate attended mandatory courses of AMGG Trainee School together with other national and international courses, in topics related to Arctic marine geology and research ethics. The candidate also actively participated in the ResClim- the research school at the University of Bergen and attended a scientific writing course offered by ResClim. Additionally, courses on Pedagogy and communicating science to media were attended at UNIS. For data collection and PhD education, the candidate participated and assisted in six research cruises with R/V *Helmer Hanssen* and two cruises with R/V *Viking Explorer*, and also assisted in laboratory work of the marine geology course, AG-211, at UNIS.

The results and progress of the PhD work were presented at national workshops and international conferences in Finland (APEX VI Conference, Oulu, 2012), India (PAGES, 4<sup>th</sup> Open Science Meeting, Goa, 2013) and Russia (PAST Gateways Conference, St. Petersburg, 2013). The results were distributed in 3 oral and 5 poster presentations, including presentation at the Research Grand Prix organised by ResClim onboard M/S *Hurtigruten* (2012) which won 2<sup>nd</sup> prize, and participation in UNIS Open Days (2012, 2013).

The thesis is broadly divided in two sections. Section I covers Chapter 1 to 7 giving an overview of the thesis. Section II presents three research papers which contributed to reconstruction of late Quaternary paleoceanography of the northern continental margin of Svalbard.

The research papers are:

### **Paper I**

T. Chauhan, T. L. Rasmussen, R. Noormets, M. Jakobsson, K. A. Hogan, 2014. **Glacial history and paleoceanography of the southern Yermak Plateau since 132 ka BP.**

*Quaternary Science Review*, 92, pp 155-169.

*doi:10.1016/j.quascirev.2013.10.023*

### **Paper II**

Teena Chauhan, Tine L Rasmussen and Riko Noormets. **Paleoceanography of the Barents Sea continental margin, north of Nordaustlandet, Svalbard during the last 74 ka.**

*Accepted for publication in Boreas*

### **Paper III**

Teena Chauhan, Riko Noormets and Tine L Rasmussen. **Glaciomarine sedimentation and bottom current activity along the north-western and northern continental margin of Svalbard during the late Quaternary.**

*Submitted to Geo-Marine Letters*



## ACKNOWLEDGMENTS

I must say that it is really hard to write this section for several reasons ☺. But then, taking this opportunity, I would like to firstly thank my family for their confidence in me and for providing endless support, especially my decision to move from +30 to -30 °C!

Several people have influenced the progress of my PhD work at different stages. My both supervisors - Assoc. Prof. Riko Noormets (UNIS) and Prof. Tine L. Rasmussen (UiT) - deserve to be on top of the list. Big thanks to Riko for giving me opportunity of this PhD position, which also brought with it the opportunities to participate in research cruises in Svalbard fjords, the Barents Sea and the high North, to attend national and international conferences, and to my surprise - interface at meetings with hi-profile officials at UNIS. I am fortunate that despite the distance, I received timely guidance in microscopy work from Tine in identifying and understanding the beautiful foraminifera of Arctic waters. I have benefited greatly from discussions with both of you on different aspects of Arctic glacial history and micropaleontology. Your suggestions have greatly improved the research papers and this thesis. I express my sincere gratitude to both, for your time and effort, for being my support system in completion of this PhD and for being wonderful supervisors ☺.

*Tänan väga Riko! Tusind tak Tine!*

I thank the captain and crew of research vessel *Helmer Hanssen* (UiT) for their help during data collection and also for arranging 'vegetarian food' for me onboard! Ångstorm Radiocarbon Laboratory, Uppsala, Sweden; 14-CHRONO Centre for Climate, Environment and Chronology, Belfast, UK and Lund Radiocarbon Dating Laboratory, Lund, Sweden are acknowledged for generating radiocarbon dates. Special thanks to Mats Rundgren from Lund Radiocarbon Laboratory. The Stable Isotope Laboratory, Stockholm is acknowledged for oxygen and carbon stable isotope measurements. I am thankful to Dr. Erik Thomsen, Aarhus University for calculating bottom water temperatures using transfer functions. I sincerely thank all my co-authors and reviewers for their contribution in improving the quality of research papers. Big thanks to Kelly A. Hogan as a co-author and especially for being a dear friend.

Thanks to UNIS Director and administration for giving a wonderful infrastructure and working environment, and for making my stay comfortable in Longyearbyen. I acknowledge Ingrid Eggenfellner for helping with administrative formalities when I arrived at UNIS in 2011. I would also like to thank Anne Bjørndal, Eva Theresa Jenssen and Stefan Nørdlie for their help. Big thanks to student advisor Tine M. Hågensen at the Faculty of Science and Technology, UiT.

I am grateful to the academic staff at UNIS who helped me in one or other way at different stages of my PhD study. I specially acknowledge Eva Falck for prolific discussions on oceanography and for helping with Norwegian translation. Big thanks to Steve Coulson, Doug Benn, Alvar Braathen, Hanne H. Christiansen and Anne Hormes. I acknowledge Sebastian Sikora for helping me with core pictures. Sarah Thompson read major sections of thesis and Peter Hill read a few sections for language correction. Thank you so much!

Special thanks to Venke Ivarrud and Heidi Sevestre for all the positive energy and smiles ☺ Keep smiling! I am grateful to Berit Jakobsen for being extremely helpful and such a wonderful librarian. *Tusen takk!*

I would like to acknowledge Karen Luise Knudsen, Aarhus University, Denmark for nurturing my interest in foraminifera research and Anne Jennings, INSTAAR, Colorado for fruitful discussions on foraminifera. I also extend my thanks to Dr. B. N. Nath at the National Institute of Oceanography, Goa, India for initially developing my research aptitude. Thanks to Faezeh M. Nick, Iben Andersen, Ragnhild Rønneberg, Dr. Kim Hølmen and Emeritus Prof. Karsten Storetvedt for all the encouragement. Thanks to friends in India for helping in Hindi translation.

Many thanks to my fellow PhDs and Post Docs at UNIS and friends at UiT for all the amazing time and support you provided over these years and big thanks to all the people that I forgot to mention here. Last but not least, I am thankful to the seven members of 'Team India' in Longyearbyen, for their help, all the good times we had and for keeping the spirit alive by adding Indian spice. *Dhanyavad!*

Longyearbyen, Svalbard, June 2015

Teena Chauhan ☺

# TABLE OF CONTENTS

Abstract.....	vii
Preface.....	ix
Acknowledgments.....	xi
Table of Contents.....	xiii
<b>SECTION I OVERVIEW-----</b>	<b>1</b>
Chapter 1 INTRODUCTION.....	3
1.1 General background.....	3
1.2 Previous studies.....	5
1.3 Objectives of the thesis.....	7
1.4 Thesis outline.....	9
Chapter 2 REGIONAL SETTING OF THE STUDY AREA -----	11
2.1 Geologic and physiographic setting.....	12
2.2 Ocean circulation and water masses.....	13
Chapter 3 MATERIALS AND METHODS -----	17
3.1 Materials.....	17
3.2 Methods.....	19
Chapter 4 FORAMINIFERA DISTRIBUTION -----	25
4.1 Modern benthic assemblages.....	26
4.2 Fossil foraminiferal assemblages in cores JM10-02GC and HH11-09GC.....	27
4.3 Ecology of most common foraminifera.....	28
Chapter 5 SUMMARIES OF PAPERS AND AUTHORS' CONTRIBUTION -----	31
5.1 Paper I.....	31
5.2 Paper II.....	32
5.3 Paper III.....	34
Chapter 6 SYNTHESIS -----	37
Chapter 7 FUTURE PERSPECTIVES -----	45
REFERENCES -----	47
<b>SECTION II RESEARCH PAPERS (I, II and III) -----</b>	<b>57</b>
Appendix A List of planktic and benthic species identified in cores JM10-02GC and HH11-09GC and taxonomy	
Appendix B Summary in Hindi	



**SECTION I**  
**Overview**



# Chapter 1

## INTRODUCTION

### 1.1 General background

Marine sediments are ‘natural archives’ of the past climate as the oceans occupy over 70% of the Earth’s surface and play a significant role in regulating the climate system (Bradley, 2015). In addition, atmospheric circulation and solar energy (insolation) are also important global climate forcing mechanisms. Since the industrial revolution, anthropogenic activities have been suggested to influence the global climate system (IPCC, 2014). The study of climate change, prior to the large-scale human impact, is important for understanding the natural variability in the climate system. This will enhance our ability to provide more reliable predictions of future climate.

Present climate warming is more pronounced in the Arctic Ocean and its surrounding seas than at lower latitudes. This is known as Arctic Amplification (Pithan and Mauritsen, 2014). Various positive feedback mechanisms, such as surface albedo changes due to receding sea-ice and glaciers and sea level rise resulting from the melting glaciers and ice caps, are leading to increased warming in the Arctic (IPCC, 2014). The amplified warming in turn influences the exchange of heat between ocean and atmosphere, the strength of ocean currents and marine life (Fig. 1.1). Berger and Loutre (2002) hypothesized that because of various feedbacks within the Earth system, the present warm period may continue for the next 50,000 years or more, even if the influence of the natural and anthropogenic climate forcing mechanisms is reduced in the future. However, climate forcings and their feedback mechanisms vary spatially and temporally due to changes in distribution of solar energy, bottom topography and ocean currents (McCarroll, 2015).

The oceanic heat transport in the Eurasian Arctic occurs through interplay between warm and saline Atlantic Water, and relatively cold and fresh Polar Water. This exchange of water masses with different densities largely controls not only the distribution of sea-ice, but also the growth and retreat of glaciers on land. For example, inflow of warm Atlantic Water in recent decades has been suggested as one potential cause for rapid acceleration of ice loss from a marine-based sector of Austfonna ice cap on Nordaustlandet, Svalbard (McMillan et al., 2014) and sea-ice loss north of Svalbard margin (Onarheim et al., 2014).

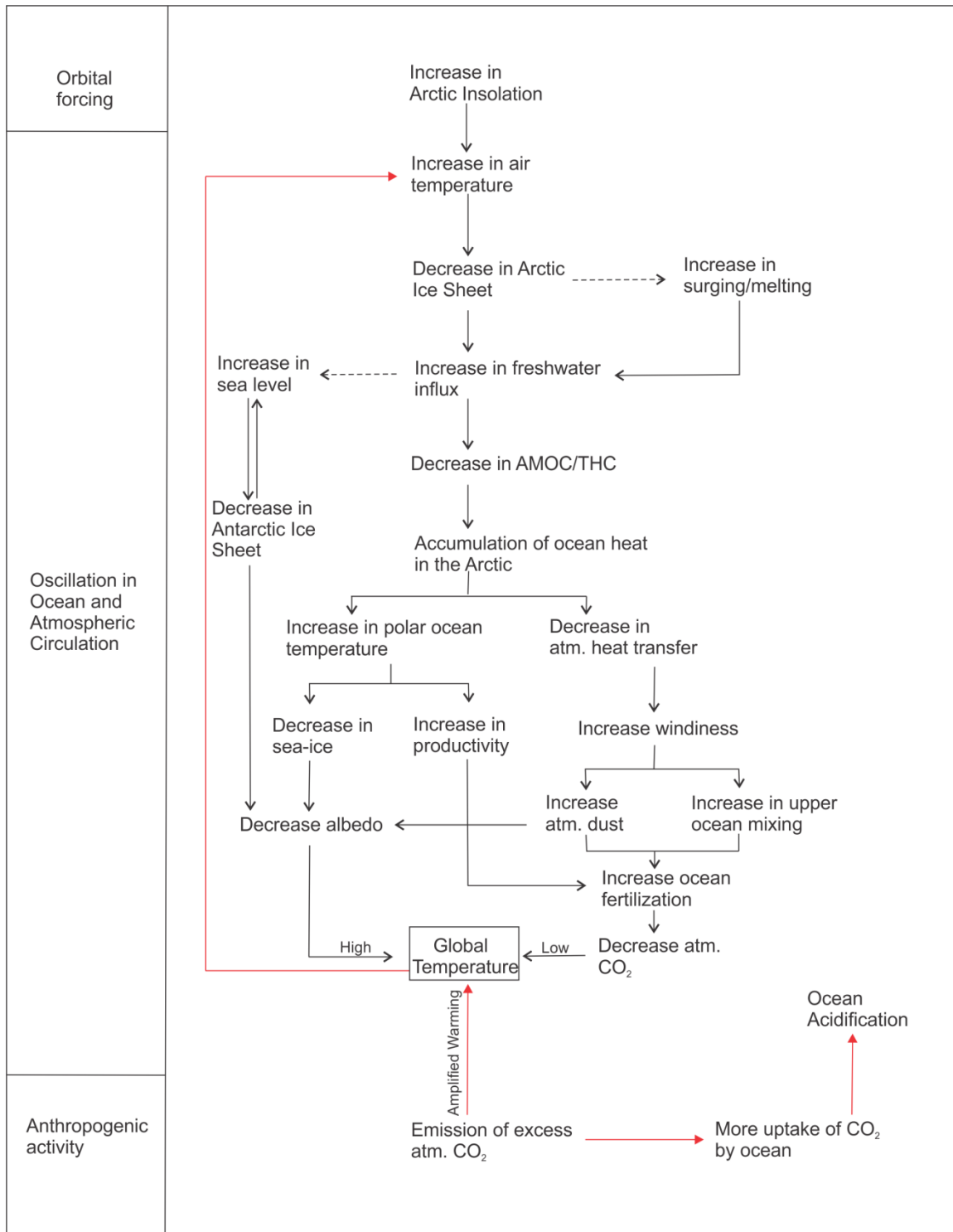


**Fig. 1.1** Main processes governing the climate warming in the Arctic (*adapted and modified from Alley (1995)*). AMOC–Atlantic Meridional Overturning Circulation; THC–Thermohaline Circulation; atm.–atmospheric; CO<sub>2</sub>–carbon-dioxide



The inflow of Atlantic Water is also a significant factor in the generation of deep water in the Nordic Seas that regulates the thermohaline circulation (THC) (Ivanova, 2009). During the last glacial-interglacial cycle, the inflow of Atlantic Water supplied heat and moisture by THC and exerted strong control on the extent of the Eurasian ice sheets (e.g., Hebbeln et al., 1994; Hebbeln and Wefer, 1997). During deglaciation periods, particularly the last deglaciation, the freshwater supply from melting ice sheets slowed down the THC and weakened the heat transfer, leading to more cooling (e.g., Knies et al., 1999; Nørgaard-Pedersen et al., 2003).

Major Arctic temperature anomalies during the late Quaternary occurred in the previous Interglacial (130 ka<sup>\*</sup>), the Last Glacial Maximum (LGM) (22 ka) and in the early Holocene Thermal Maximum (8 ka) (Miller et al., 2010, 2013). Temperature anomalies influenced the sea-ice cover, ocean circulation and the stability of the marine-based Svalbard-Barents Sea Ice Sheet (SBIS), which covered the Barents Sea several times during the Quaternary. A present-day analogue to the SBIS is the West Antarctica Ice Sheet - a marine-based ice sheet covering West Antarctica. Better understanding of the ocean current systems, glacial processes, and the associated climatic controls that led to the disintegration of the SBIS will help to assess the current state of the West Antarctica Ice Sheet and its potential instability.

The exchange of Atlantic and Polar Water masses result in distinct changes in the geological, biological and oceanographic processes, such as sea-ice extent, freshwater and nutrients inflow, biota and organic carbon flux, etc. These processes are pronounced at the continental margins of the Eurasian Arctic, and therefore ideal locations for climate reconstruction. The Atlantic Water flows as surface water mass via West Spitsbergen Current along the western Svalbard margin and on losing heat at the north-western Svalbard margin, it submerges under the Polar Water and flows as subsurface water mass along the northern Svalbard margin. Therefore, the continental margins north-west and north of Svalbard are the key location for studying the variability of Atlantic Water inflow to the Arctic Ocean and its influence on the stability of the SBIS during the last glacial-interglacial cycles.

## **1.2 Previous studies**

Previous studies have reconstructed the paleoceanography of the western Svalbard margin and the Fram Strait (e.g., Hebbeln et al., 1994, 1998; Dokken and Hald, 1996; Hebbeln and

---

\*ka = kiloannum/thousand years

Wefer, 1997; Hald et al., 2001, 2004; Nørgaard-Pedersen et al., 2003; Birgel and Hass, 2004; Jessen et al., 2010; Dylmer et al., 2013; Werner et al., 2013; Rasmussen et al., 2014b). These studies cover different time periods and provide a background for understanding the variability of surface Atlantic Water and its influence on the extent of the SBIS west of Svalbard. However, knowledge about the variability of submerged Atlantic Water and its influence on the SBIS north of Svalbard is limited.

Off the north-western Svalbard margin, the magnetic properties of sediments from the eastern slope of Yermak Plateau were used to establish magneto-stratigraphy and short term polarity events within the last 170 ka (Nowaczyk et al., 1994). These results have been used for stratigraphic correlation and developing a regional chronology. Based on the sortable silt and dinoflagellate record from the eastern Yermak Plateau, Howe et al. (2008) suggested that the mid- and late Weichselian was characterized by polar conditions with unsteady bottom currents due to abundant ice-rafted debris (IRD), whereas advection of the Atlantic Water during the LGM-early Holocene interval resulted in open water conditions. Foraminifera-based study from the northern Yermak Plateau (Wollenburg et al., 2004) and IP25 biomarker-based study from the western Yermak Plateau (Muller et al., 2009) shows that near-perennial sea-ice cover, which expanded during the LGM, reduced due to advection of warm Atlantic Water at 14 ka. These studies also suggest that during the Holocene, seasonal sea-ice cover expanded at the northern and western Yermak Plateau.

At the southern Yermak Plateau, the longest paleo-record was obtained by the Ocean Drilling Program (ODP) on Leg 151. During ODP coring, three sediment cores 910, 911 and 912 were recovered. Studies of ODP sediment cores gave an overview of the paleoceanography of the region (Hevrøy et al., 1996; Hull et al., 1996; Rack et al., 1996; Thiede and Myhre, 1996). Based on mineralogy and organic geochemistry of the sediments from the southern and northern Yermak Plateau, Vogt et al. (2001) suggested a strong influx of Atlantic Water during Marine Isotope Stage (MIS) 4/3 and MIS 2/1 causing northward shift of the sea-ice edge. A distinct organic carbon layer sourced from the southern Svalbard was identified as an evidence of the SBIS advance during the LGM. Spielhagen et al. (2004) investigated cores from the Arctic Ocean, the Yermak Plateau and the Fram Strait, using stable isotope analysis and abundance of planktic foraminifera and IRD to present oceanographic evolution of last 200 ka. Based on the results, they suggested that freshwater and IRD input probably had common source with the major outflow of freshwater that occurred at  $c^{\dagger}$ . 130 ka, 80-75 ka and 52 ka. The results further suggested that the major Atlantic Water inflow occurred during

---

<sup>†</sup>*c.* = *circa*

Eemian and Holocene and to a lesser degree within stadials and glacial stages of MIS 6, MIS 4 and MIS 2. A recent micropaleontological study from the south-western slope of Yermak Plateau has presented evidence of a continuous influx of Atlantic Water during MIS 4–2. The results indicate that the strength and temperature of the Atlantic Water mass varied significantly in pace with Dansgaard-Oeschger events and Heinrich events (Rasmussen et al., 2014a).

At the northern Svalbard margin, late Quaternary paleoceanographic evolution was studied using organic carbon concentration (Knies and Stein, 1998), sedimentological and geochemical data (Knies et al., 1999) and the benthic foraminiferal record (Wollenburg et al., 2001) in a sediment core from the lower continental slope (PS2138). The results show that advection of warm Atlantic Water in subsurface occurred during interglacial periods of MIS 5 and the Holocene. During glacial periods, the short intervals of enhanced inflow of Atlantic Water and polynya formation provided moisture for the growth of the SBIS. The concentration of marine organic matter increased during 15.9–11.2 ka due to melting sea-ice and an influx of warm Atlantic Water (Knies and Stein, 1998). Concurrently, foraminiferal studies from the northern Svalbard shelf covering the last deglaciation and the Holocene period suggested initiation of warm Atlantic Water inflow at *c.* 15 ka after the LGM (Koç et al., 2002; Slubowska et al., 2005).

These studies mainly illustrate the influence of Atlantic Water on the sedimentation environment and on the fluctuation of the SBIS. Long-term Atlantic Water variability, using both planktic and benthic foraminifera together with the physical properties of the sediments at the north-western and the northern continental margin of Svalbard, has not been presented so far.

### **1.3 Objectives of the thesis**

The aim of this study is to enhance knowledge about climate evolution along the northern Barents Sea margin during the late Quaternary. The study focusses on the variation in inflow of warm Atlantic Water to the Arctic Ocean, the response of the SBIS to this variation and resulting changes in continental margin sedimentation. To achieve this aim, the following objectives were defined:

1. To reconstruct the variation in Atlantic Water inflow to the north-western and northern Svalbard margin during the Late Quaternary glacial-interglacial periods, and identify its influence on sea-ice extent and ice sheet fluctuations.

2. To compare and correlate the paleoceanographic conditions using the benthic foraminifera assemblage in order to trace the inflow of Atlantic Water on the north-western and northern Svalbard margin.
3. To characterize the depositional environments using paleo-bottom current strength and organic carbon flux inferred from the organic carbon and grain size record on the north-western and northern Svalbard margin.

To reconstruct the Atlantic Water variability and define past climatic changes, microfossils in marine sediments and the composition of sediments are used. Microfossils, such as 'foraminifera' are a reliable proxy for paleoceanographic reconstructions because these single cell micro-organisms are abundant on continental shelves and slopes, and they respond to a number of environmental variables. They precipitate calcium carbonate from the sea water to form their tests, preserving the chemical properties of sea water at the time of the formation. On dying, their tests are buried in marine sediments and constitute the pool of microfossils (subject to the sea bottom environment being suitable for preservation). The assemblage of benthic and planktic foraminifera species and geochemical properties of their tests in the successive layers of sediments enable the study of the past environment. Bergsten (1994) and Wollenburg et al. (2000) studied the living foraminifera and defined the modern assemblages and their preferences in terms of habitat, food, sea water salinity and temperature in the north-western and northern Svalbard margin, respectively. Knowledge obtained from these and several other studies of living foraminifera in the Arctic (e.g. Jennings and Helgadottir, 1994; Seidenkrantz, 1995; Hald and Korsun, 1997; Wollenburg and Mackensen, 1998; Korsun and Hald, 2000; Polyak et al., 2002; Sejrup et al., 2004), is applied to the microfossil assemblage recovered from sediment cores in order to reconstruct the paleoceanographic conditions. In this study, both planktic and benthic foraminifera are investigated to infer variations in water masses and bottom conditions, and to study the interactions of the Atlantic and Polar Waters.

In marine sediments, grain size variations reflect the hydraulic parameters of the depositional environment (e.g., Flemming, 1982; Kuijpers et al., 2003; Bourget et al., 2010). Reconstruction of paleo-bottom current strength is based on grain size analyses of the sediments, in particular, sortable silt (10–63  $\mu\text{m}$  size fraction), which is a proxy for near bottom current strength (McCave et al., 1996). To study the depositional environment, preserved organic carbon content and IRD content ( $> 150 \mu\text{m}$ ) in marine sediments are investigated. IRD content, which is a function of sea water temperature, provides vital

information about the iceberg distribution, sediment source and melt rate (Piper and Brisco, 1975; Bischof et al., 1990).

## **1.4 Thesis outline**

The thesis is divided into two sections. Section I includes seven chapters giving an overview of the PhD Thesis. Chapter 1 provides general background, short summary of previous studies and objectives of the thesis. Chapter 2 explains the geologic, physiographic and oceanographic setting of the study area. Materials and methods used during the PhD study are described in Chapter 3. Background information about foraminifera preferences, modern day assemblage thriving in the study areas and fossil assemblage found in two sediment cores are described in Chapter 4. The ecology and scanning electron microscope images of most abundant foraminifera species are also presented. Chapter 5 presents main results through summaries of the three research papers and the contribution of each author in papers. Chapter 6 is a synthesis of the whole of my PhD work. Future perspectives are described in Chapter 7 followed by list of references used in Section I. Section II consists of three research papers. A list of planktic and benthic foraminifera identified and picked for foraminiferal assemblage and various analyses is presented in Appendix A. Appendix B contains short summary of the PhD Thesis in Hindi language.



## REGIONAL SETTING OF THE STUDY AREA

The southern Yermak Plateau on the north-western Svalbard margin and the upper continental slope, north of Nordaustlandet on the northern Svalbard margin were selected to study the Atlantic Water variability and response of the SBIS during the Late Quaternary (Fig. 2.1). The geologic, physiographic and oceanographic settings of the study area are presented below.

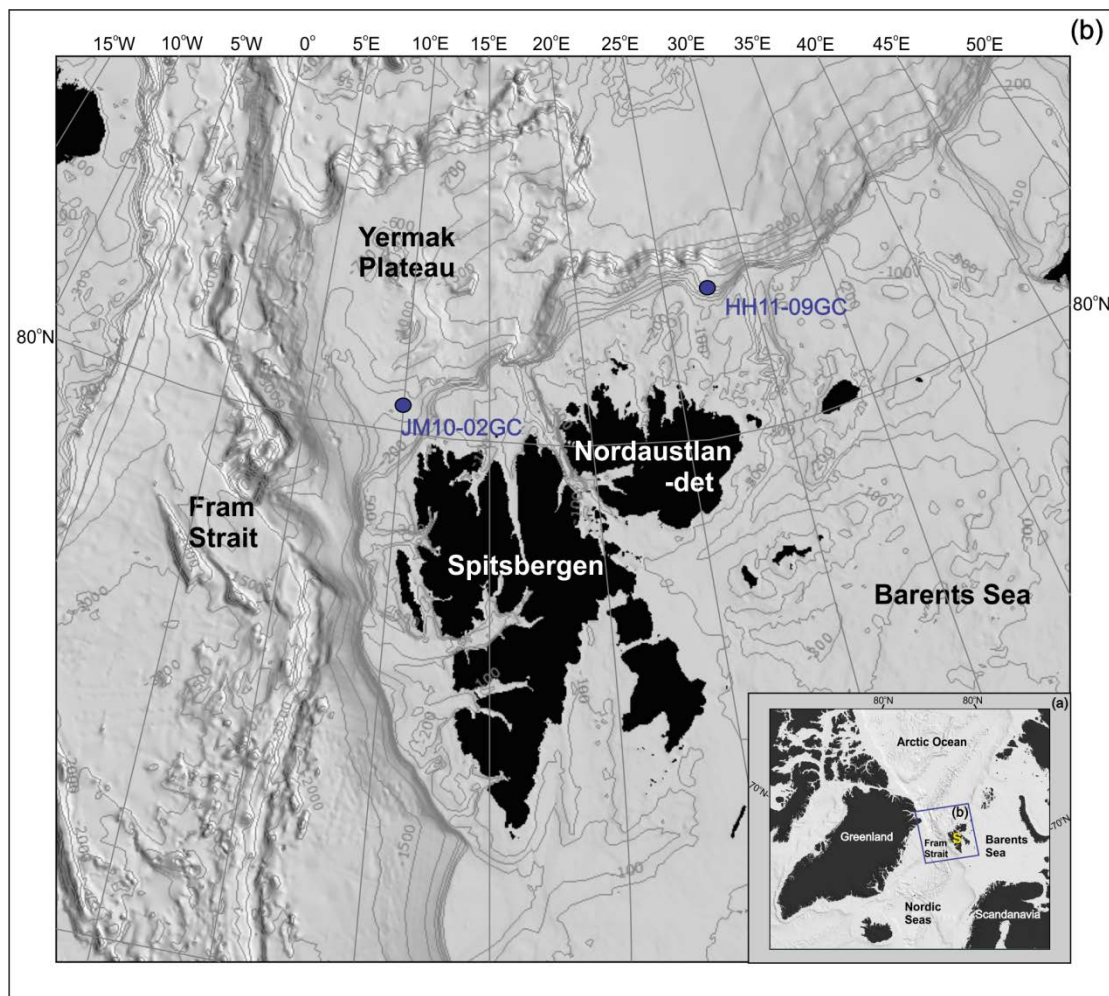


**Fig. 2.1** (a) Overview map of the Arctic Ocean, the Fram Strait and the Nordic Seas showing the location of Svalbard archipelago (S); (b) Map of the northern Nordic Seas and the Barents Sea showing the position of two investigated cores (blue circles) from the north-western (JM10-02GC) and the northern continental margin of Svalbard (HH11-09GC). Bathymetric map is from the International Bathymetric Chart of the Arctic Ocean (IBCAO) v3 (Jakobsson et al., 2012).

## 2.1 Geologic and physiographic setting

### *Southern Yermak Plateau*

The submarine Yermak Plateau extends north-west of the Svalbard into the Fram Strait, the only deep water connection between the Arctic Ocean and the world oceans. It is a topographic obstacle in the flow path of Atlantic Water to the Arctic Ocean (Fig. 2.1). The plateau trends northward for about 200 km, then north-east for 150 km with an average water depth of 700–800 m over large part and 400 m in shallower regions (Eiken, 1992). The two major depressions bordering the Yermak Plateau are the Danskøya Basin, situated between the north-western Svalbard and the southern Yermak Plateau, and the Sophia Basin, east of the Yermak Plateau.

The basement rock on the southern Yermak Plateau is probably an extension of the late Precambrian strata, mainly gneisses, which are outcropped on the north-western Svalbard (Hjelle and Lauritzen, 1982; Eiken, 1992). The basement of the plateau is covered with 2 km of Cenozoic sediments (Geissler et al., 2011). Eiken (1992) proposed that sediments of Miocene and Plio-Pleistocene age show the influence of bottom currents, suggesting that branching of the West Spitsbergen Current occurred approximately during that time. The surface of the southern Yermak Plateau shows different sets of ploughmarks, which were formed by icebergs drifting over the plateau during the late Quaternary glaciations (Vogt et al., 1994; Dowdeswell et al., 2010; Noormets et al., 2010).

### *Continental margin north of Nordaustlandet*

The continental shelves west and north of Svalbard are 50–80 km wide (Eiken, 1992). At the continental shelf break north of Svalbard, a steep passive continental margin, with slopes up to 10° (average 4°), forms the boundary of the Eurasian basin in the Arctic Ocean. On the inner shelf, north of Nordaustlandet, the sediment cover is thin, probably due to erosion by the former ice sheet whereas sediment cover at the outer shelf is 3 to 3.5 km thick (Geissler and Jokat, 2004). Geissler and Jokat (2004) further documented evidence of intensive slumping on the continental slope between 15°E and 30°E, north of Nordaustlandet. According to Bart and Anderson (1995), aggradation or slumping occurs during relatively short-lived grounding events. Geissler and Jokat (2004) also proposed that the former ice sheet north of Nordaustlandet drained at a few locations through ice streams between 15°E and 30°E.



Due to regional thermal events, the igneous basement is outcropped on northern Nordaustlandet and probably continues on the continental shelf and slope under the sediment cover (Eiken, 1992) The outer shelf north of Nordaustlandet features different glacial landforms, for instance, grounding zone wedges, grooves, transverse moraines, mega-scale glacial lineations and iceberg ploughmarks, which were formed by the SBIS during the late Weichselian glaciation (Noormets et al., 2012). Large iceberg ploughmarks (up to 100 m deep) from MIS 6 have also been reported on the upper continental slope at the northern Svalbard margin between 19°E and 20°E (Dowdeswell et al., 2010).

## **2.2 Ocean circulation and water masses**

Warm and saline Atlantic surface water derived from the Gulf Stream in the North Atlantic Ocean flows northward through the Nordic Seas. Along the margin of western Norway, the current is known as the Norwegian Atlantic Current and on the western Svalbard margin as the West Spitsbergen Current. Cold Polar Water of the East Greenland Current flows southward along the eastern Greenland margin through the Denmark Strait into the North Atlantic Ocean (Fig. 2.2). The sea-ice supplied to the East Greenland Current comes from two branches of Transpolar Drift. One branch from the north enters the Lena Trough and merges with East Greenland Current and the other branch from the north-east, crosses the Yermak Plateau before merging with the first branch (Gascard et al., 1995).

The physical properties of the West Spitsbergen Current and the East Greenland Current are similar but the two currents are different in terms of their stability. The West Spitsbergen Current is considered a variable current whereas the East Greenland Current is relatively stable (Gascard et al., 1988). Gascard et al. (1995) described the West Spitsbergen Current as jet, 20 miles wide, with high speeds in the centre (up to 40 cm/s) and lower speeds at the edges (10 cm/s), and a strong acceleration between 79°N and 80°N. The West Spitsbergen Current interacts with the bottom topography of the continental shelf and slope west of Svalbard (Fig. 2.2). The west coast of Svalbard is also affected by the coastal current - the East Spitsbergen Current, which flows southward from the Arctic Ocean via the north-west Barents Sea into the Fram Strait (Johannessen, 1986).

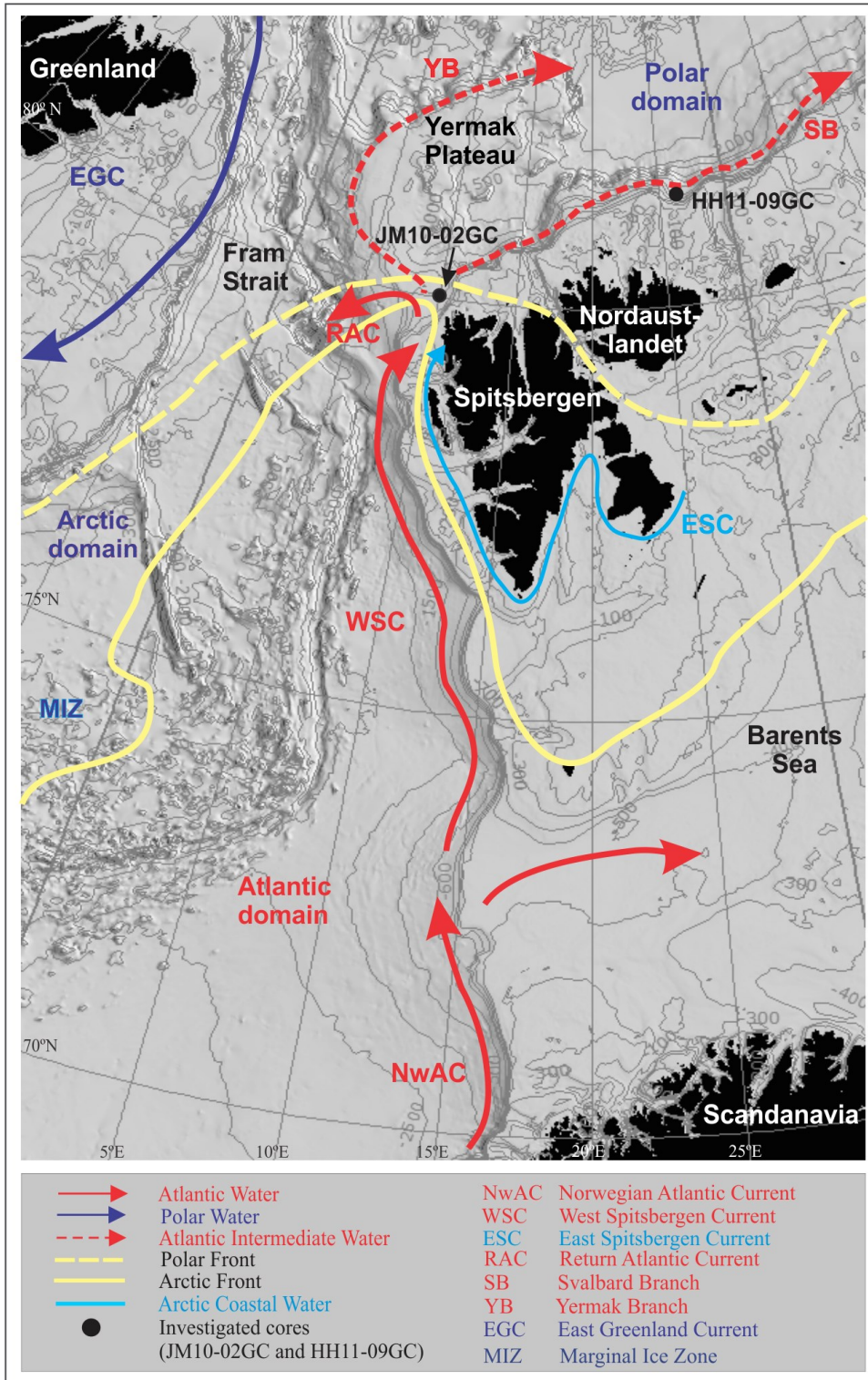


**Fig. 2.2** Map of the northern Nordic Seas and Barents Sea showing main water masses, surface currents and oceanic fronts. Bathymetric map is from the International Bathymetric Chart of the Arctic Ocean (IBCAO) v3 (Jakobsson et al., 2012).

The Atlantic Water of the West Spitsbergen Current flows over the western shelf and slope of Svalbard as a surface water mass. In the northern part of the Fram Strait, the Atlantic Water loses heat and submerges under the icy and cold Polar Water of the Arctic Ocean and flows as a subsurface water mass north of Svalbard. Around 80° N, water masses shallower than 500 m deflect eastwards and flow along the northern Svalbard margin (Svalbard Branch), whereas the deep water mass below 500 m depth (Yermak Branch) follows the continental slope and flows north up to 81° N and then east around the north-western tip of the Yermak Plateau (Fig. 2.2). A third branch of the West Spitsbergen Current turns counter-clockwise towards the west and submerges beneath the colder sea-ice covered Polar Water of the East Greenland Current. It then continues southward as Atlantic Intermediate Water known as the Return Atlantic Current (Rudels et al., 2012).

Currently, the narrow marginal ice zone (MIZ) occurs on the southern Yermak Plateau between the Polar and Arctic Fronts (Fig. 2.2). The MIZ is characterized by seasonal sea-ice cover and high surface productivity (Guest et al., 1995). Perennially sea-ice covered Polar Waters, with a temperature  $< 0$  °C and salinity  $< 34.4\text{‰}$  occur north of the Polar Front whereas the sea-ice free Atlantic Surface Waters with temperature of 5–7 °C and salinity  $> 34.9\text{‰}$  occur south of the Arctic Front. Mixing of the Atlantic and Polar Waters between these oceanic fronts results in intermediate conditions, with temperatures of 0–4 °C and salinity between 34.4‰ and 34.9‰. These waters are known as Arctic Waters (Johannessen, 1986; Swift, 1986) (Fig. 2.2). The bottom currents over the Yermak Plateau are variable but generally flow parallel to the sea-ice margin. Due to the seasonal presence of the sea-ice margin, part of the current deflects to the east where it joins the Svalbard Branch (Bourke et al., 1988). On the northern Svalbard margin, seasonal sea-ice cover exists in modern hydrographic settings and Atlantic Water in the subsurface extends to the bottom of shelf and upper slope region. Below the Atlantic Water, relatively cold Lower Arctic Intermediate Water, with salinity  $\geq 34.9\text{‰}$ , is found on the mid to lower slope (Rudels et al., 2012).



## MATERIALS AND METHODS

## 3.1 Materials

Two sediment cores from the Barents Sea continental margins are investigated in this study (Fig. 2.1). Gravity core JM10-02GC was retrieved from the north-west continental margin of Svalbard in 2010 and HH11-09GC was recovered from the northern Svalbard margin in 2011 on R/V *Helmer Hanssen* (known as R/V *Jan Mayen* until 2010) (Figs. 3.1 and 3.2; Table 3.1). In addition, 30 cm of undisturbed sediment was retrieved from the core cutter and catcher of the core HH11-09GC. CTD (conductivity, temperature, density) data was collected at both core locations prior to the coring.

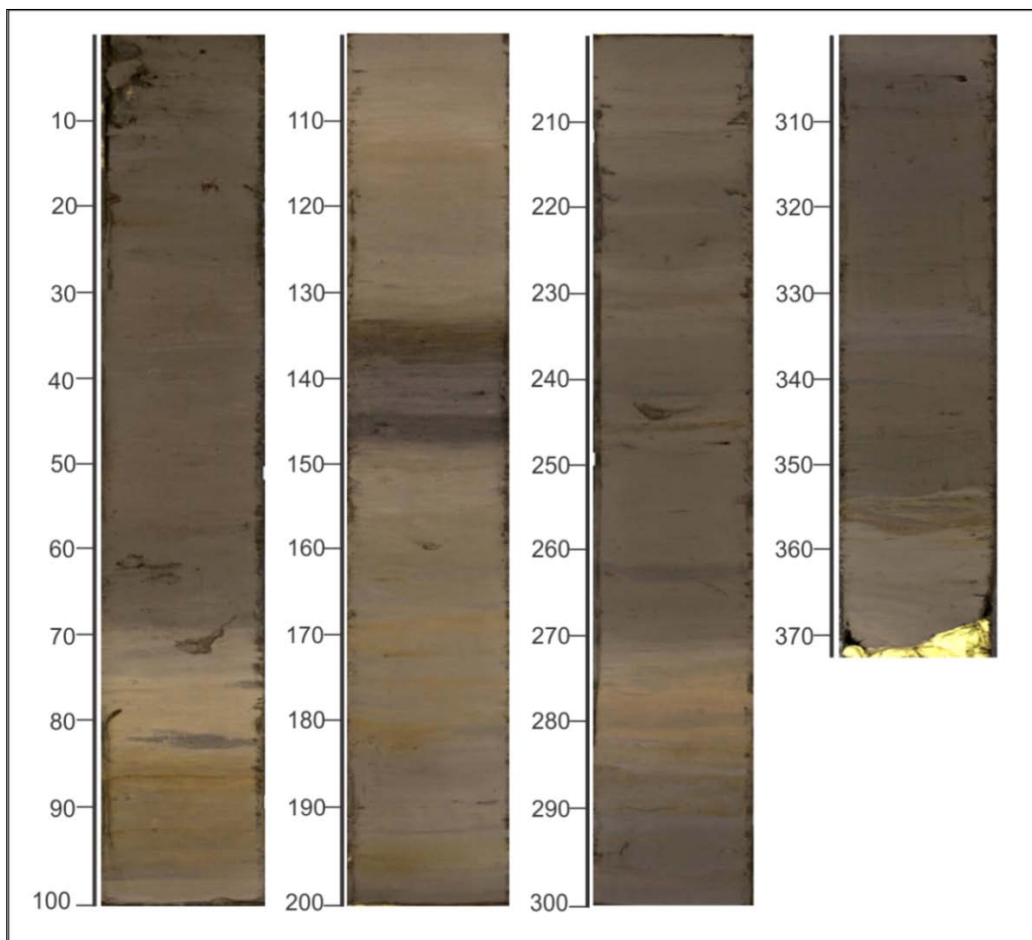


**Fig. 3.1** Digital image of gravity core JM10-02GC from the southern Yermak Plateau. For location of the core see Fig. 2.1

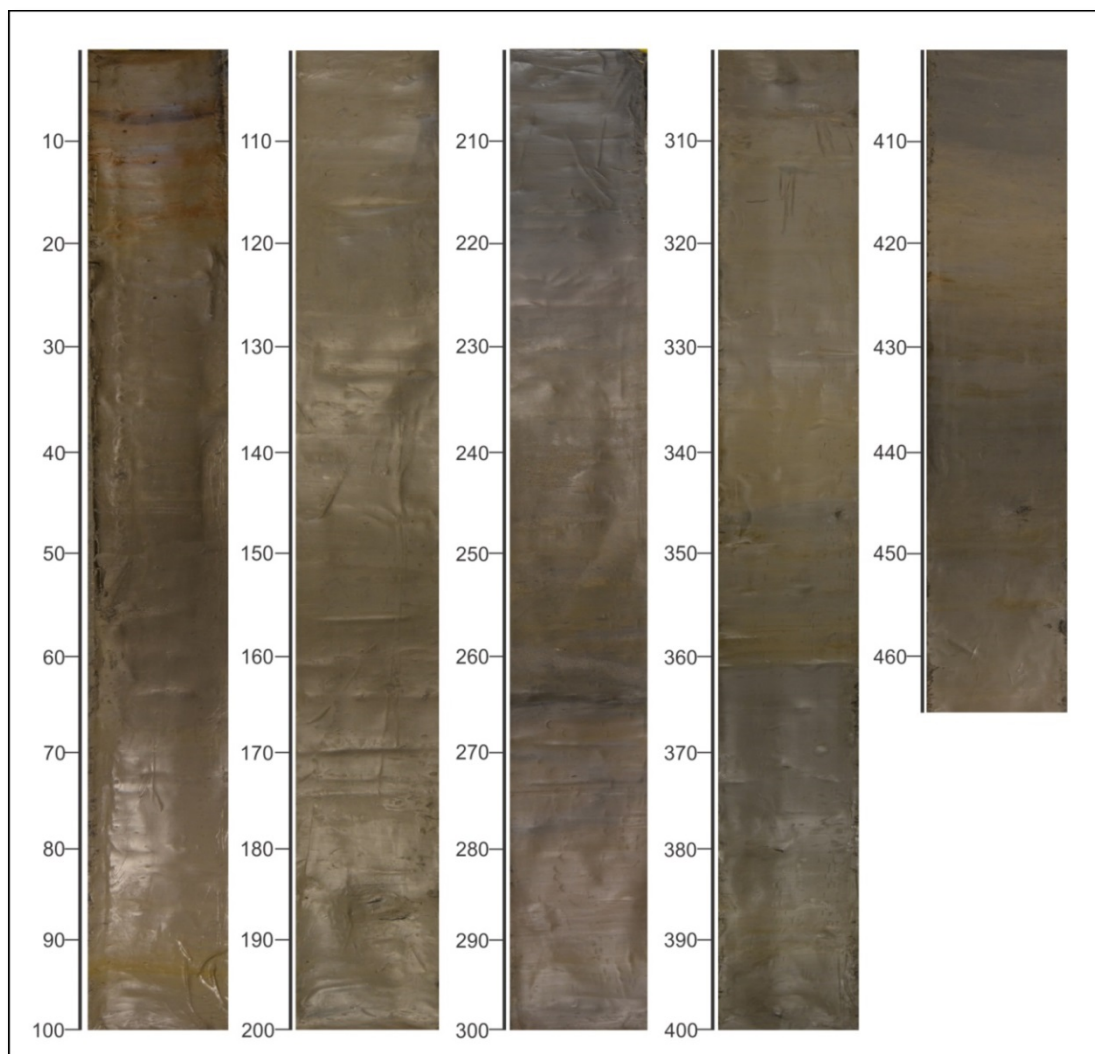


**Fig. 3.2** Digital image of gravity core HH11-09GC from the upper continental slope, north of Nordaustlandet. For location of the core see Fig. 2.1

**Table 3.1** Details of gravity cores investigated in this study

<b>Location</b>	<b>Core name</b>	<b>Coordinates</b>	<b>Water depth</b>	<b>Core length</b>	<b>Month, Year</b>
Southern Yermak Plateau	JM10-02GC	80°03' N 9°50' E	501 m	368 cm	September, 2010
Upper slope, north of Nordaustlandet	HH11-09GC	81°16' N 26°13' E	488 m	466 cm	September, 2011



## 3.2 Methods

### *Lithological-log and geotechnical properties*

Both gravity cores were cut into 1 m sections and each section was split length-wise into two halves. The digital image of core JM10-02GC was taken on the archive half of the core at the Department of Geology, UiT The Arctic University of Norway. The working half was described for visible changes in colour (using Munsell soil colour chart), texture, sedimentary structures and grain size (Fig. 3.3). Magnetic susceptibility was measured at 1 cm interval using a Bartington MS2 point sensor. Shear strength was measured at 2 cm interval using the fall cone method of Hansbo (1957). In core HH11-09GC, the colour of the sediment was measured on the sediment surface with a Colortron Spectrophotometer (Andrews and Freeman, 1996). The measurements were taken at 1 cm interval. The digital imaging of core HH11-09GC and the measurements of the geotechnical properties of both cores were carried out at the University Centre in Svalbard (UNIS).

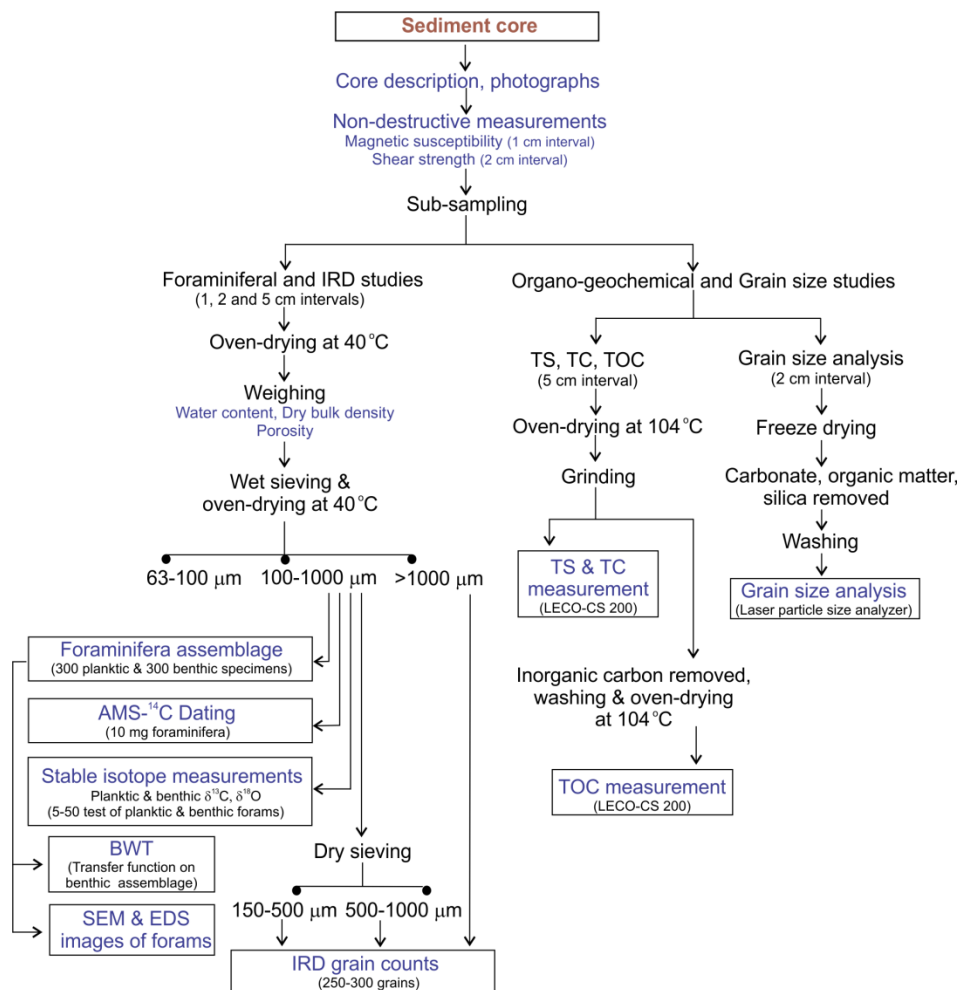


**Fig. 3.3** Outline of methodological approach (black text) and analyses performed (blue text). Refer section 3.2 for details.

### ***Foraminiferal studies***

Based on changes in lithology, 81 sediment samples were taken at 5 cm intervals in core JM10-02GC. In core HH11-09GC, 115 samples were taken at 5, 2 or 1 cm intervals and in addition, one sample from the middle of the core cutter and catcher, respectively. For each sample, 1 cm thick slice was extracted. The extracted samples were weighed and dried in an oven at 40 °C. The dried samples were weighed again and the water content was calculated. Porosity and dry bulk density ( $\text{g cm}^{-3}$ ) were calculated using the formulas:

$$\text{Porosity} = \text{Water content} / \text{Volume}$$

$$\text{Dry bulk density} = \text{Wet bulk density} - (1.026 \times (\text{Porosity}/100))$$

where Wet bulk density = Wet weight / Volume

$$\text{Volume} (\pi r^2 h) = 39.28 \text{ cm}^3 \text{ (} r = 5 \text{ cm; } h = 1 \text{ cm)}$$

The dried residues were subsequently wet sieved through stacked sieves of 63, 100 and 1000  $\mu\text{m}$  mesh sizes, and upon drying, the weight % of each grain size fraction was calculated. Up to 300 planktic and 300 benthic specimens were picked from the residues of size fraction 100–1000  $\mu\text{m}$ . Samples with 0–50 specimens were noted as barren intervals and were not considered for interpretation. Of the total picked planktic foraminifera, the number of *Neogloboquadrina pachyderma* sinistral species was counted in both cores, additionally the number of *Turborotalita quinqueloba* species was counted in core HH11-09GC. All picked benthic foraminifera were identified to species level. The relative abundance (%) of identified planktic and benthic species were calculated in relation to their total counts. The concentrations of planktic and benthic foraminifera were calculated as the number of foraminifera per gram dry weight sediment ( $\text{no. g}^{-1}$ ). Using these two concentrations, the planktic/benthic (P/B) ratio was calculated. Fluxes of planktic and benthic specimens ( $\text{no. cm}^{-2} \text{ ka}^{-1}$ ) were calculated using the formula:

$$\text{Flux} = \text{Foraminifera concentration (no. g}^{-1}) \times \text{Mass accumulation rate (MAR)}$$

where, MAR ( $\text{g cm}^{-2} \text{ ka}^{-1}$ ) = Linear sedimentation rate ( $\text{cm ka}^{-1}$ ) x Dry bulk density ( $\text{g cm}^{-3}$ )

### ***SEM and EDS images***

The scanning electron micrographs and elemental composition images of selected foraminifera specimens were taken with a Hitachi TM3000 Scanning Electron Microscope



(SEM) integrated with Quantax 70 Energy Dispersive Spectroscopy (EDS) System at the Department of Geology, UiT The Arctic University of Norway.

### ***Bottom water temperature***

Absolute bottom water temperatures were calculated for both cores using transfer functions based on the benthic foraminiferal assemblages using the C2 program (Juggins, 2007). The calculations were based on the database of Sejrup et al. (2004) with the addition of new data from the Barents Sea by Saher et al. (2009). Following the recommendations of Sejrup et al. (2004), the Weighted Averaging Partial Least-Squares (WAPLS) method and 1-component were used.

### ***Accelerator Mass Spectrometry (AMS) <sup>14</sup>C dating***

Based on foraminifera abundance, sample intervals were selected for AMS-<sup>14</sup>C dating. Approximately 2–10 mg of foraminifera tests (100–1200 individual tests) were picked from each sample. In core JM10-02GC, eleven samples were dated at the Ångström Radiocarbon Laboratory, Uppsala, Sweden and at the <sup>14</sup>CHRONO Centre for Climate, Environment and Chronology, Belfast, UK. A reservoir correction of 440±52 years (Mangerud et al., 2006) was applied and the corrected ages were calibrated to calendar years using the Fairbanks calibration curve (Fairbanks et al., 2005).

In core HH11-09GC, eleven foraminiferal samples were dated at the Radiocarbon Laboratory of Lund University, Sweden and four bivalve shell samples at the Ångström Radiocarbon Laboratory of Uppsala University, Sweden. Conventional ages were calibrated to calendar ages using the Calib 7.02 and Marine 13 Radiocarbon Age calibration curve. Since the present difference in reservoir age is small compared to the uncertainty of the dating, an integrated standard reservoir correction (-405 years) was applied (Stuiver and Reimer 1993; Reimer et al., 2013). Calibrated age range with 1 sigma standard deviation (68.3%) is used and the mid-point of ±1σ age range was calculated.

### ***Stable isotope analysis***

For stable oxygen and carbon isotope analyses ( $\delta^{18}\text{O}$ ,  $\delta^{13}\text{C}$ ), 5–50 tests of planktic and benthic foraminifera were picked from the 100–1000 μm size fraction. Square shaped four chambered specimens of planktic species *N. pachyderma* (test size 150–250 μm) and the benthic species *Cassidulina neoteretis*, *Islandiella norcrossi*, *Melonis barleeanus* and

*Cibicides lobatulus* were selected. The benthic species were selected based on the presence of a relatively large number of tests in the samples and good preservation. Benthic  $\delta^{18}\text{O}$  values from *C. lobatulus*, *M. barleeanus* and *C. neoteretis* were corrected for isotopic disequilibrium by +0.64, +0.4 and +0.16‰, respectively (Duplessy et al., 1980; Poole et al., 1994). The offset of *I. norcrossi* is uncertain therefore it was not corrected (Ślubowska-Woldengen et al., 2007). Analyses were performed at the Stable Isotope Laboratory, Stockholm University, Sweden.

### ***IRD analysis***

The residue of the 100–1000  $\mu\text{m}$  size fraction was subsequently dry sieved using 150  $\mu\text{m}$  and 500  $\mu\text{m}$  sieves for the counts of IRD (ice-rafted debris). A number of 250–300 mineral grains were counted from each sample and the concentration of IRD (no. IRD  $\text{g}^{-1}$ ) was calculated for three size fractions. The different size fractions of IRD were categorized as coarse IRD ( $> 1000 \mu\text{m}$ ), medium IRD (500–1000  $\mu\text{m}$ ) and fine IRD (150–500  $\mu\text{m}$ ).

### ***Organo-geochemical measurements***

Total carbon, total organic carbon (TOC) and total sulphur (TS) measurements were performed on a total of 200 samples from both cores in a LECO-CS200 induction furnace at the Department of Geology, UiT The Arctic University of Norway. Approximately 2 grams of sediment was collected at 5 cm interval from both the cores and the wet sediment was dried overnight in oven at 104 °C and ground. For measurement of total carbon and TS, ~0.2–0.4 g of powdered sediment was used. For TOC measurement another portion of ~0.2–0.4 g of grinded sediment was first decalcified using 10% hydrochloric acid, washed 8 times in porous crucibles, dried again at 104 °C in oven and then analyzed. Total inorganic carbon was calculated by subtracting TOC (%) from total carbon (%). The content of calcium carbonate ( $\text{CaCO}_3$ ) was calculated using the formula by Espitalié et al. (1977):

$$\text{CaCO}_3 (\%) = \text{Total inorganic carbon} (\%) \times 8.333$$

where 8.333 = stoichiometric conversion factor

### ***Grain size analysis***

For the grain size analysis, approximately 2 grams of sediment was sampled at 2 cm intervals. A total of 185 samples were analyzed from core JM10-02GC, and 248 samples from core HH11-09GC. The wet sediments were freeze-dried and treated with acetic acid and

hydrogen peroxide to remove carbonate and organic matter. Fifteen samples from core HH11-09GC containing sponge spicules were treated with 1M sodium hydroxide to remove silica. After each treatment the samples were washed with distilled water to neutralize and adjust pH to approximately 7. Before the grain size analyses, 1–2 drops of Calgon (sodium hexametaphosphate) was added to each sample and treated with an ultrasound and a magnetic stirrer to disperse the grains. While the samples were stirred, approximately 5 ml of solution was pipetted out and injected into the Beckman Coulter LS 13320 Laser Particle Size Analyser. Statistical parameters (mean, sorting and skewness) were calculated geometrically in metric scale according to Folk and Ward (1957) using the GRADISTAT software (Blott and Pye 2001).



# FORAMINIFERA DISTRIBUTION

The distribution and abundance of planktic and benthic foraminiferal species in sediments is a function of two parameters: 1) the original environmental conditions, which control the distribution of foraminifera and 2) the taphonomic processes in the water column and the sediment (Murray, 2006; Jones, 2014).

The conceptual model TROX-2 (TROphic conditions and OXYgen concentrations) proposed by van der Zwaan et al. (1999) is a modified version of the origin model of Corliss and Emerson (1990). In the original model, the interplay of food (particulate organic carbon and surface productivity) and oxygen was considered the controlling factor for the distribution of benthic foraminifera. Later, geochemical changes and competition for labile organic matter were also taken into account. However, Murray (2006) suggested that in deeper water, on the outer shelf and upper slope, the key controlling factors are food supply, energy levels (especially currents) and the nature of the substrate. Wollenburg and Kuhnt (2000) studied living benthic foraminifera in slope sediments from the Arctic Ocean and suggested that the biodiversity is mainly controlled by food supply, and the role of temperature is relatively insignificant. This has been challenged in later studies, where temperature appears to exert a major control on deep-sea biodiversity (Yasuhara and Danovaro, 2014 and references therein).

Murray (2006) describes several taphonomic processes that influence the distribution of benthic foraminifera in the sediments. These include post-mortem processes such as destruction of tests, transport, and bioturbation; dissolution of calcareous tests due to corrosive pore water or cold, dense polar bottom water; destruction of agglutinated tests due to bacterial or chemical decay of the cement; mass flow of sediments and the influence of strong tides and currents. For the paleoecological or paleoceanographic interpretation from fossil foraminiferal assemblages the effects of these processes must be taken into account.

## 4.1 Modern benthic assemblages

### *North-west Svalbard margin – Southern Yermak Plateau*

Living benthic foraminifera from the southern Yermak Plateau at 552 m water depth are dominated by *Adercotryma glomerata*, *C. neoteretis*, *C. lobatulus*, *Elphidium excavatum*, *M. barleeanus*, *Stetsonia arctica*, *Textularia torquata* and *Trochammina* spp. All are typical of the northern North Atlantic Ocean (Bergsten, 1994). Subdominant species are *Cassidulina reniforme*, *Epistominella exigua*, *Pullenia bulloides*, *Hyperammina* spp. and *Fursenkoina fusiformis*. Species that are abundant in the fossil populations are also generally abundant in the living assemblage. Studies by Bergsten (1994) and Wollenburg and Mackensen (1998) suggest that the agglutinated species are relatively abundant (48–55%) compared to the calcareous species on the southern Yermak Plateau. This abundance is due to influence of corrosive conditions caused by the high surface productivity in the area (Wollenburg and Mackensen, 1998). The sediments also contain few planktic specimens because of dissolution of calcium carbonate (Spielhagen et al., 2005). The average primary productivity of this region falls in the range of 100–120 g C m<sup>-2</sup> y<sup>-1</sup> (Reigstad et al., 2011).

### *Northern Svalbard margin – Upper slope, north of Nordaustlandet*

The closest records of modern benthic foraminiferal assemblage data are from a study off Kvitøya Trough at ~700 m water depth at the northern Barents Sea margin (Wollenburg and Mackensen, 1998). The dominant calcareous species are *C. neoteretis*, *Pullenia osloensis*, *Eilohedra nipponica*, *Melonis zaandamae*, *Lobatula lobatula*, *Epistominella arctica* and *Lagenammia difflugiformis arenulata*. The subdominant species are *Ceratobulimina artica*, *F. fusiformis*, and *Triloculina frigida*. Among the agglutinated species *Reophax* sp., *Reophax gutifer*, *Rhizammina algaeformis*, *Hippocrepina flexibilis* and *Placopsilinella aurantiaca* are dominant. The average primary productivity of the northern Svalbard margin is only about half of the primary productivity from the north-west Svalbard margin, and in the range of 50–60 g C m<sup>-2</sup> y<sup>-1</sup> (Reigstad et al., 2011). The lower productivity here is mainly due to near-permanent sea-ice cover.

## 4.2 Fossil foraminiferal assemblages in cores JM10-02GC and HH11-09GC

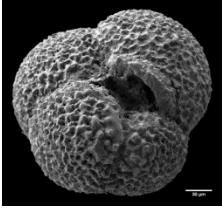
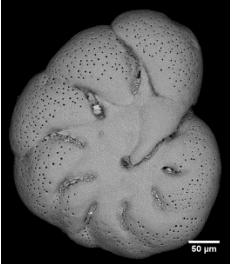
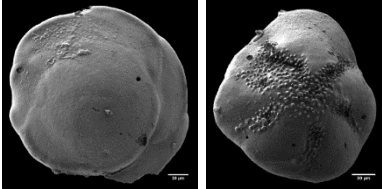
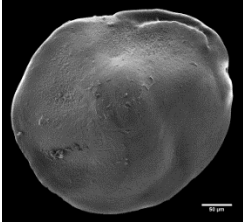
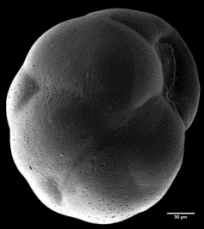
About 42 different species of benthic foraminifera were recorded in core JM10-02GC from the southern Yermak Plateau (Appendix A). The dominant benthic species groups in decreasing order of abundance are (1) *C. neoteretis*, *I. norcrossi*, *C. reniforme*; (2) *E. excavatum*, *Nonionellina labradorica*, *C. lobatulus* and (3) *M. barleeanus*, *Buccella* spp., *Astrononion gallowayi*. The most abundant planktic species throughout the core is *N. pachyderma*.

In core HH11-09GC from north of Nordaustlandet, a total of 44 benthic foraminiferal species have been identified (Appendix A). The abundant benthic species group in descending order are (1) *C. neoteretis*, *I. norcrossi*, *C. reniforme*, *E. excavatum*, *Elphidium* spp., *Buccella* spp., *M. barleeanus* and (2) *C. lobatulus*, *A. gallowayi*, *N. labradorica*, *P. bulloides*. The dominant planktic foraminiferal species in the core are *N. pachyderma* and *T. quinqueloba*.

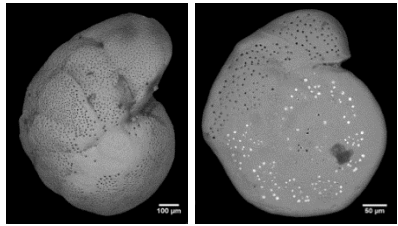
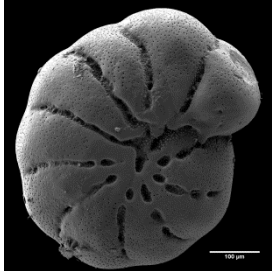
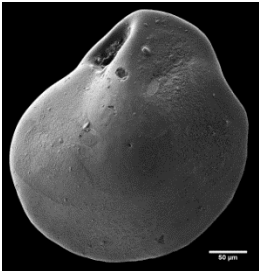
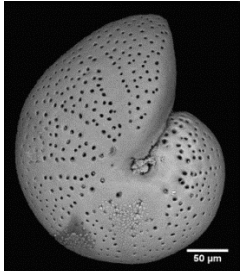

A group of subtropical-boreal benthic species ('Atlantic species') (cf. Rasmussen and Thomsen, 2005) are present at certain intervals in cores JM10-02GC (0–6%) and HH11-09GC (0–10%). These species include: *Anomalinoidea minimus*, *Cibicides pachyderma*, *Cornuloculina inconstans*, *Eggerella bradyi*, *Eilohedra nipponica*, *Gyroidina umbonata*, *Pyrgo* sp., *Marginulinopsis costata*, *Pullenia subcarinata*, *Pyrgo williamsoni*, *Pyrgoella irregularis*, *Robertinoidea* sp., *Sagrina subspinescens*, *Sphaeroidina bulloides*, *Triloculina oblonga* and *Valvulineria arctica*.

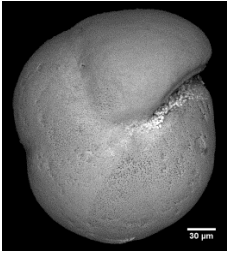
Eleven species of agglutinated foraminifera, ranging from 30–60% of the total benthic foraminifera counts were present in the top 18 cm of core HH11-09GC. These are *Labrospira crassimargo*, *Centropyxis arenatus*, *Usbekistania charoides*, *Rhabdammina abyssorum*, *Rhabdammina* sp., *Lagenammina micacea*, *Rheophax* sp., *Testulosiphon indivisus*, *Lagenammina difflugiformis*, *Lepidodeuterammina ochracea* and *Trochammina* spp.

### 4.3 Ecology of most common foraminifera

Foraminifera species	Ecological preferences and references
<p data-bbox="197 394 588 456"><i>Neogloboquadrina pachyderma</i> (sinistral)</p> 	<p data-bbox="624 495 1278 524">Polar conditions; Arctic and Polar Water at the surface.</p> <p data-bbox="624 562 1145 591">Carstens et al. (1997), Simstich et al. (2003)</p>
<p data-bbox="248 714 528 743"><i>Astrononion gallowayi</i></p> 	<p data-bbox="624 781 1401 844">Occurs in areas of coarse sediment. Indicator of enhanced bottom current activity.</p> <p data-bbox="624 882 1410 981">Sejrup et al. (1981), Mackensen et al. (1985), Korsun and Polyak (1989), Polyak and Solheim (1994), Wollenburg and Mackensen (1998), Polyak et al. (2002), Jennings et al. (2004), Murray (2006)</p>
<p data-bbox="309 1059 475 1088"><i>Buccella</i> spp.</p> 	<p data-bbox="624 1128 1430 1191">Prefers low temperatures and use algal blooms at the sea-ice margin as food source. They indicate cold condition with seasonal sea-ice.</p> <p data-bbox="624 1229 1410 1258">Mudie et al. (1984), Polyak and Solheim (1994), Steinsund (1994)</p>
<p data-bbox="266 1332 536 1361"><i>Cassidulina neoteretis</i></p> 	<p data-bbox="624 1364 1453 1494">Infaunal species that prefers fine-grained, terrigenous mud. Abundant in glaciomarine environments with stable salinity and temperature. Confined to areas influenced by often cool Atlantic Water with/without Polar Water or sea-ice at the surface.</p> <p data-bbox="624 1532 1445 1662">Green (1960), Mackensen and Hald (1988), Jennings and Helgadottir (1994), Seidenkrantz (1995), Polyak and Mikhailov (1996), Hald and Korsun (1997), Lubinski et al. (2001), Rytter et al. (2002), Husum and Hald (2004), Jennings et al. (2004), Wollenburg et al. (2004)</p>
<p data-bbox="256 1691 533 1720"><i>Cassidulina reniforme</i></p> 	<p data-bbox="624 1758 1453 1856">Arctic species. Associated with cold Atlantic Water in faunas of relatively high diversity. Also found in proximal glaciomarine environments in faunas of low diversity.</p> <p data-bbox="624 1895 1370 1957">Sejrup et al. (1981), Mackensen et al. (1985), Hald and Korsun (1997), Korsun and Hald (2000)</p>



<p><i>Cibicides lobatulus</i></p> 	<p>Epifaunal species found in coarser sediments. Often attached to hard substrates. Shows good correlation with high energy environments.</p> <p>Mackensen et al. (1985), Hald and Steinsund (1992), Hald and Korsun (1997), Murray (2006)</p>
<p><i>Elphidium excavatum</i></p> 	<p>Arctic-Polar species abundant in polar conditions and in cold bottom water. Highly adaptable to changes in food availability and thus tolerates variable environmental conditions with low salinity and low temperatures and high turbidity. Dominant in front of glaciers and in ice marginal conditions.</p> <p>Linke and Lutze (1993), Steinsund (1994), Hald and Korsun (1997), Korsun and Hald (2000), Polyak et al. (2002), Sejrup et al. (2004)</p>
<p><i>Islandiella norcrossi</i></p> 	<p>Arctic-Polar species. Prefers relatively high and stable bottom water salinities. Indicator of high organic content of the sediment, increased productivity and presence of the sea-ice edge and seasonal sea-ice.</p> <p>Steinsund (1994), Korsun and Hald (1998), Polyak et al. (2002), Murray (2006), Ślubowska-Woldengen et al. (2008)</p>
<p><i>Melonis barleeanus</i></p> 	<p>Infaunal Arctic-Boreal species. Related to chilled Atlantic Water, high salinities, open water to seasonal sea-ice cover and fine sediments. High sedimentation rates and steady supply of food through partially degraded organic matter</p> <p>Caralp (1989), Korsun and Polyak (1989), Linke and Lutze (1993), Steinsund (1994), Hald and Steinsund (1996), Heinz et al. (2001), Polyak et al. (2002), Jennings et al. (2004)</p>
<p><i>Nonionellina labradorica</i></p> 	<p>Arctic-Polar species. Prefers cold water (&lt; 2 °C) of normal salinity &gt; 34.5‰ and is abundant in areas with high organic matter and high seasonal productivity in ice marginal zones or oceanic fronts.</p> <p>Mudie et al. (1984), Corliss (1991), Steinsund (1994), Hald and Korsun (1997), Korsun and Hald (1998), Korsun and Hald (2000), Polyak et al. (2002), Sejrup et al. (2004), Murray (2006)</p>

<p><i>Pullenia bulloides</i></p> 	<p>Infaunal species associated with high organic flux and influence of Atlantic Water especially in terms of bottom water temperature. Prefers a narrow salinity interval close to 35‰ and temperature between 2 °C and 4 °C.</p> <p>Haake and Pflaumann (1989), Bauch et al. (1996), Fronval and Jansen (1997), Rasmussen et al. (1999), Rytter et al. (2002), Risebrobakken et al. (2010)</p>
<p><b>‘Atlantic species’</b></p> <p><i>Anomalinoides minimus</i>  <i>Cibicides pachyderma</i>  <i>Cornuloculina inconstans</i>  <i>Eggerella bradyi</i>  <i>Eilohedra nipponica</i>  <i>Gyroidina umbonata</i>  <i>Marginulinopsis costata</i>  <i>Pullenia subcarinata</i>  <i>Pyrgo</i> sp.  <i>Pyrgo williamsoni</i>  <i>Pyrgoella irregularis</i>  <i>Robertinoides</i> sp.  <i>Sagrina subspinescens</i>  <i>Sphaeroidina bulloides</i>  <i>Triloculina oblonga</i>  <i>Valvulineria arctica</i></p> <p>(For more SEM images refer to plates in paper II)</p>	<p>The group has southern affinity and lives in warmer Atlantic Water. They are adapted to low productivity.</p> <p>Meltwater and sea-ice cover during Heinrich events prevented heat loss and caused bottom water warming providing favourable conditions for this group of species.</p> <p>Thomas et al. (1995), Rasmussen et al. (1996a, b), Wollenburg and Mackensen (1998), Rasmussen (2005), Rasmussen and Thomsen (2005), Rasmussen et al. (2007), Wollenburg et al. (2001, 2004, 2007)</p>

### SUMMARIES OF PAPERS AND AUTHORS' CONTRIBUTION

#### 5.1 Paper I

T. Chauhan, T. L. Rasmussen, R. Noormets, M. Jakobsson, K. A. Hogan, 2014. **Glacial history and paleoceanography of the southern Yermak Plateau since 132 ka BP.**

*Quaternary Science Review*, 92, pp 155-169. doi:10.1016/j.quascirev.2013.10.023

The aim of this study is to reconstruct the variation of the Atlantic Water inflow to the southern Yermak Plateau and its correlation to movement of the sea-ice margin and the SBIS during the late Quaternary. The Yermak Plateau extends north-west from the continental margin of Svalbard and is located at the entrance to the Arctic Ocean. It constitutes a relatively shallow topographic obstacle for the transport of Atlantic Water northwards. The 3.7 m long sediment core (JM10-02GC) was retrieved from 501 m water depth on the southern Yermak Plateau, which is currently in the narrow MIZ between the Polar Front and the Arctic Front. The sediment core covers the last 132 ka. The reconstruction of the water masses is based on the distribution patterns of benthic and planktic foraminiferal species, stable oxygen and carbon isotope records of benthic and planktic foraminifera, IRD and magnetic susceptibility of the sediments.

The results show that the influence of the Atlantic Water between MIS 5 and MIS 3 was weak except in MIS 5e (Eemian), 5a and in a few intervals in MIS 3. During most part of MIS 5 and MIS 4, seasonal sea-ice margin extended close to the core site. The benthic foraminiferal species *I. norcrossi* and *E. excavatum* were associated with these periods of seasonal sea-ice cover. However, short periods with relatively stronger influence of subsurface Atlantic Water led to the thinning of sea-ice and open water conditions with higher surface productivity. These periods are characterized by high abundance of *C. neoteretis*. Following these short periods of productivity, the formation of seasonal sea-ice in the MIZ and associated very high productivity probably increased the supply of organic matter to the sea floor and resulted in the dissolution of calcium carbonate. The benthic foraminiferal record shows several barren intervals mainly because of dissolution. Another

reason for intervals barren of foraminifera was deposition of ice-rafted material. Stronger advection of subsurface Atlantic Water occurred during MIS 2, which resulted in high productivity of planktic and benthic foraminifera. The open water conditions during glacial period indicate that the sea-ice margin had retreated to the north. This period of extended open water correlates with growth of the SBIS. The foraminifera-barren interval dating 24–23 ka within MIS 2 was associated with high flux of ice-rafted material, which was released due to the advance of the SBIS to the shelf edge in southern and western Svalbard. Low planktic  $\delta^{18}\text{O}$  values at 17.3 ka and decrease in relative abundance of *N. pachyderma* and *C. neoteretis* marks the initiation of the last deglaciation period. The Holocene started with advection of relatively warm Atlantic Water, indicated by presence of *P. bulloides*. The Holocene record was incomplete due to erosion or non-deposition of sediments.

### ***Contribution of single author***

Teena Chauhan did all the laboratory work on sediment cores, microscopy work on planktic and benthic foraminifera assemblage, IRD and sample preparation for  $^{14}\text{C}$  radiocarbon dating and stable isotope analysis. She is also responsible for drafting manuscript and drawing all figures. Tine L. Rasmussen supervised the microscopy work, participated in interpretation and discussion of results and critical revision of manuscript. Riko Noormets contributed by acquisition of sediment core and supervision of the laboratory work on sediment core. Martin Jakobsson gave feedback on stable isotope results. Kelly A. Hogan participated in the discussions of the sedimentological aspects and corrected the language. All co-authors have discussed the ideas presented and have reviewed the manuscript.

## **5.2 Paper II**

Teena Chauhan, Tine L. Rasmussen and Riko Noormets. **Paleoceanography of the Barents Sea continental margin, north of Nordaustlandet, Svalbard during the last 74 ka.**

*Accepted for publication in Boreas*

The goal of this study is to reconstruct the paleoceanography of the poorly studied region of the northern Svalbard margin and to correlate the results with the data from the north-western Svalbard margin in order to study the inflow of Atlantic Water along the northern Barents Sea margin. At present, the continental margin north of Nordaustlandet is covered by seasonal sea-ice. The influx of Atlantic Water occurs as a subsurface flow with the core of

warm water flowing between 100 m and 600 m water depth. The 4.6 m long sediment core (HH11-09GC) taken on the upper slope from 488 m water depth covers the last 74 ka. The reconstruction is based on the distribution of planktic and benthic foraminiferal faunas, planktic and benthic stable isotopes, lithological parameters and concentration of IRD. In addition, bottom water temperature was calculated by transfer functions based on the benthic foraminiferal species assemblage data of this core and the core from the southern Yermak Plateau (JM10-02GC). The ‘Atlantic species’ are identified in both cores and using this new data set, the age model of JM10-02GC core has been slightly revised.

Several short-lasting periods during MIS 5a, late MIS 4 and in MIS 3 were characterized by increase in relative abundance of *C. neoteretis* reflecting stronger influence of subsurface inflow of Atlantic Water. The period of Atlantic Water influx during the glacial period of late MIS 4 probably caused formation of polynya, whereas during MIS 5a and MIS 3 advection of subsurface Atlantic Water in combination with the relatively high insolation caused acceleration of melting of the SBIS and sea-ice. Stronger influence of subsurface Atlantic Water was recorded in late MIS 3 and for the LGM in MIS 2 with sea-ice marginal conditions (high *I. norcrossi*). The cold conditions caused the SBIS to grow and advance to the shelf edge at *c.* 65 ka in MIS 4 and later at 23–22 ka in MIS 2. The last deglaciation started at 16.9 ka with increase in insolation and inflow of warm Atlantic Water (high bottom water temperature), which probably accelerated the melting of the ice sheet. However, the elevated freshwater supply (low planktic  $\delta^{18}\text{O}$  values) caused stratification of the water column and reduced ocean circulation. The time period corresponded to Heinrich event H1 in the North Atlantic. Moreover, a large amount of IRD was released at 15.6 ka, reflecting the major disintegration of the SBIS in the north of the Barents Sea. The influx of warm Atlantic Water caused rapid decrease in sea-ice at 15.5 ka (Bølling-Allerød interstadial) and later at 14 ka and 12.8 ka, meltwater discharge weakened the ocean circulation. Sediments of early Holocene age were absent, either due to erosion or non-deposition. The late Holocene was characterized by cold conditions and near-perennial sea-ice cover with an exception at 1.5 ka, when stronger advection of Atlantic Water and reduced cover of sea-ice persisted for a short period. The correlation of these results with the data from the southern Yermak Plateau suggests that the magnitude of Atlantic Water inflow together with insolation, meltwater supply and sea-ice export were controlling factors in the paleoceanographic development of these areas.

### ***Contribution of single author***

Teena Chauhan participated during acquisition of the sediment core and did all the laboratory work on sediment core (logging, measuring geo-technical properties, sub-sampling, sieving), microscopy work on planktic and benthic foraminifera assemblage, IRD and sample preparation for  $^{14}\text{C}$  radiocarbon dating and stable isotope analysis, together with preparation of all figures and writing first draft of manuscript. Tine L. Rasmussen contributed by writing method and result section on bottom water temperatures, participated in the discussion and critical review of the manuscript. Riko Noormets contributed by acquisition of the sediment core and participated in the review process.

## **5.3 Paper III**

Teena Chauhan, Riko Noormets and Tine L. Rasmussen. **Glaciomarine sedimentation and bottom current activity along the north-western and northern continental margin of Svalbard during the late Quaternary**

*Submitted to Geo-Marine Letters on 7<sup>th</sup> May 2015*

The aim of the study is to reconstruct the physical characteristics of the paleo-bottom water current and variations in the flow of the West Spitsbergen Current and the associated changes in the sedimentary environments on the north-western and northern Svalbard margin during the late Quaternary. The concentration of organic carbon was measured and detailed grain size analyses were performed in core JM10-02GC from the southern Yermak Plateau and core HH11-09GC from the upper slope, north of Nordaustlandet. In particular, the ‘sortable silt’ proxy has been used to reconstruct paleo-bottom current strength.

From the sortable silt and its relation to the content of sand and clay, five main grain size distribution (GSD) types were distinguished to investigate the strength of the bottom currents and the transport of sediment at the cores sites. MIS 5e (Eemian) and MIS 5a were characterized by strong bottom currents in connection with high insolation and inflow of warm Atlantic Water. During MIS 4, weak bottom currents and poor ventilation persisted, except at 64 ka on the north-western margin and at 62 ka on the northern Svalbard margin, where strong bottom currents dominated, probably due to dense water formation. It is suggested that super-cooling underneath of a floating ice shelf caused down-flow of dense

water at 64 ka, whereas north of Nordaustlandet polynyas were formed at 62 ka and extensive sea-ice formation led to brine rejection and probably dense water formation. During the MIS 4/3 transition, the retreating SBIS supplied excess freshwater and high content of probably subglacial organic carbon. The stratification of the upper water column apparently reduced the bottom current strength and favoured settling of clay size particles and preservation of organic carbon at the sea bottom. MIS 3 was a relatively stable period with moderate bottom current strength, and expansion of sea-ice cover. North of Nordaustlandet at around 30.5 ka in the late MIS 3, distinct fluctuations in grain size indicated that the ice shelf of the SBIS was grounded on the nearby shelf. At the beginning of MIS 2, the Atlantic Water advected to the southern Yermak Plateau had moderate bottom current strength, whereas north of Nordaustlandet the Atlantic Water was cold, but the strength of the bottom currents was relatively high. The sediment deposited during the LGM was mainly ice-rafted at the north-western margin (24–23 ka), while at the northern Svalbard margin they originated from down slope processes, where sediment delivery and dumping occurred due to the SBIS advance to the shelf edge (23–22 ka). At the onset of the last deglaciation, sediment supply was limited to proximal sources, such as meltwater plumes, icebergs and sea-ice melt-out and the increase in freshwater flux probably weakened the ocean circulation and enabled preservation of organic carbon. During the cold conditions of the late Holocene, strong currents generated locally at the north-western margin, while at the northern Svalbard margin, the bottom current strength was low and stable due to near-perennial sea-ice cover.

#### ***Contribution of single author***

Teena Chauhan was responsible for laboratory work on sediment cores, measurements of grain size and sample preparation for organo-geochemical analysis. The first draft of manuscript and all figures were prepared by Teena Chauhan. Riko Noormets participated in discussion of results, writing a section of the introduction chapter and critical review of the manuscript. Tine L. Rasmussen contributed in formulation of research questions, and to the discussions. All co-authors actively contributed to the improvement of the various versions of the manuscript.





## Chapter 6

### SYNTHESIS

The dissertation focuses on the reconstruction of past climate, mainly oceanographic variability and glaciomarine sedimentation at the Arctic continental margin north-west and north of Svalbard during the late Quaternary. The thesis consists of three research papers. In the first and second paper the paleoceanographic development of the north-western Svalbard margin (southern Yermak Plateau; Paper I) and the northern Svalbard margin (upper continental slope north of Nordaustlandet; Paper II) is presented. The emphasis is on improving the understanding of natural variability of the Atlantic Water inflow to the Arctic Ocean during the last interglacial-glacial-interglacial cycle and its relation to ice sheet extent, sea-ice cover and general ocean circulation. The distribution patterns of benthic and planktic foraminiferal faunas and their stable isotope records were studied. The concentration of IRD and lithological properties of sediments supported to understand the relation between the Atlantic Water inflow and the evolution of the SBIS. Furthermore, the benthic assemblages and the paleoceanographic events of both locations were compared to understand the variation in the paleoenvironmental conditions (Paper II).

Variation in bottom current activity within glacial-interglacial periods has never been investigated before in the study areas. In the third paper, proxies for paleo-bottom current strength and the influence of bottom currents on the depositional environment of the north-western and northern Svalbard margin are presented. Grain size distribution of the sediments, in particular the sortable silt size fraction (10–63  $\mu\text{m}$ ) has been studied and the distribution of organic carbon in the sediment analyzed for better understanding of the depositional environment. Additionally, the physical evidence for bottom current strength and the indirect evidence for activity of the flow of Atlantic Water obtained from the foraminiferal studies have been compared (Paper III).

In summary, the aim of this dissertation is (a) to reconstruct the natural variability of Atlantic Water inflow, its impact on sea-ice cover and freshwater supply, its relation to bottom current strength and depositional environments, and (b) to delineate the response of the northern part of the SBIS to this variation during the late Quaternary. The main results of the

reconstruction of paleo-environmental conditions are described below and illustrated in schematic diagram (Fig. 6.1).

## **Interglacial periods**

Sediment core JM10-02GC from the southern Yermak Plateau covers the last interglacial period, the Eemian (MIS 5e). Core HH11-09GC from the upper slope north of Nordaustlandet covers MIS 5a. The Eemian interglacial was characterized by strong inflow of warm Atlantic Water with strong bottom currents. The environmental conditions during MIS 3 were generally cold with weaker flow of Atlantic Water compared to the Eemian interglacial. Seasonal sea-ice cover expanded with episodic events of stronger influence of Atlantic Water at the bottom (increase in relative abundance of *C. neoteretis*) and the bottom current strength was generally moderate throughout MIS 3. The short periods of Atlantic Water advection and associated higher productivity were followed by increased supply of organic carbon to the sea floor. The high concentration of organic matter in the sediment may have caused corrosion, which is not favourable for calcium carbonate preservation and may explain the foraminifera-barren intervals in the records. The dissolution was more pronounced on the southern Yermak Plateau due to its position within the high productivity MIZ compared to the relatively stable conditions at the upper slope north of Nordaustlandet. Intervals equivalent in time with Heinrich events H6–H3 were distinguished within MIS 3, with similar characteristics as the Heinrich events of the North Atlantic. This signifies that events in the south also had an impact on the oceanographic regime with similar influence of icebergs and meltwater at high northern latitudes. Sediments of early Holocene were absent in both cores, either due to erosion or non-deposition. Thus, comparison between the last interglacial and the Holocene period is not possible. The late Holocene was cold and due to excessive heat loss of the Atlantic Water, dense water formed and strong currents were generated locally on the southern Yermak Plateau. Consequently, the influence of Atlantic Water was further reduced at the upper slope, north of Nordaustlandet and near-perennial sea-ice cover expanded except for a short interval of increased Atlantic Water advection at *c.* 1.5 ka.

The results also show that at the onset of interglacial/interstadial periods the SBIS destabilized and ice-rafting accelerated, such as at the beginning of MIS 5e, 5c, 5a and early

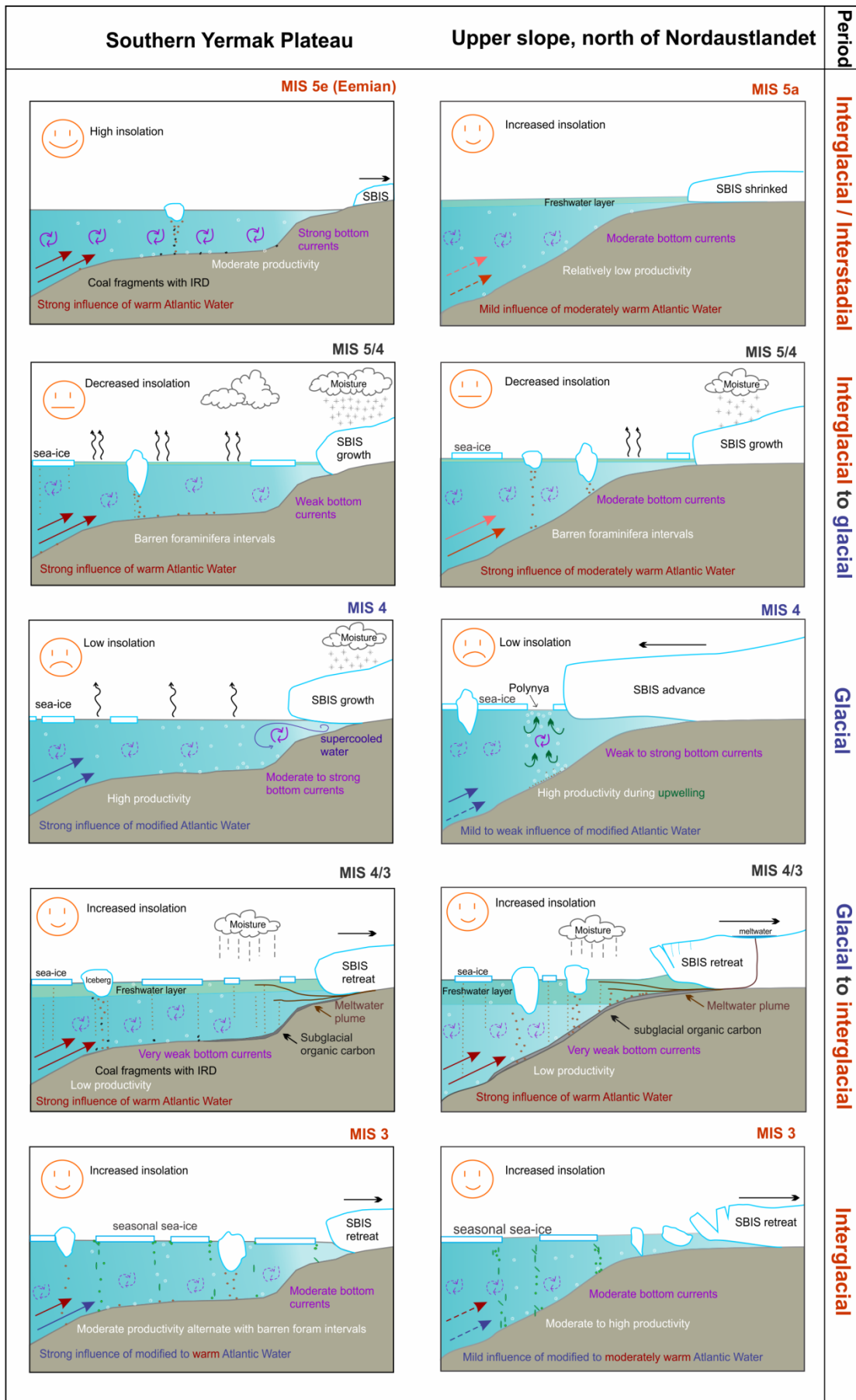
MIS 3 (and probably during the early Holocene as well). Moreover, the grain size data together with other evidence indicate that the SBIS was grounded for a short period of time at the northern Barents Sea shelf, north of Nordaustlandet, due to abrupt fall in sea-level at c. 30.5 ka.

One of the forcing mechanisms behind these events was probably an increase in ocean temperature that promoted melting of the ice sheet and sea-ice. High insolation during interglacials could have reduced the difference between ocean and air temperature, implying less exchange of heat and, thus, warmer conditions. Relatively low insolation during MIS 3 and the late Holocene compared to MIS 5 could be one of the reasons of colder conditions. During these periods, high productivity related to Atlantic Water inflow and ice marginal conditions led to increased organic carbon supply to the sea bottom.

### **Interglacial to glacial transition periods**

The glacial inception at the MIS 5/4 (71 ka) and MIS 3/2 (28 ka) transitions were characterized by moderate bottom current strength. During the MIS 5/4 transition, the sediments at the north-western and the northern Svalbard margin were barren of planktic and benthic foraminifera. This suggests occurrence of poor ventilation, poor calcium carbonate preservation or very low productivity conditions. Relatively good ventilation and low organic carbon content probably led to good preservation of calcium carbonate in the sediments during the MIS 3/2 transition, where relatively high abundances of *I. norcrossi* and *C. neoteretis* indicate cold conditions with seasonal sea-ice cover. The MIS 5/4 transition was also characterized by high content of IRD, that indicates the advance of the SBIS was rapid.

High content of IRD at MIS 5/4 transition and high surface productivity at MIS 3/2 transition occurred primarily due to advection of warm Atlantic Water, but in combination with low insolation. Contrary to the interglacial periods, the low insolation during these transition periods enabled excessive heat loss from the Atlantic Water to the atmosphere. Hebbeln et al. (1994) suggested that the increased rate of evaporation provided moisture for the growth of the SBIS.



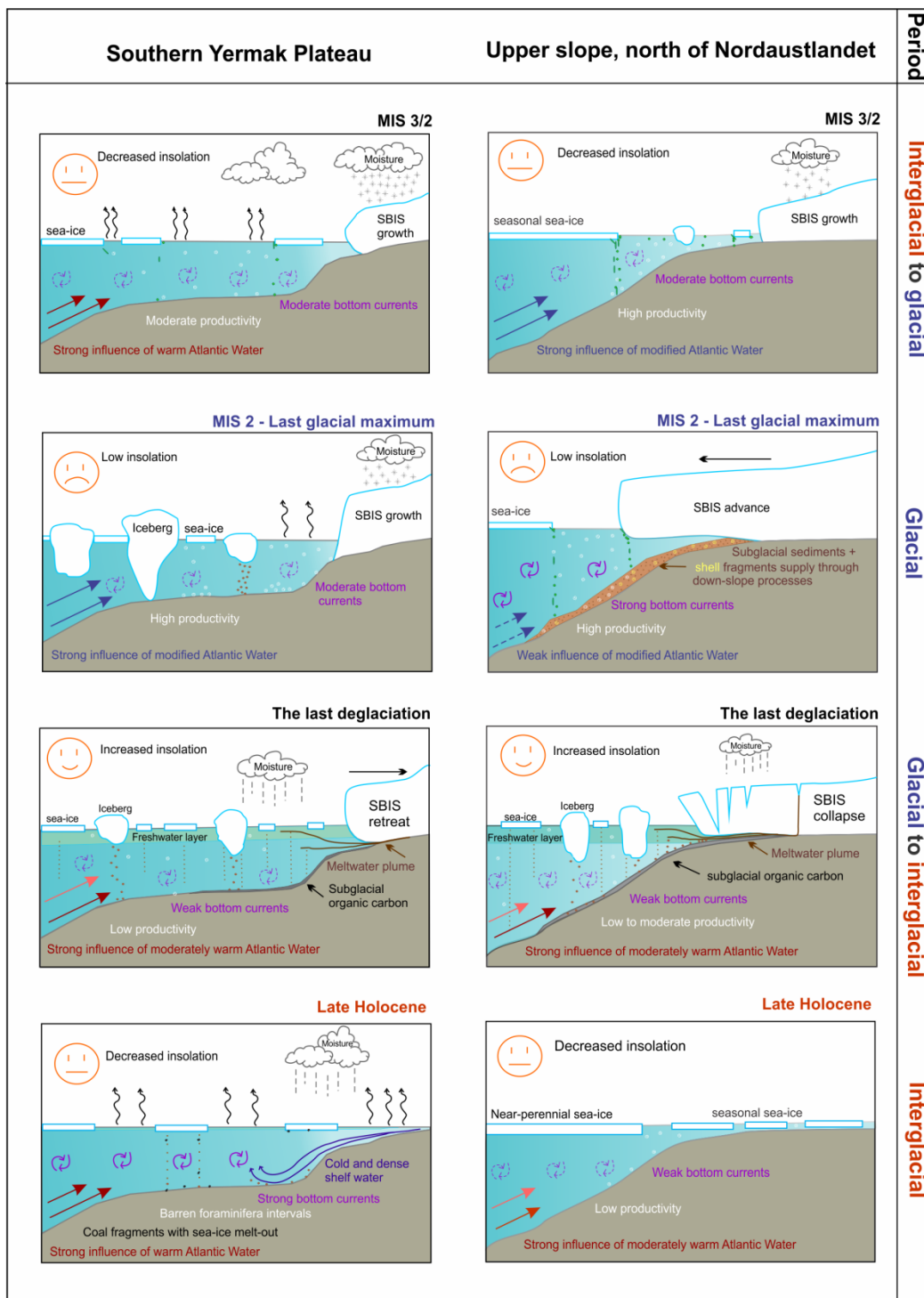


**Fig. 6.1** Schematic diagram (not to scale) summarizing the key results based on interplay of climate, oceanographic and ice sheet processes, and their effect on sedimentary environment on the north-western (southern Yermak Plateau) and northern (north of Nordaustlandet) Svalbard margins at various key time periods since MIS 5.

## Glacial Period

Sediments from the glacial periods MIS 4 (71–60 ka) and MIS 2 (28–11 ka) are present in both cores. Foraminiferal species, which today thrive in subsurface Atlantic Water in polar conditions such as the planktic species *N. pachyderma* and the benthic species *C. neoteretis*, *C. reniforme* and *I. norcrossi*, are dominant. During MIS 4, the influence of the Atlantic Water was relatively weak with moderate bottom current strength and weak bottom water ventilation. Events of dense water formation generating strong bottom currents were also recorded during MIS 4. They were associated with the formation of dense shelf waters at the north-western margin (at 64 ka) and with sea-ice formation following the polynyal activity at the northern Svalbard margin (at 62 ka).

Although the paleoceanographic development appears similar between the two glacial periods and between the two study areas, some differences were also recorded. For example, during MIS 2 the influence of Atlantic Water was high with moderate bottom current strength at the southern Yermak Plateau, whereas at the upper slope north of Nordaustlandet the influence of Atlantic Water was weak and bottom current strength was high. Generally, calcium carbonate dissolution occurred at the southern Yermak Plateau due to increased open water conditions and higher productivity. In contrast, at the upper slope north of Nordaustlandet the lower productivity and continuous influence of subsurface Atlantic Water resulted in better preservation of calcium carbonate.

During MIS 4, the SBIS advanced to the northern Barents Sea margin at *c.* 65 ka and consequently, IRD was deposited on the upper slope, north of Nordaustlandet. During the LGM in MIS 2, the sediment supply at the southern Yermak Plateau was mainly from ice-rafted material at 24–23 ka. It has been suggested that the source of icebergs and debris at the southern Yermak Plateau was from a series of mass-wasting events at the western Svalbard margin and advance of the SBIS at the southern Svalbard (Andersen et al., 1996; Vogt et al., 2001; Jessen et al., 2010). However, north of Nordaustlandet, the down-slope processes due to the SBIS advance to the shelf edge supplied reworked sediments and shell fragments between 23 and 22 ka. The dissimilarity in depositional environment in the intervals of advance of the SBIS during the LGM is interpreted to be mainly due to the topographic differences between the two areas.

Together with low insolation, the relatively strong influence of the Atlantic Water facilitated the growth of the SBIS and caused high productivity periods at the southern Yermak Plateau. This result is in agreement with published studies from the western Svalbard margin (Hebbeln et al., 1994; Hald et al., 2001). At the same time, the weak influence of Atlantic Water compared to Polar Water on the upper slope enabled sea-ice expansion. Due to an increase in ice volume, the SBIS advanced to the southern, western and northern margin of the Barents Sea during the LGM over approximately the same time interval. Similar environmental conditions may have occurred at other high latitude regions of the Eurasian Arctic. It is suggested that interplay between Atlantic Water inflow and Polar Water outflow from the Arctic Ocean was one of the key forcing mechanisms in growth and decay of the SBIS and the sea-ice.

### **Glacial to interglacial (deglaciation periods)**

Core JM10-02GC from the southern Yermak Plateau covers three deglaciation periods (MIS 6/5, MIS 4/3 and MIS 2/1), whereas core HH11-09GC from the north of Nordaustlandet, covers two (MIS 4/3 and MIS 2/1). The deglaciation periods were associated with inflow of relatively warm subsurface Atlantic Water (high bottom water temperature) and were also characterized by increased influx of meltwater from the retreating ice sheet, melting of sea-ice and icebergs, as indicated by low planktic  $\delta^{18}\text{O}$  values. The bottom current strength was reduced due to the presence of a thick freshwater layer at the surface causing stratification of water column. This resulted in poor ventilation and anoxic conditions at the seafloor. The supply of organic carbon was high and probably released from melting of the ice sheet, in particular during the MIS 4/3 transition (around 60 ka) and during the last deglaciation at c. 19 ka.

Due to retreat of the SBIS, the sediments were enriched in IRD and drop-stones during the deglaciation periods. During the last deglaciation, the major collapse of the SBIS north of the Barents Sea occurred at 15.6 ka. The inflow of warm Atlantic Water was renewed after 15.5 ka together with an increase in supply of terrigenous sediments. This correlates with the beginning of the Bølling-Allerød interstadials. The meltwater pulse at 14 ka was similar in magnitude to the pulse recorded at 60 ka, which resulted in preservation of very high content

of organic carbon, probably due to poor ventilation. The ocean circulation was likely to have been significantly reduced during these meltwater events.

The influx of warm Atlantic Water with a gradual increase in insolation was the primary force behind the deglaciation and resulted in melting of sea-ice and ice sheets. However, increase in freshwater supply from sea-ice and the SBIS acted as a positive feedback, further reducing the strength of currents and ocean circulation.

Overall, it can be concluded that the primary forcing mechanisms, in regulating the ocean circulation during the late Quaternary were changes in insolation together with variability in the inflow of Atlantic Water. Freshwater supply also had strong influence on the oceanographic conditions. This study shows that the continuous presence and variable strength of the subsurface Atlantic Water along the north-western and northern Svalbard margin had a significant effect on the extent of the sea-ice cover and the stability of the SBIS since the start of MIS 4. Over the Yermak Plateau there was stronger influence of Atlantic Water near the surface with more open water conditions and seasonal sea-ice cover. In contrast, at the northern Svalbard margin the influence of Atlantic Water was weak and the inflow was under the cold Polar Water and/or near-perennial sea-ice cover. The influence of these climate forcing mechanisms varied temporally within glacial and interglacial periods and spatially between locations with same water depth. The influence on the local sedimentary and oceanographic environment varied significantly. This underlines the importance of considering the regional environmental parameters and feedback mechanisms in reconstructions of the past climate.



### FUTURE PERSPECTIVES

The sediment cores from the north-western and northern continental margin of Svalbard have been studied using planktic and benthic foraminifera and sediment grain size data. The study presents new insights about the variability in subsurface Atlantic Water inflow to the Arctic Ocean during the last two glacial and interglacial periods and its influence on the extent of the SBIS. However, methods to create a detailed chronology still need to be improved, for areas devoid of foraminifera. The foraminifera-barren intervals or intervals with very low abundance of foraminifera could not be dated and only tentatively correlated using oxygen isotope stratigraphy. The Optically Stimulated Luminescence (OSL) method could potentially be used for dating these intervals, provided suitable material is present in the sediment (Rhodes, 2011; Jacobs, 2008). Several studies have shown affirmative result based on the OSL dating method (Jakobsson et al., 2003; Kortekaas et al., 2007; Sugisaki et al., 2010).

Also, the early Holocene history of the region is not well understood. Early Holocene sediments were absent in both cores of this study. Similar trends are observed in cores from the western Svalbard slope at a water depth <1200 m due to strong bottom current activity (Jessen et al., 2010). Thick sequences of Holocene sediment can be retrieved from the fjords, which act as sediment traps (e.g., Slubowska et al., 2005; Slubowska-Woldengen et al., 2007; Forwick and Vorren, 2009; Skirbekk et al., 2010). However, to obtain a high resolution sequence of Holocene age from the slope, deep sites must be visited. Detailed data of Holocene age will also be useful to investigate the similarities and dissimilarities between the Holocene and MIS 5e (Eemian) interglacial periods at high latitude.

In addition to commonly used transfer functions, the paleo-temperature can be reconstructed based on Magnesium/Calcium (Mg/Ca) ratios provided suitable foraminiferal species are present in the records (Lea et al., 2000). Boron/Calcium (B/Ca) ratios and  $\delta^{11}\text{B}$  values in planktic foraminifera are proxies for carbonate ion concentration and pH - factors important for calcium carbonate ( $\text{CaCO}_3$ ) preservation and carbon-dioxide ( $\text{CO}_2$ ) in the water (Lohmann, 1995; Broecker and Clark, 2001).

Likewise, reconstruction of variations in past sea-ice cover during the Quaternary is another emerging research question.  $IP_{25}$  (Ice Proxy with 25 carbon atoms) has been widely used in Arctic sediments to derive seasonal sea-ice/stable sea-ice marginal conditions (Belt et al., 2008; Belt and Muller, 2013). Study of more records from around Svalbard will be useful to validate the results. Moreover, studies based on the distribution patterns of modern foraminiferal faunas from seasonal sea-ice covered areas around Svalbard will improve knowledge about the preferences of benthic foraminifera. To better understand the ocean circulation in the Arctic, knowledge regarding the variability of Polar Water outflow from the Arctic Ocean is equally important to Atlantic Water inflow variability. Studies are needed from the areas that are influenced by the East Greenland Current.

Another question arising from this study is provenance of IRD and the sediments released from melting of sea-ice and meltwater plumes from the ice sheet, and whether the source was proximal or distal. For instance, investigating the composition and grain size of sediments and IRD from a series of sediment cores along a transect from near-shore to offshore, north of Nordaustlandet, could enhance our knowledge on the melting and calving processes of SBIS during the past glacial-interglacial cycles. This knowledge could then be used to better understand the evolution and processes of the marine-based West Antarctic Ice Sheet, which is a modern analogue of the former SBIS.

## REFERENCES

- Alley, R.B., 1995. Resolved: The Arctic Controls Global Climate Change, in: Walker O. Smith, J., Grebmeier, J.M. (Eds.), *Arctic Oceanography: Marginal Ice Zones and Continental Shelves*. American Geophysical Union, Washington, DC, p. 263.
- Andersen, E.S., Dokken, T.M., Elverhøi, A., Solheim, A., Fossen, I., 1996. Late quaternary sedimentation and glacial history of the western Svalbard continental margin. *Marine Geology* 133, 123-156.
- Andrews, J., Freeman, W., 1996. The measurement of sediment color using the colortron spectrophotometer. *Arctic and Alpine Research*, 524-528.
- Bart, P.J., Anderson, J.B., 1995. Seismic record of glacial events affecting the Pacific margin of the northwestern Antarctic Peninsula. *Geology and seismic stratigraphy of the Antarctic margin* 68, 75-95.
- Bauch, H.A., Erlenkeuser, H., Grootes, P.M., Jouzel, J., 1996. Implications of Stratigraphic and Paleoclimatic Records of the Last Interglaciation from the Nordic Seas. *Quaternary Research* 46, 260-269.
- Belt, S.T., Massé, G., Vare, L.L., Rowland, S.J., Poulin, M., Sicre, M.-A., Sampei, M., Fortier, L., 2008. Distinctive  $^{13}\text{C}$  isotopic signature distinguishes a novel sea ice biomarker in Arctic sediments and sediment traps. *Marine Chemistry* 112, 158-167.
- Belt, S.T., Müller, J., 2013. The Arctic sea ice biomarker IP25: a review of current understanding, recommendations for future research and applications in palaeo sea ice reconstructions. *Quaternary Science Reviews* 79, 9-25.
- Berger, A., Loutre, M., 2002. An exceptionally long interglacial ahead? *Science* 297, 1287.
- Bergsten, H., 1994. Recent benthic foraminifera of a transect from the North Pole to the Yermak Plateau, eastern central Arctic Ocean. *Marine Geology* 119, 251-267.
- Birgel, D., Hass, H.C., 2004. Oceanic and atmospheric variations during the last deglaciation in the Fram Strait (Arctic Ocean): a coupled high-resolution organic-geochemical and sedimentological study. *Quaternary Science Reviews* 23, 29-47.
- Bischof, J., Koch, J., Kubisch, M., Spielhagen, R.F., Thiede, J., 1990. Nordic Seas surface ice drift reconstructions: evidence from ice rafted coal fragments during oxygen isotope stage 6. *Geological Society, London, Special Publications* 53, 235-251.
- Blott, S.J., Pye, K., 2001. GRADISTAT: a grain size distribution and statistics package for the analysis of unconsolidated sediments. *Earth surface processes and Landforms* 26, 1237-1248.
- Bourget, J., Zaragosi, S., Ellouz-Zimmermann, S., Ducassou, E., Prins, M., Garlan, T., Lanfume, V., Schneider, J.-L., Rouillard, P., Giraudeau, J., 2010. Highstand vs. lowstand turbidite system growth in the Makran active margin: Imprints of high-frequency external controls on sediment delivery mechanisms to deep water systems. *Marine Geology* 274, 187-208.
- Bourke, R.H., Weigel, A.M., Paquette, R.G., 1988. The Westward Turning Branch of the West Spitsbergen Current. *J. Geophys. Res.* 93, 14065-14077.
- Bradley, R.S., 2015. Chapter 6 - Marine Sediments, in: Bradley, R.S. (Ed.), *Paleoclimatology (Third Edition)*. Academic Press, San Diego, pp. 195-277.

- Broecker, W., Clark, E., 2001. An evaluation of Lohmann's foraminifera weight dissolution index. *Paleoceanography* 16, 531-534.
- Caralp, M., 1989. Abundance of *Bulimina exilis* and *Melonis barleeanum*: Relationship to the quality of marine organic matter. *Geo-Marine Letters* 9, 37-43.
- Carstens, J., Hebbeln, D., Wefer, G., 1997. Distribution of planktic foraminifera at the ice margin in the Arctic (Fram Strait). *Marine Micropaleontology* 29, 257-269.
- Corliss, B.H., Emerson, S., 1990. Distribution of Rose Bengal stained deep-sea benthic foraminifera from the Nova Scotian continental margin and Gulf of Maine. *Deep Sea Research Part A. Oceanographic Research Papers* 37, 381-400.
- Corliss, B.H., 1991. Morphology and microhabitat preferences of benthic foraminifera from the northwest Atlantic Ocean. *Marine Micropaleontology* 17, 195-236.
- Dokken, T.M., Hald, M., 1996. Rapid climatic shifts during isotope stages 2–4 in the Polar North Atlantic. *Geology* 24, 599-602.
- Dowdeswell, J., Jakobsson, M., Hogan, K., O'Regan, M., Backman, J., Evans, J., Hell, B., Löwemark, L., Marcussen, C., Noormets, R., 2010. High-resolution geophysical observations of the Yermak Plateau and northern Svalbard margin: implications for ice-sheet grounding and deep-keeled icebergs. *Quaternary Science Reviews* 29, 3518-3531.
- Duplessy, J.-C., Moyes, J., Pujol, C., 1980. Deep water formation in the North Atlantic Ocean during the last ice age. *Nature* 286, 479-482.
- Dylmer, C., Giraudeau, J., Eynaud, F., Husum, K., Vernal, A.D., 2013. Northward advection of Atlantic water in the eastern Nordic Seas over the last 3000 yr. *Climate of the Past* 9, 1505-1518.
- Espitalié J., Laporte J. L., Madec M., Marquis F., Leplat, P., Paulet J. and Boutefeu A., 1977. Méthode rapide de caractérisation des roches meres, de leur potential pétrolier et de leur degré d'évolution. *Revue de l'Institut Français du Pétrole* 32, 23-42.
- Eiken, O., 1992. An outline of the northwestern Svalbard continental margin, in: Vorren, T.O., Bergsager E., Dahl-Stamnes Ø.A., et al. (Ed.), *Arctic Petroleum Potential*, NPF Special Publication 2. Elsevier, Amsterdam, pp. 619-629.
- Fairbanks, R.G., Mortlock, R.A., Chiu, T.-C., Cao, L., Kaplan, A., Guilderson, T.P., Fairbanks, T.W., Bloom, A.L., Grootes, P.M., Nadeau, M.-J., 2005. Radiocarbon calibration curve spanning 0 to 50,000 years BP based on paired  $^{230}\text{Th}/^{234}\text{U}/^{238}\text{U}$  and  $^{14}\text{C}$  dates on pristine corals. *Quaternary Science Reviews* 24, 1781-1796.
- Flemming, B., 1982. Sediment mixing: its natural occurrence and textural expression, 11th International Congress on Sedimentology, Hamilton, pp. 22-27.
- Folk, R.L., Ward, W.C., 1957. Brazos River bar: a study in the significance of grain size parameters. *Journal of Sedimentary Research* 27, 3-26.
- Forwick, M., Vorren, T.O., 2009. Late Weichselian and Holocene sedimentary environments and ice rafting in Isfjorden, Spitsbergen. *Palaeogeography, Palaeoclimatology, Palaeoecology* 280, 258-274.
- Fronval, T., Jansen, E., 1997. Eemian and Early Weichselian (140–60 ka) Paleoceanography and paleoclimate in the Nordic Seas with comparisons to Holocene conditions. *Paleoceanography* 12, 443-462.

- Gascard, J.-C., Richez, C., Rouault, C., 1995. New Insights on Large-Scale Oceanography in Fram Strait: The West Spitsbergen Current, in: Walker O. Smith, J., Grebmeier, J.M. (Eds.), *Arctic Oceanography: Marginal Ice Zones and Continental Shelves*. American Geophysical Union, Washington, DC, p. 131.
- Gascard, J.C., Kergomard, C., Jeannin, P.F., Fily, M., 1988. Diagnostic study of the Fram Strait marginal ice zone during summer from 1983 and 1984 Marginal Ice Zone Experiment Lagrangian observations. *Journal of Geophysical Research: Oceans (1978–2012)* 93, 3613-3641.
- Geissler, W.H., Jokat, W., 2004. A geophysical study of the northern Svalbard continental margin. *Geophysical Journal International* 158, 50-66.
- Geissler, W.H., Jokat, W., Brekke, H., 2011. The Yermak Plateau in the Arctic Ocean in the light of reflection seismic data—implication for its tectonic and sedimentary evolution. *Geophysical Journal International* 187, 1334-1362.
- Green, K.E., 1960. Ecology of some Arctic foraminifera. *Micropaleontology* 6, 57-78.
- Guest, P.S., Davidson, K.L., Overland, J.E., Frederickson, P.A., 1995. Atmospheric-Ocean Interactions in the Marginal Ice Zones of the Nordic Seas, in: Walker O. Smith, J., M. Grebmeier, J. (Eds.), *Arctic Oceanography: Marginal Ice Zones and Continental Shelves*. American Geophysical Union, Washington DC, p. 51.
- Haake, F.-W., Pflaumann, U.W.E., 1989. Late Pleistocene foraminiferal stratigraphy on the Vøring Plateau, Norwegian Sea. *Boreas* 18, 343-356.
- Hald, M., Steinsund, P.I., 1992. Distribution of surface sediment benthic foraminifera in the southwestern Barents Sea. *The Journal of Foraminiferal Research* 22, 347-362.
- Hald, M., Steinsund, P., 1996. Benthic foraminifera and carbonate dissolution in the surface sediments of the Barents and Kara Seas, in: Stein, R., Ivanov, G., Levitan, M., Fahl, K. (Eds.), *Surface-sediment composition and sedimentary processes in the central Arctic Ocean and along the Eurasian Continental Margin*, *Berichte zur Polarforschung* 212, 285-307.
- Hald, M., Korsun, S., 1997. Distribution of modern benthic foraminifera from fjords of Svalbard, European Arctic. *The Journal of Foraminiferal Research* 27, 101-122.
- Hald, M., Dokken, T., Mikalsen, G., 2001. Abrupt climatic change during the last interglacial–glacial cycle in the polar North Atlantic. *Marine Geology* 176, 121-137.
- Hald, M., Ebbesen, H., Forwick, M., Godtlielsen, F., Khomenko, L., Korsun, S., Ringstad Olsen, L., Vorren, T.O., 2004. Holocene paleoceanography and glacial history of the West Spitsbergen area, Euro-Arctic margin. *Quaternary Science Reviews* 23, 2075-2088.
- Hansbo, S., 1957. A new approach to the determination of the shear strength of clay by the fall-cone test. *Royal Swedish Geotechnical Institute Proceedings* 14, p. 47.
- Hebbeln, D., Dokken, T., Andersen, E.S., Hald, M., Elverhoi, A., 1994. Moisture supply for northern ice-sheet growth during the Last Glacial Maximum. *Nature* 370, 357-360.
- Hebbeln, D., Wefer, G., 1997. Late Quaternary Paleoceanography in the Fram Strait. *Paleoceanography* 12, 65-78.
- Hebbeln, D., Henrich, R., Baumann, K.H., 1998. Paleoceanography of the last interglacial/glacial cycle in the Polar North Atlantic. *Quaternary Science Reviews* 17, 125-153.

- Heinz, P., Kitazato, H., Schmiedl, G., Hemleben, C., 2001. Response of deep-sea benthic foraminifera from the Mediterranean Sea to simulated phytoplankton pulses under laboratory conditions. *The Journal of Foraminiferal Research* 31, 210-227.
- Hevrøy, K., Lavik, G., Jansen, E., 1996. QUATERNARY PALEOCEANOGRAPHY AND PALEOCLIMATOLOGY OF THE FRAM STRAIT/YERMAK PLATEAU REGION: EVIDENCE FROM SITES 909 AND 912, in: Thiede, J., Myhre, A. M., Firth, J. V., Johnson, G. L., Ruddiman, W.F. (Eds.), *Proceedings of the Ocean Drilling Program, Scientific Results* 151, 469-482.
- Hjelle, A., Lauritzen, Ø., 1982. Geological Map of Svalbard 1: 500000 Sheet 3G, Spitsbergen northern part. Norsk Polarinstitutt, Oslo.
- Howe, J.A., Shimmield, T.M., Harland, R.E.X., Eyles, N., 2008. Late Quaternary contourites and glaciomarine sedimentation in the Fram Strait. *Sedimentology* 55, 179-200.
- Hull, D.M., Osterman, L.E., Thiede, J., 1993. BIOSTRATIGRAPHIC SYNTHESIS OF LEG 151, NORTH ATLANTIC-ARCTIC GATEWAYS, in: Thiede, J., Myhre, A. M., Firth, J. V., Johnson, G. L., Ruddiman, W.F. (Eds.), *Proceedings of the Ocean Drilling Program, Scientific Results* 151, 627-644.
- Husum, K., Hald, M., 2004. Modern foraminiferal distribution in the subarctic Malangen fjord and adjoining shelf, northern Norway. *The Journal of Foraminiferal Research* 34, 34-48.
- IPCC, 2014. Summary for Policymakers, in: Field, C.B., Barros, V.R., Dokken, D.J., Mach, K.J., Mastrandrea, M.D., Bilir, T.E., Chatterjee, M., Ebi, K.L., Estrada, Y.O., Genova, R.C., Girma, B., Kissel, E.S., Levy, A.N., MacCracken, S., Mastrandrea, P.R., White, L.L. (Eds.), *Climate Change 2014: Impacts, Adaptation, and Vulnerability. Part A: Global and Sectoral Aspects. Contribution of Working Group II to the Fifth Assessment Report of the Intergovernmental Panel on Climate Change*. Cambridge University Press, Cambridge, United Kingdom, and New York, NY, USA, pp. 1-32.
- Ivanova, E., 2009. The global thermohaline paleocirculation. Springer Science & Business Media, pp. 314.
- Jacobs, Z., 2008. Luminescence chronologies for coastal and marine sediments. *Boreas* 37, 508-535.
- Jakobsson, M., Backman, J., Murray, A., Løvlie, R., 2003. Optically Stimulated Luminescence dating supports central Arctic Ocean cm-scale sedimentation rates. *Geochemistry, Geophysics, Geosystems* 4, doi: 10.1029/2002GC000423.
- Jakobsson, M., Mayer, L., Coakley, B., Dowdeswell, J. A., Forbes, S., Fridman, B., Hodnesdal, H., Noormets, R., Pedersen, R., Rebesco, M., Schenke, H. W., Zarayskaya, Y., Accettella, D., Armstrong, A., Anderson, R. M., Bienhoff, P., Camerlenghi, A., Church, I., Edwards, M., Gardner, J. V., Hall, J. K., Hell, B., Hestvik, O., Kristoffersen, Y., Marcussen, C., Mohammad, R., Mosher, D., Nghiem, S. V., Pedrosa, M. T., Travaglini, P. G., Weatherall, P., 2012. The International Bathymetric Chart of the Arctic Ocean (IBCAO) Version 3.0. *Geophysical Research Letters* 39, L12609.
- Jennings, A.E., Helgadottir, G., 1994. Foraminiferal assemblages from the fjords and shelf of eastern Greenland. *The Journal of Foraminiferal Research* 24, 123-144.
- Jennings, A.E., Weiner, N.J., Helgadottir, G., Andrews, J.T., 2004. Modern foraminiferal faunas of the southwestern to northern Iceland shelf: oceanographic and environmental controls. *The Journal of Foraminiferal Research* 34, 180-207.

- Jessen, S.P., Rasmussen, T.L., Nielsen, T., Solheim, A., 2010. A new Late Weichselian and Holocene marine chronology for the western Svalbard slope 30,000–0 cal years BP. *Quaternary Science Reviews* 29, 1301-1312.
- Johannessen, O.M., 1986. Brief overview of the physical oceanography, in: B.G.Hurdle (Ed.), *The Nordic Seas*. Springer, New York, pp. 103-127.
- Jones, R.W., 2014. *Foraminifera and their Applications*. Cambridge University Press, pp. 391
- Juggins, S., 2007. C2 Version 1.5 User guide. Software for ecological and palaeoecological data analysis and visualisation. Newcastle University, Newcastle upon Tyne, UK 73.
- Knies, J., Stein, R., 1998. New aspects of organic carbon deposition and its paleoceanographic implications along the Northern Barents Sea Margin during the last 30,000 years. *Paleoceanography* 13, 384-394.
- Knies, J., Vogt, C., Stein, R., 1999. Late Quaternary growth and decay of the Svalbard/Barents Sea ice sheet and paleoceanographic evolution in the adjacent Arctic Ocean. *Geo-Marine Letters* 18, 195-202.
- Koç, N., Klitgaard-Kristensen, D., Hasle, K., Forsberg, C.F., Solheim, A., 2002. Late glacial paleoceanography of Hinlopen Strait, northern Svalbard. *Polar Research* 21, 307-314.
- Korsun, S., Polyak, L., 1989. Distribution of benthic foraminiferal morphogroups in the Barents Sea. *Oceanology* 29, 838-844.
- Korsun, S., Hald, M., 1998. Modern Benthic Foraminifera off Novaya Zemlya Tidewater Glaciers, Russian Arctic. *Arctic and Alpine Research* 30, 61-77.
- Korsun, S., Hald, M., 2000. Seasonal dynamics of benthic foraminifera in a glacially fed fjord of Svalbard, European Arctic. *The Journal of Foraminiferal Research* 30, 251-271.
- Kortekaas, M., Murray, A., Sandgren, P., Björck, S., 2007. OSL chronology for a sediment core from the southern Baltic Sea: A continuous sedimentation record since deglaciation. *Quaternary Geochronology* 2, 95-101.
- Kuijpers, A., Troelstra, S., Prins, M., Linthout, K., Akhmetzhanov, A., Bouryak, S., Bachmann, M., Lassen, S., Rasmussen, S., Jensen, J., 2003. Late Quaternary sedimentary processes and ocean circulation changes at the Southeast Greenland margin. *Marine Geology* 195, 109-129.
- Lea, D.W., Pak, D.K., Spero, H.J., 2000. Climate impact of late Quaternary equatorial Pacific sea surface temperature variations. *Science* 289, 1719-1724.
- Linke, P., Lutze, G.F., 1993. Microhabitat preferences of benthic foraminifera—a static concept or a dynamic adaptation to optimize food acquisition? *Marine Micropaleontology* 20, 215-234.
- Lohmann, G., 1995. A model for variation in the chemistry of planktonic foraminifera due to secondary calcification and selective dissolution. *Paleoceanography* 10, 445-457.
- Lubinski, D.J., Polyak, L., Forman, S.L., 2001. Freshwater and Atlantic water inflows to the deep northern Barents and Kara seas since ca 13 <sup>14</sup>C ka: foraminifera and stable isotopes. *Quaternary Science Reviews* 20, 1851-1879.
- Mackensen, A., Sejrup, H.P., Jansen, E., 1985. The distribution of living benthic foraminifera on the continental slope and rise off southwest Norway. *Marine Micropaleontology* 9, 275-306.

- Mackensen, A., Hald, M., 1988. *Cassidulina teretis* Tappan and *C. laevigata* d'Orbigny; their modern and late Quaternary distribution in northern seas. *The Journal of Foraminiferal Research* 18, 16-24.
- Mangerud, J., Bondevik, S., Gulliksen, S., Karin Hufthammer, A., Høisæter, T., 2006. Marine  $^{14}\text{C}$  reservoir ages for 19th century whales and molluscs from the North Atlantic. *Quaternary Science Reviews* 25, 3228-3245.
- McCarroll, D., 2015. 'Study the past, if you would divine the future': a retrospective on measuring and understanding Quaternary climate change. *Journal of Quaternary Science* 30, 154-187.
- McCave, I., Manighetti, B., Robinson, S., 1996. Sortable silt and fine sediment size/composition slicing: parameters for palaeocurrent speed and palaeoceanography. *Oceanographic Literature Review* 1, 45.
- McMillan, M., Shepherd, A., Gourmelen, N., Dehecq, A., Leeson, A., Ridout, A., Flament, T., Hogg, A., Gilbert, L., Benham, T., van den Broeke, M., Dowdeswell, J.A., Fettweis, X., Noël, B., Strozzi, T., 2014. Rapid dynamic activation of a marine-based Arctic ice cap. *Geophysical Research Letters* 41, 2014GL062255.
- Miller, G.H., Alley, R.B., Brigham-Grette, J., Fitzpatrick, J.J., Polyak, L., Serreze, M.C., White, J.W.C., 2010. Arctic amplification: can the past constrain the future? *Quaternary Science Reviews* 29, 1779-1790.
- Miller, G.H., Brigham-Grette, J., Alley, R.B., Anderson, L., Bauch, H.A., Douglas, M.S.V., Edwards, M.E., Elias, S.A., Finney, B.P., Fitzpatrick, J.J., Funder, S.V., Geirsdóttir, A., Herbert, T.D., Hinzman, L.D., Kaufman, D.S., MacDonald, G.M., Polyak, L., Robock, A., Serreze, M.C., Smol, J.P., Spielhagen, R., White, J.W.C., Wolfe, A.P., Wolff, E.W., 2013. PALEOCLIMATE-Paleoclimate History of the Arctic, in: Mock, S.A.E.J. (Ed.), *Encyclopedia of Quaternary Science (Second Edition)*. Elsevier, Amsterdam, pp. 113-125.
- Mudie, P.J., Keen, C.E., Hardy, I.A., Vilks, G., 1984. Multivariate analysis and quantitative paleoecology of benthic foraminifera in surface and Late Quaternary shelf sediments, northern Canada. *Marine Micropaleontology* 8, 283-313.
- Müller, J., Massé, G., Stein, R., Belt, S.T., 2009. Variability of sea-ice conditions in the Fram Strait over the past 30,000 years. *Nature geoscience* 2, 772-776.
- Murray, J.W., 2006. *Ecology and applications of Benthic foraminifera*. Cambridge University Press, Cambridge, p. 426.
- Noormets, R., Dowdeswell, J.A., Jakobsson, M., O'Cofaigh, C., 2010. New evidence on past ice flow and iceberg activity on the southern Yermak Plateau, 2010 Fall Meeting, AGU, San Francisco, Calif.
- Noormets, R., Hogan, K., Austin, W., Chauhan, T., Roy, S., Rasmussen, T., Dowdeswell, J., 2012. Submarine glacial landform assemblages on the outer continental shelf north of Nordaustlandet, Svalbard, The 6th Arctic Paleoclimate and Its Extremes (APEX) Meeting. Oulu University, Oululanka Research Station, Finland, p. 70.
- Nørgaard-Pedersen, N., Spielhagen, R.F., Erlenkeuser, H., Grootes, P.M., Heinemeier, J., Knies, J., 2003. Arctic Ocean during the Last Glacial Maximum: Atlantic and polar domains of surface water mass distribution and ice cover. *Paleoceanography* 18, 1063.



- Nowaczyk, N.R., Frederichs, T.W., Eisenhauer, A., Gard, G., 1994. Magnetostratigraphic Data From Late Quaternary Sediments From the Yermak Plateau, Arctic Ocean: Evidence for four Geomagnetic Polarity Events Within the Last 170 Ka of the Brunhes Chron. *Geophysical Journal International* 117, 453-471.
- Onarheim, I.H., Smedsrud, L.H., Ingvaldsen, R.B., Nilsen, F., 2014. Loss of sea ice during winter north of Svalbard. *Tellus A* 66, 23933.
- Piper, D., Brisco, C., 1975. Deep-water continental-margin sedimentation, DSDP Leg 28, Antarctica, in: Hayes, D.E., L. A. Frakes et al. (Eds.), *Initial Reports of the Deep Sea Drilling Project*, Washington, pp. 727-755.
- Pithan, F., Mauritsen, T., 2014. Arctic amplification dominated by temperature feedbacks in contemporary climate models. *Nature Geosci* 7, 181-184.
- Polyak, L., Solheim, A., 1994. Late-and postglacial environments in the northern Barents Sea west of Franz Josef Land. *Polar Research* 13, 197-207.
- Polyak, L., Mikhailov, V., 1996. Post-glacial environments of the southeastern Barents Sea: foraminiferal evidence. *Geological Society, London, Special Publications* 111, 323-337.
- Polyak, L., Korsun, S., Febo, L.A., Stanovoy, V., Khusid, T., Hald, M., Paulsen, B.E., Lubinski, D.J., 2002. Benthic foraminiferal assemblages from the southern Kara Sea, a river-influenced Arctic marine environment. *The Journal of Foraminiferal Research* 32, 252-273.
- Poole, D. A. R., Dokken, T. M., Hald, M., Polyak, L., 1994. Stable isotope fractionation in recent benthic foraminifera from the Barents and Kara Seas (unpublished manuscript). In *Neogene and Quaternary Paleoenvironments on the North Norwegian Shelf*, Ph. D. Thesis, Department of Geology, University of Tromsø, Norway, pp 82.
- Rack, F.R., Finndin, R., Moran, K., 1996. ANALYSIS AND INTERPRETATION OF X-RAY IMAGES OF SEDIMENT CORES FROM HOLE 910D, YERMAK PLATEAU: PRELIMINARY RESULTS, in: Thiede, J., Myhre, A. M., Firth, J. V., Johnson, G. L., Ruddiman, W.F. (Eds.), *Proceedings of the Ocean Drilling Program, Scientific Results* 151, 377-388.
- Rasmussen, T.L., Thomsen, E., Labeyrie, L., van Weering, T.C.E., 1996a. Circulation changes in the Faeroe-Shetland Channel correlating with cold events during the last glacial period (58–10 ka). *Geology* 24, 937-940.
- Rasmussen, T.L., Thomsen, E., Van Weering, T.C.E., Labeyrie, L., 1996b. Rapid changes in surface and deep water conditions at the Faeroe Margin during the last 58,000 years. *Paleoceanography* 11, 757-771.
- Rasmussen, T.L., Balbon, E., Thomsen, E., Labeyrie, L., Van Weering, T.C.E., 1999. Climate records and changes in deep outflow from the Norwegian Sea~ 150–55 ka. *Terra Nova* 11, 61-66.
- Rasmussen, T.L., 2005. Systematic paleontology and ecology of benthic foraminifera from the Plio-Pleistocene Kallithea Bay section, Rhodes, Greece. *Cushman Foundation Special Publication* 39, 53-157.
- Rasmussen, T.L., Thomsen, E., 2005. Foraminifera and paleoenvironment of the Plio-Pleistocene Kallithea Bay section, Rhodes, Greece: Evidence for cyclic sedimentation and shallow-water sapropels. *Cushman Foundation for Foraminiferal Research, Special Publication* 39, 15-51.

- Rasmussen, T.L., Thomsen, E., Ślubowska, M.A., Jessen, S., Solheim, A., Koç, N., 2007. Paleooceanographic evolution of the SW Svalbard margin (76°N) since 20,000 14C yr BP. *Quaternary Research* 67, 100-114.
- Rasmussen, T.L., Thomsen, E., Nielsen, T., 2014a. Water mass exchange between the Nordic seas and the Arctic Ocean on millennial timescale during MIS 4–MIS 2. *Geochemistry, Geophysics, Geosystems* 15, 530-544.
- Rasmussen, T.L., Thomsen, E., Skirbekk, K., Ślubowska-Woldengen, M., Klitgaard Kristensen, D., Koç, N., 2014b. Spatial and temporal distribution of Holocene temperature maxima in the northern Nordic seas: interplay of Atlantic-, Arctic-and polar water masses. *Quaternary Science Reviews* 92, 280-291.
- Reigstad, M., Carroll, J., Slagstad, D., Ellingsen, I., Wassmann, P., 2011. Intra-regional comparison of productivity, carbon flux and ecosystem composition within the northern Barents Sea. *Progress in Oceanography* 90, 33-46.
- Reimer, P.J., Bard, E., Bayliss, A., Beck, J.W., Blackwell, P.G., Ramsey, C.B., Buck, C.E., Cheng, H., Edwards, R.L., Friedrich, M., Grootes, P.M., Guilderson, T.P., Haflidason, H., Hajdas, I., C, H., Heaton, T.J., Hoffmann, D.L., Hogg, A.G., Hughen, K.A., Kaiser, K.F., Kromer, B., Manning, S.W., M, N., Reimer, R.W., Richards, D.A., Scott, D.B., Southon, J.R., Staff, R.A., Turney, C.S.M., Plicht, J.v.d., 2013. IntCal13 and Marine13 radiocarbon age calibration curves 0–50,000 years cal BP. *Radiocarbon* 55, 1869-1887.
- Rhodes, E.J., 2011. Optically stimulated luminescence dating of sediments over the past 200,000 years. *Annual Review of Earth and Planetary Sciences* 39, 461-488.
- Risebrobakken, B., Moros, M., Ivanova, E.V., Chistyakova, N., Rosenberg, R., 2010. Climate and oceanographic variability in the SW Barents Sea during the Holocene. *The Holocene*, 1–13, doi: 10.1177/0959683609356586.
- Rudels, B., Anderson, L., Eriksson, P., Fahrbach, E., Jakobsson, M., Jones, E. P., Melling, H., Prinsenberg, S., Schauer, U., Yao, T., 2012. Observations in the ocean. *Arctic Climate Change*, Springer, p. 117–198.
- Rytter, F., Knudsen, K.L., Seidenkrantz, M.S., Eiríksson, J., 2002. Modern distribution of benthic foraminifera on the North Icelandic shelf and slope. *The Journal of Foraminiferal Research* 32, 217-244.
- Saher, M., Kristensen, D.K., Hald, M., Korsun, S., Jørgensen, L.L., 2009. Benthic foraminifera assemblages in the Central Barents Sea: an evaluation of the effect of combining live and total fauna studies in tracking environmental change. *Norwegian Journal of Geology* 89, 149-161.
- Seidenkrantz, M.-S., 1995. *Cassidulina teretis* Tappan and *Cassidulina neoteretis* new species (Foraminifera): stratigraphic markers for deep sea and outer shelf areas. *Journal of Micropalaeontology* 14, 145-157.
- Sejrup, H., Birks, H., Klitgaard Kristensen, D., Madsen, H., 2004. Benthonic foraminiferal distributions and quantitative transfer functions for the northwest European continental margin. *Marine Micropalaeontology* 53, 197-226.
- Sejrup, H.P., Fjaeran, T., Hald, M., Beck, L., Hagen, J., Miljeteig, I., Morvik, I., Norvik, O., 1981. Benthonic foraminifera in surface samples from the Norwegian continental margin between 62 degrees N and 65 degrees N. *The Journal of Foraminiferal Research* 11, 277-295.

- Simstich, J., Sarnthein, M., Erlenkeuser, H., 2003. Paired  $\delta^{18}\text{O}$  signals of *Neogloboquadrina pachyderma* (s) and *Turborotalita quinqueloba* show thermal stratification structure in Nordic Seas. *Marine Micropaleontology* 48, 107-125.
- Skirbekk, K., Kristensen, D.K., Rasmussen, T.L., Koç, N., Forwick, M., 2010. Holocene climate variations at the entrance to a warm Arctic fjord: evidence from Kongsfjorden trough, Svalbard. *Geological Society, London, Special Publications* 344, 289-304.
- Ślubowska-Woldengen, M., Rasmussen, T.L., Koç, N., Klitgaard-Kristensen, D., Nilsen, F., Solheim, A., 2007. Advection of Atlantic Water to the western and northern Svalbard shelf since 17,500 cal yr BP. *Quaternary Science Reviews* 26, 463-478.
- Ślubowska-Woldengen, M., Koc, N., Rasmussen, T.L., Klitgaard-Kristensen, D., Hald, M., Jennings, A.E., 2008. Time-slice reconstructions of ocean circulation changes on the continental shelf in the Nordic and Barents Seas during the last 16,000 cal yr BP. *Quaternary Science Reviews* 27, 1476-1492.
- Ślubowska, M.A., Koç, N., Rasmussen, T.L., Klitgaard-Kristensen, D., 2005. Changes in the flow of Atlantic water into the Arctic Ocean since the last deglaciation: evidence from the northern Svalbard continental margin, 80 N. *Paleoceanography* 20, PA4014.
- Spielhagen, R.F., Baumann, K.-H., Erlenkeuser, H., Nowaczyk, N.R., Nørgaard-Pedersen, N., Vogt, C., Weiel, D., 2004. Arctic Ocean deep-sea record of northern Eurasian ice sheet history. *Quaternary Science Reviews* 23, 1455-1483.
- Spielhagen, R.F., Erlenkeuser, H., Siegert, C., 2005. History of freshwater runoff across the Laptev Sea (Arctic) during the last deglaciation. *Global and Planetary Change* 48, 187-207.
- Steinsund, P.I., 1994. Benthic foraminifera in surface sediments of the Barents and Kara seas: Modern and late Quaternary applications, PhD Thesis, University of Tromsø, Tromsø, Norway, p. 111.
- Stuiver, M., Reimer, J., 1993. Extended  $^{14}\text{C}$  data base and revised CALIB 3.014 C age calibration program. *EDITORIAL COMMENT* 35, 215-230.
- Sugisaki, S., Buylaert, J.-P., Murray, A., Tsukamoto, S., Nogi, Y., Miura, H., Sakai, S., Iijima, K., Sakamoto, T., 2010. High resolution OSL dating back to MIS 5e in the central Sea of Okhotsk. *Quaternary Geochronology* 5, 293-298.
- Swift, J.H., 1986. The Arctic Waters, in: B.G. H. (Ed.), *The Nordic Seas*. Springer, New York, pp. 129-153.
- Thiede, J., Myhre, A.M., 1996. The palaeoceanographic history of the North Atlantic–Arctic gateways, in: Thiede, J., Myhre, A. M., Firth, J. V., Johnson, G. L., Ruddiman, W.F. (Eds.), *Proceedings of the Ocean Drilling Program, Scientific Results* 151, pp. 645-658.
- Thomas, E., Booth, L., Maslin, M., Shackleton, N., 1995. Northeastern Atlantic benthic foraminifera during the last 45,000 years: changes in productivity seen from the bottom up. *Paleoceanography* 10, 545-562.
- Van der Zwaan, G., Duijnste, I., Den Dulk, M., Ernst, S., Jannink, N., Kouwenhoven, T., 1999. Benthic foraminifers: proxies or problems?: a review of paleocological concepts. *Earth-Science Reviews* 46, 213-236.
- Vogt, C., Knies, J., Spielhagen, R.F., Stein, R., 2001. Detailed mineralogical evidence for two nearly identical glacial/deglacial cycles and Atlantic water advection to the Arctic Ocean during the last 90,000 years. *Global and Planetary Change* 31, 23-44.

- Vogt, P.R., Crane, K., Sundvor, E., 1994. Deep Pleistocene iceberg plowmarks on the Yermak Plateau: sidescan and 3.5 kHz evidence for thick calving ice fronts and a possible marine ice sheet in the Arctic Ocean. *Geology* 22, 403-406.
- Werner, K., Spielhagen, R.F., Bauch, D., Hass, H.C., Kandiano, E., 2013. Atlantic Water advection versus sea-ice advances in the eastern Fram Strait during the last 9 ka: Multiproxy evidence for a two-phase Holocene. *Paleoceanography* 28, 283-295.
- Wollenburg, J.E., Mackensen, A., 1998. Living benthic foraminifers from the central Arctic Ocean: faunal composition, standing stock and diversity. *Marine Micropaleontology* 34, 153-185.
- Wollenburg, J.E., Kuhnt, W., 2000. The response of benthic foraminifers to carbon flux and primary production in the Arctic Ocean. *Marine Micropaleontology* 40, 189-231.
- Wollenburg, J.E., Kuhnt, W., Mackensen, A., 2001. Changes in Arctic Ocean paleoproductivity and hydrography during the last 145 kyr: The benthic foraminiferal record. *Paleoceanography* 16, 65-77.
- Wollenburg, J.E., Knies, J., Mackensen, A., 2004. High-resolution paleoproductivity fluctuations during the past 24 kyr as indicated by benthic foraminifera in the marginal Arctic Ocean. *Palaeogeography, Palaeoclimatology, Palaeoecology* 204, 209-238.
- Wollenburg, J.E., Mackensen, A., Kuhnt, W., 2007. Benthic foraminiferal biodiversity response to a changing Arctic palaeoclimate in the last 24.000 years. *Palaeogeography, Palaeoclimatology, Palaeoecology* 255, 195-222.
- Yasuhara, M., Danovaro, R., 2014. Temperature impacts on deep-sea biodiversity. *Biological Reviews*, doi: 10.1111/brv.12169.

**SECTION II**  
**Research Papers**



T. Chauhan, T. L. Rasmussen, R. Noormets, M. Jakobsson, K. A. Hogan, 2014.  
**Glacial history and paleoceanography of the southern Yermak Plateau  
since 132 ka BP.**

*Quaternary Science Review*, 92, pp 155-169

[doi:10.1016/j.quascirev.2013.10.023](https://doi.org/10.1016/j.quascirev.2013.10.023)







# Glacial history and paleoceanography of the southern Yermak Plateau since 132 ka BP



T. Chauhan <sup>a,b,\*</sup>, T.L. Rasmussen <sup>b</sup>, R. Noormets <sup>a</sup>, M. Jakobsson <sup>c</sup>, K.A. Hogan <sup>d</sup>

<sup>a</sup> Department of Arctic Geology, The University Centre in Svalbard (UNIS), P.O. Box 156, N-9171 Longyearbyen, Svalbard, Norway

<sup>b</sup> Department of Geology, University of Tromsø, NO-9037 Tromsø, Norway

<sup>c</sup> Department of Geological Sciences, Stockholm University, 10691 Stockholm, Sweden

<sup>d</sup> Scott Polar Research Institute, University of Cambridge, Lensfield Road, Cambridge CB2 1ER, UK

## ARTICLE INFO

### Article history:

Received 15 February 2013

Received in revised form

3 October 2013

Accepted 20 October 2013

Available online 4 December 2013

### Keywords:

Yermak Plateau (YP)

Marginal Ice Zone (MIZ)

Planktic and benthic foraminifera

Stable isotopes

Ice-rafted debris (IRD)

Svalbard–Barents Sea Ice Sheet (SBIS)

## ABSTRACT

The southern Yermak Plateau (YP) is situated at the entrance to the Arctic Ocean in the narrow Marginal Ice Zone (MIZ) between the Polar and Arctic Fronts, north-west of Svalbard. A gravity core JM10-02GC has been analysed in order to reconstruct paleoceanographic conditions and the movement of the sea ice margin as well as the glacier ice conditions of the Svalbard–Barents Sea Ice Sheet (SBIS) during the Last Interglacial–Glacial cycle. The distribution of planktic and benthic foraminifera, planktic and benthic oxygen and carbon isotopes and variations in ice-rafted debris (IRD) has been investigated. The sediment core covers the time interval from the Marine Isotope Stage (MIS) 6/5e transition (Termination II, c. 132 ka BP) to the early Holocene. During Termination II (TII), the SBIS retreated and the sea ice margin was in distal position whereas during MIS 5 to MIS 4 the sea ice margin was close to the core site. Several core intervals interpreted as representing MIS 5e, MIS 5c, MIS 5a, MIS 3 and MIS 1 were barren of calcareous microfossils whereas the intervals representing MIS 4 and MIS 2 were characterised by high productivity (HP) of planktic and benthic foraminifera. These “glacial” HP zones were associated with the open water conditions resulting from the advection of Atlantic Water (AW) and retreat of the sea ice margin. The barren zones during MIS 5, MIS 3 and MIS 1 resulted from the proximity of the sea ice margin whereas during MIS 2 the likely cause was an advance of the SBIS.

© 2013 Elsevier Ltd. All rights reserved.

## 1. Introduction

At the northern latitudes, the interaction between the Polar and Atlantic Surface Waters determine the position of oceanographic fronts. A narrow strip of surface water is bordered by the Polar Front to the north and the Arctic Front to the south at the southern YP (Fig. 1). Perennially sea ice covered Polar Waters with temperature  $<0$  °C and salinity 30–34‰ occur north of the Polar Front whereas the sea ice free Atlantic Surface Waters with temperature 5–7 °C and salinity  $>35$ ‰ occur south of the Arctic Front. Between these fronts the Arctic Waters, which consist of mixed Atlantic and Polar Waters, show intermediate conditions with temperature of 0–4 °C and salinity between 34.6 and 34.9‰ (Johannessen, 1986; Swift, 1986). This zone of Arctic Surface Water also represents the

MIZ characterised with seasonal sea ice cover and high surface productivity (Guest et al., 1995).

The YP is located at the eastern margin of the Fram Strait which is the only deep water connection between the sub-polar seas and the Arctic Ocean. It forms the main topographic obstacle to the inflow of warm AW to the Arctic Ocean via the West Spitsbergen Current (WSC). In addition, the YP is located near the north-western Svalbard continental slope, which is an ideal position for recording changes in the extent of the SBIS. During glacial–interglacial cycles, large variations in the flow of surface water masses, the position of the Polar and Arctic Fronts, and the location of the MIZ occurred over southern YP. Therefore, the combined effect of climate change, sea ice cover, ice sheet extent and variations in ocean circulation are most likely captured in the sedimentary record in this area.

Previous studies from the area have focused mainly on planktic stable isotopes, abundance of planktic foraminifera and various sedimentological parameters such as the distribution of IRD from deep water sites (e.g. Knies et al., 2001; Vogt et al., 2001; Spielhagen et al., 2004). In this paper, a core from the southern YP is analysed for

\* Corresponding author. Department of Arctic Geology, The University Centre in Svalbard (UNIS), P.O. Box 156, N-9171 Longyearbyen, Svalbard, Norway. Tel.: +47 7902 3399; fax: +47 7902 3301.

E-mail addresses: [teena.chauhan@unis.no](mailto:teena.chauhan@unis.no), [chauhan2081@gmail.com](mailto:chauhan2081@gmail.com) (T. Chauhan).

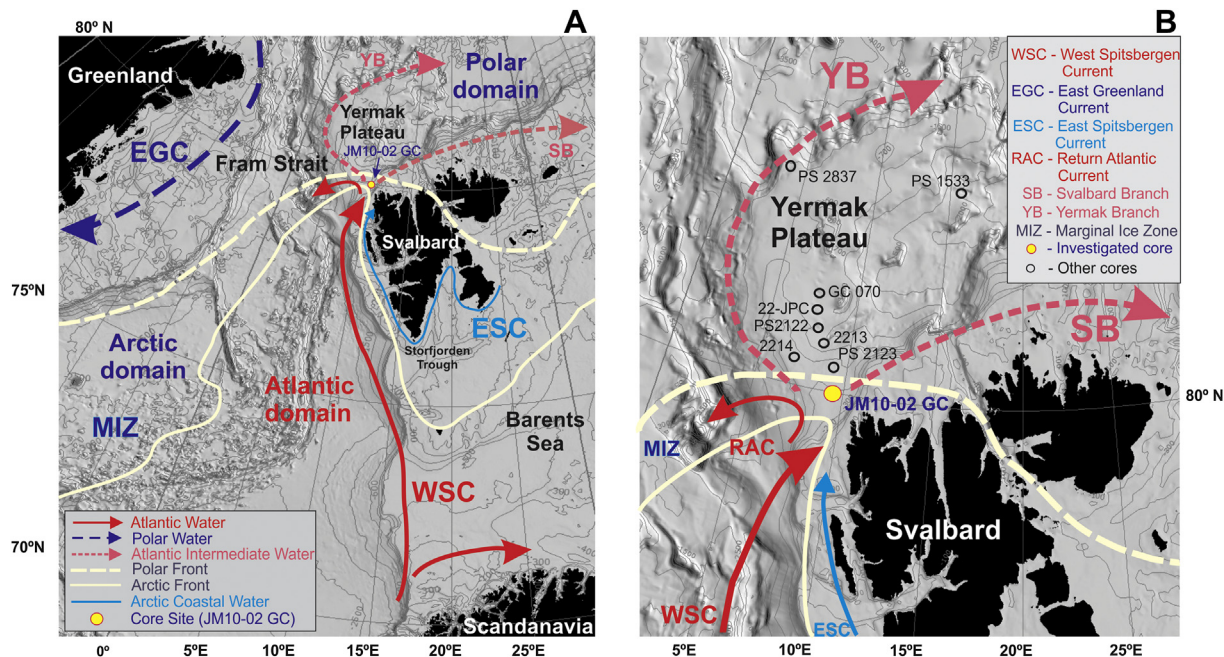


Fig. 1. Study Area. A. Location map of Fram Strait and Svalbard. B. Map of the Yermak Plateau showing positions of the core JM10-02GC (yellow circle) and the previously studied cores. Bathymetric contours are from the International Bathymetric Chart of the Arctic Ocean (IBCAO) v3 (Jakobsson et al., 2012).

the distribution patterns of planktic and benthic foraminifera, ice-rafted debris (IRD) and planktic and benthic stable isotopes. The investigation reveals paleoceanographic changes from the TII (MIS 6/5e) to the early Holocene. The core JM10-02GC was taken on the path of the AW where it impinges on the upper slope in a relatively shallow water depth (501 m). By analysing both benthic and planktic foraminifera and their stable isotope ratios the flow of AW over the sea bottom and at the subsurface has been reconstructed. This study provides the most detailed record of benthic foraminifera from the YP so far.

## 2. Material and methods

A 3.68 m long gravity core JM10-02GC was retrieved from a water depth of 501 m on the southern YP (80°03' N 9°50' E) on R/V Jan Mayen in 2010 (Fig. 1B). The top 10 cm of the core was somewhat disturbed. Lithology, magnetic susceptibility and shear strength were logged at 1 cm intervals. A Bartington MS2 with surface scanning point sensor was used to measure the magnetic susceptibility. The shear strength was measured by fall cone test (Hansbo, 1957).

81 sediment samples were taken at 5 cm intervals. For each sample a 1 cm thick slice was extracted for micro-paleontological studies. The samples were weighed and dried in an oven at 40 °C. They were subsequently wet sieved through stacked sieves of 63 μm, 100 μm and 1 mm mesh sizes. The dried residues were weighed and the weight % of each grain size fraction was calculated. From the >100 μm size fraction samples, up to 300 planktic and 300 benthic foraminiferal specimens were picked. Intervals that were barren of foraminifera and samples with less than 50 specimens are described as barren intervals in the text. Of the total picked planktic foraminifera the number of *Neogloboquadrina pachyderma* sinistral (s) species was counted and its relative abundance was calculated. All picked benthic foraminifera were identified to species level. The concentrations of planktic and benthic foraminifera were calculated as number of foraminifera per gram dry weight sediment (no./g).

Fluxes of planktic and benthic specimens (no./cm<sup>2</sup>/ka) were calculated using the formula:

$$\text{no./g} \times \text{Mass Accumulation Rate (MAR)}$$

where, MAR = Linear Sedimentation Rate (LSR) (cm/ka) × Dry Bulk Density (DBD) (g/cm<sup>3</sup>).

Eight samples were dated by Accelerator Mass Spectrometry (AMS-<sup>14</sup>C) at the Ångström Radiocarbon Laboratory, Uppsala, Sweden and at the <sup>14</sup>CHRONO Centre for Climate, Environment and Chronology, Belfast, UK. A reservoir correction of 440 ± 52 years (Mangerud et al., 2006) was applied to seven samples and six of the corrected ages were calibrated to calendar years using the Fairbanks calibration curve (Fairbanks et al., 2005). The lowermost sample dated at 270 cm core-depth gave an infinite age (>48 <sup>14</sup>C ka BP). In the following text, all calibrated ages are referred to as 'ka BP' and uncalibrated radiocarbon ages as '<sup>14</sup>C ka BP'. With the exception of the age of the topmost sample, which was from mixed planktic species, all the ages were obtained from monospecific samples of *N. pachyderma* s (Table 1).

Square shaped four chambered specimens of *N. pachyderma* s and the benthic species *Cassidulina neoteretis*, *Islandiella norcrossi*, *Melonis barleeanus* and *Cibicides lobatulus* were selected for stable oxygen and carbon isotope analyses (Fig. 2c, d, e). The four different benthic species were selected based on their good preservation and relatively large number of tests in the samples. Carbon isotope values of the epibenthic species *C. lobatulus* are a proxy for water mass ventilation (Duplessy et al., 1988). *C. lobatulus* and *M. barleeanus* were corrected for isotopic disequilibrium by +0.64 and +0.4‰, respectively (Duplessy et al., 1980). The other two benthic species were not corrected. Analyses were performed at the Stable Isotope Laboratory, Stockholm University, Sweden.

For IRD, the >100 μm fraction was dry sieved using stacked 150 μm and 500 μm sieves; 200–250 mineral grains were counted and the concentration of IRD (no. IRD/g) was calculated for each size fraction adding the counts of the >1 mm size grains. These three size fractions of IRD are categorised as coarse IRD (>1 mm),

**Table 1**  
AMS <sup>14</sup>C dates and sedimentation rates for the core JM10-02GC and the nearby core PS2123 (Vogt et al., 2001).

JM10-02GC (this study)					PS2123		
Depth (cm)	Material used	Radiocarbon <sup>14</sup> C age	Calibrated age (ka)	Sedimentation rate (cm/ka)	Depth (cm)	Age (ka)	Sedimentation (ka) rate (cm/ka)
50	Mixed Foraminifers	12,941 ± 91	14,470 ± 260	3.47	170	12.00	14.33
65	<i>N. pachyderma</i> s	15,054 ± 62	17,347 ± 255	5.17	268	23.29	8.57
115	<i>N. pachyderma</i> s	18,514 ± 95	21,481 ± 244	12.10	404	58.73	3.82
120	<i>N. pachyderma</i> s	18,891 ± 77	22,058 ± 174	8.33	488	73.45	5.88
157	<i>N. pachyderma</i> s	21,817 ± 111	25,646 ± 256	10.27	628	122.00	2.73
160	<i>N. pachyderma</i> s	23,353 ± 123	27,509 ± 241	1.57			
225	<i>N. pachyderma</i> s	46,567 ± 2091	–	3.17			
270	<i>N. pachyderma</i> s	>48,874	–	1.74			
368	Not dated		~132 <sup>a</sup>	1.74			

<sup>a</sup> The basal age (~132 ka BP) at 368 cm core-depth is based on oxygen isotope and magnetic susceptibility correlation of the core PS1533 (Nowaczyk et al., 1994; Spielhagen et al., 2004) from northern YP and the nearby core PS2123 (Vogt et al., 2001) with the core JM10-02GC (this study) (Figs. 3 and 4).

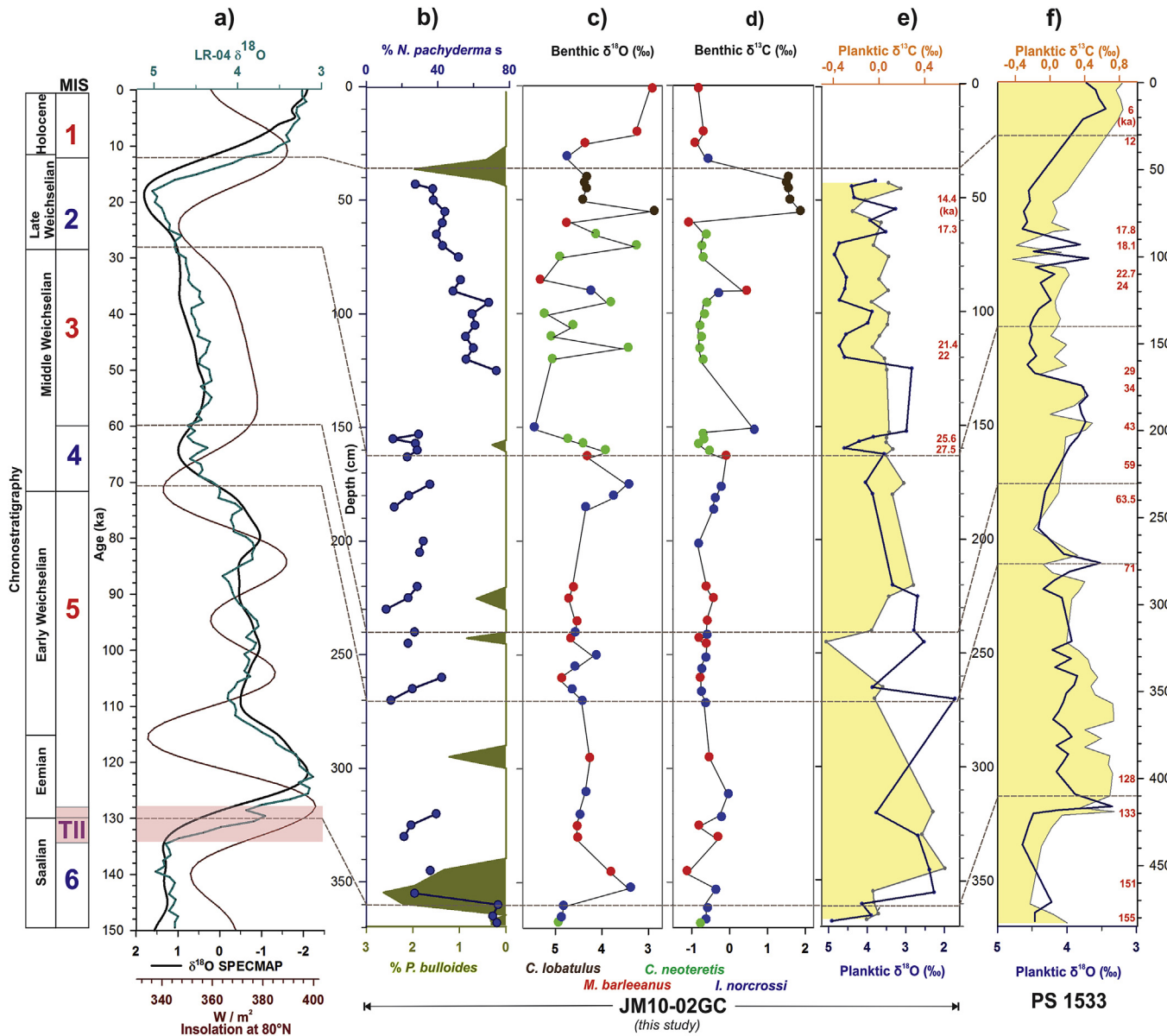


**Fig. 2.** Correlation of stable isotope records. (a) Correlation of global  $\delta^{18}\text{O}$  isotope curves of SPECMAP (Martinson et al., 1987) and LR-04 benthic stack (Lisiecki and Raymo, 2005). Insolation at  $80^\circ\text{N}$  is according to Berger (1978); (b) Occurrence of benthic species *P. bulloides* (%) (green shade) is used to identify MIS 5e and MIS 5a. The concentration of planktic species *N. pachyderma* s (%) (blue dots) shows gaps in the record due to barren sections; (c)  $\delta^{18}\text{O}$  and (d)  $\delta^{13}\text{C}$  isotope records of benthic foraminifera based on four benthic species; (e)  $\delta^{18}\text{O}$  (blue line) and  $\delta^{13}\text{C}$  (yellow shade) isotope records of planktic foraminifera; (f) planktic  $\delta^{18}\text{O}$  (blue line) and  $\delta^{13}\text{C}$  (yellow shade) record of the core PS1533 according to Nowaczyk et al. (1994); Spielhagen et al. (2004). The numbers in red along the right side of panels (e) and (f) are ages in ka. The boundaries of different MIS are marked on the basis of age model by Martinson et al. (1987) and AMS-<sup>14</sup>C dates obtained in this study. The location of the cores is shown in Fig. 1B.



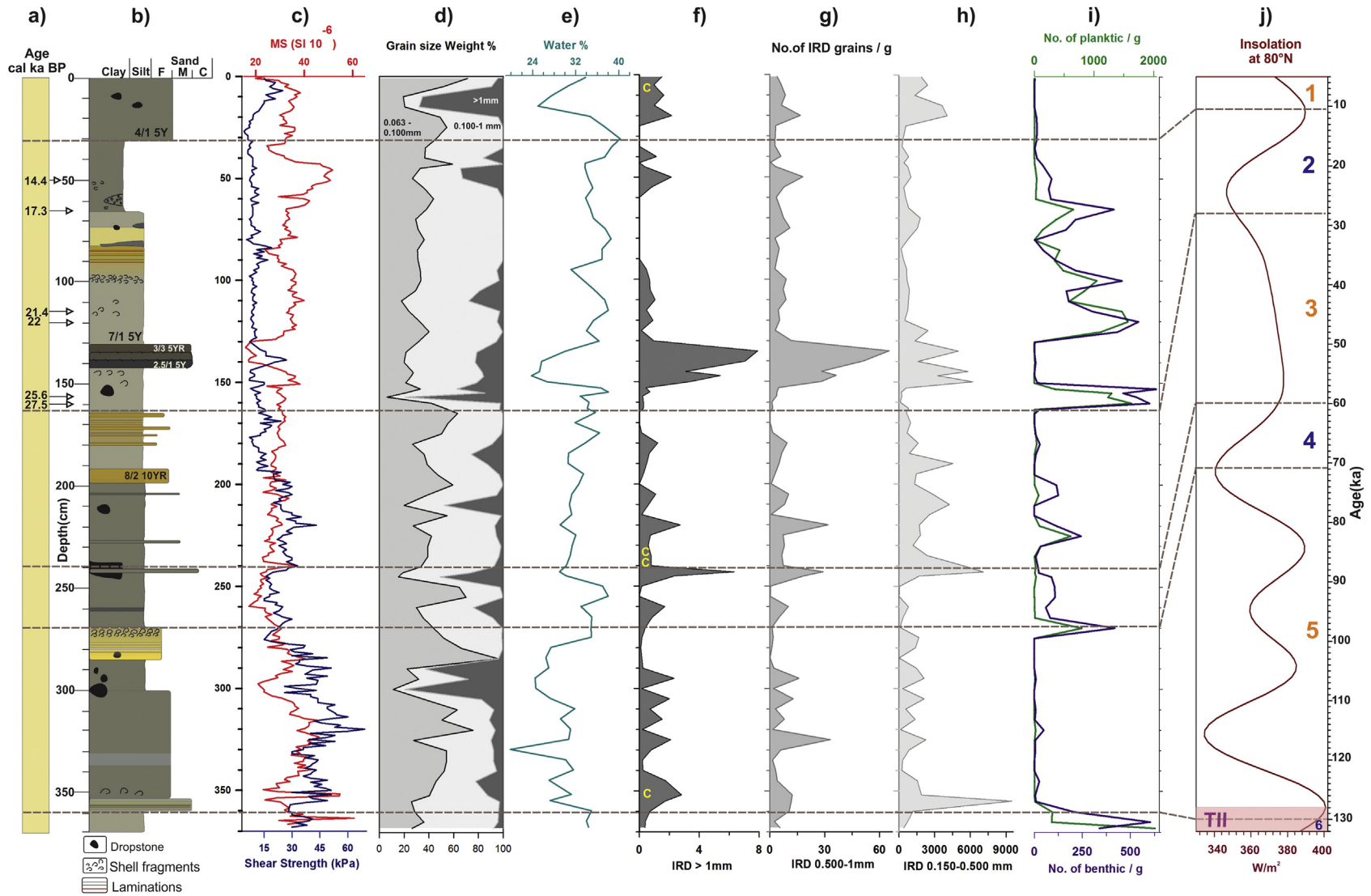


**Fig. 3.** JM10-02GC logs: (a) Calibrated <sup>14</sup>C age in ka; (b) Lithology; (c) Magnetic susceptibility (red) and Shear strength (blue); (d) Grain size distribution; (e) Water content; (f), (g) and (h) amount of IRD in different fractions, 'C' indicates coal fragments; (i) Concentration of planktic (green) and benthic foraminifera (purple); (j) Insolation curve at 80°N (Berger, 1978). Numbers in orange and blue colour show Marine Isotope Stages (MIS). TII marks the Termination II.

medium IRD (0.500–1 mm) and fine IRD (0.150–0.500 mm), respectively (Fig. 3f, g, h).

### 3. Oceanographic setting and distribution of foraminifera

#### 3.1. Modern settings

The present day hydrography at the southern YP is characterised by warm and saline AW of the WSC that flows northward and eastwards along the western and northern Svalbard margin respectively (Rudels et al., 2011) (Fig. 1). Cold Polar Surface Water of the East Greenland Current (EGC) flows southward along the eastern Greenland continental margin (Fig. 1). The west coast of Svalbard is also affected by the coastal current, the East Spitsbergen Current (ESC), which flows southward from the Arctic Ocean via the NW Barents Sea into the Fram Strait (Johannessen, 1986) (Fig. 1). Around 80°N, water masses shallower than 500 m deflect eastwards and flow along the northern shelf of Svalbard (Svalbard Branch), whereas the deep water mass below 500 m depth follows the continental slope and flows north up to 81°N (Yermak Branch) and then east around the north-western tip of the YP (Fig. 1). A third branch turns counter-clockwise towards the west and submerges beneath the colder sea ice covered Polar Water of the EGC and continues southward as Atlantic Intermediate Water called the Return Atlantic Current (RAC). The bottom currents over the YP are weak and variable and it generally flows parallel to the sea ice margin. Due to the presence of the sea ice margin part of the current deflects to the east where it joins the Svalbard Branch (Bourke et al., 1988).

According to Ślubowska-Woldengen et al. (2007), the present day water masses from north-west Svalbard consist of Polar Water ( $T = 6.4\text{ }^{\circ}\text{C}$  and  $S = 34.4\text{ PSU}$ ) and Arctic Surface Water ( $T = 7.1\text{ }^{\circ}\text{C}$ ,  $S = 34.9\text{ PSU}$ ) in the upper layers followed by AW ( $T = 7.3\text{ }^{\circ}\text{C}$  and  $S = 35.2\text{ PSU}$ ) in the intermediate layer and Lower Arctic Intermediate Water (LAIW) ( $T = 2.99\text{ }^{\circ}\text{C}$  and  $S = 35.0\text{ PSU}$ ) in the bottom layer. However, the salinity and temperature profiles from the core site collected in August 2010 show the relatively cold ( $T = \text{c. } 4.25\text{ }^{\circ}\text{C}$ ) and fresh ( $S = 34.1\text{--}34.3\text{ PSU}$ ) surface layer down to c. 20–25 m water depth (Fig. 4). From 20–25 m to 60–70 m water depth temperature and salinity increases abruptly to c.  $5\text{--}5.3\text{ }^{\circ}\text{C}$  and  $34.7\text{--}35.1\text{ PSU}$ , respectively. Further down in the water column the temperature decreases gradually from c.  $4\text{ }^{\circ}\text{C}$  at 70–80 m depth to  $1.5\text{ }^{\circ}\text{C}$  at 500 m depth whereas the salinity remains relatively stable at c.  $35.05\text{ PSU}$  between 70 and 500 m (Fig. 4).

Living benthic foraminifera from the southern YP are dominated by species typical of the northern North Atlantic Ocean (*Cassidulina reniforme*, *C. neoteretis*, *Elphidium excavatum*, *Melonis barleeanus* and *C. lobatulus*; Bergsten (1994)). Subordinate species are *Epistominella exigua*, *Pullenia bulloides*, *Hyperammina* spp. and *Fursenkoina fusiformis*. Species that are abundant in the fossil populations are generally also abundant in the living assemblage. Studies by Bergsten (1994) and Wollenburg and Mackensen (1998) suggest that the agglutinated species are relatively abundant (48–55%) compared to the calcareous species on the southern YP. This abundance is due to influence of corrosive bottom water that forms in the presence of seasonal sea ice and the associated high surface productivity in the area (Wollenburg and Mackensen, 1998). The sediments also contain few planktic specimens because of carbonate dissolution (Spielhagen et al., 2005).

#### 3.2. Distribution of benthic and planktic foraminifera species and their ecology

More than 20 different species of benthic foraminifera were recorded in the core JM10-02GC (Appendix A). The benthic species *C. neoteretis*, *I. norcrossi* and *C. reniforme* are dominant (40–60%),

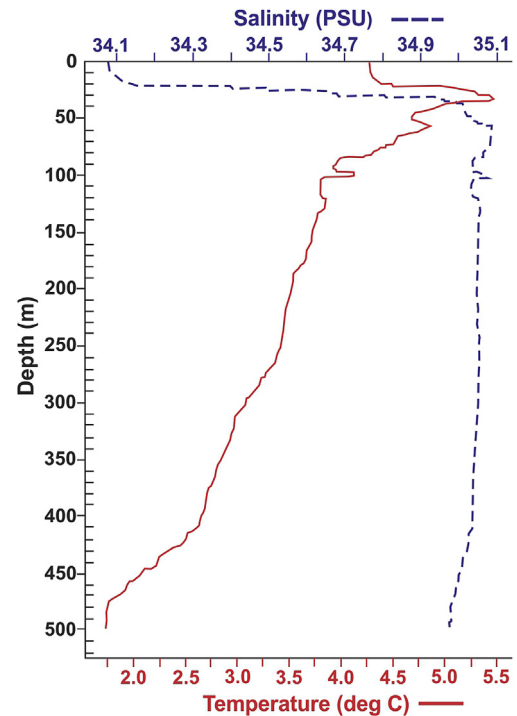
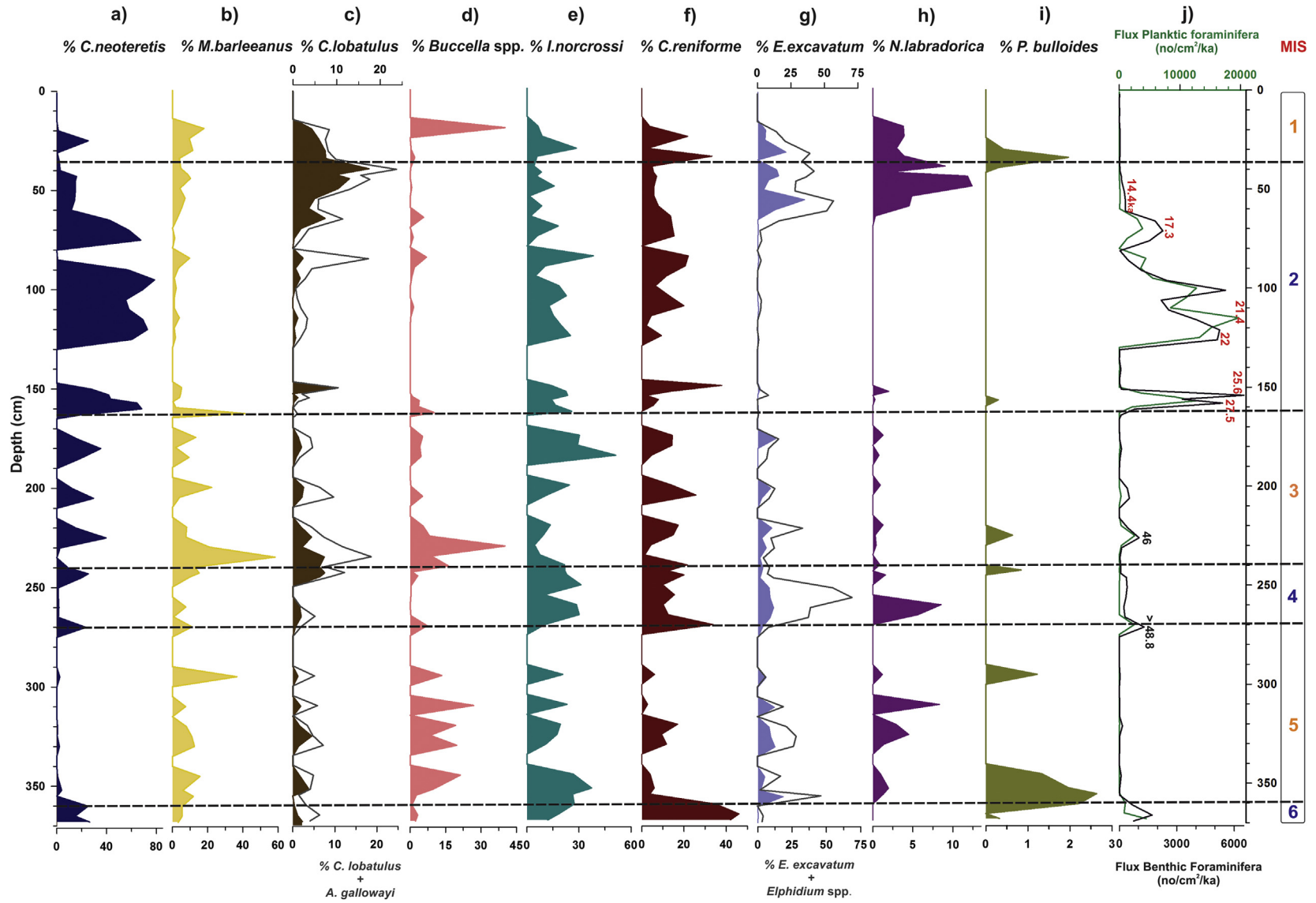


Fig. 4. Temperature and salinity profiles from the core site, collected in August 2010 on R/V Jan Mayen (presently Helmer Hanssen).

followed by two groups of species in decreasing order of abundance- *E. excavatum*, *Nonionella labradorica* and *C. lobatulus* (20–30%) constitute the first group and *M. barleeanus*, *Buccella* spp., and *Astrononion gallowayi* constitute the second group (10–20%) (Fig. 5). The most abundant planktic species throughout the core is *N. pachyderma* s (c. 20–80%) (Fig. 2b).

The dominant benthic species *C. neoteretis* and *C. reniforme* are indicators of glacialmarine environments and the presence of chilled and saline AW in the subsurface below a layer of Polar Surface Water (Jennings and Helgadottir, 1994; Polyak and Solheim, 1994; Rasmussen et al., 1996a, 1996b; Hald and Korsun, 1997; Lubinski et al., 2001; Rytter et al., 2002; Jennings et al., 2004). *C. reniforme* prefers lower temperature and high salinity (Steinsund, 1994). *Buccella* spp. and *I. norcrossi* prefer low temperatures and often occur together. They use the algal blooms at sea ice margins as food source (Steinsund, 1994). Their abundance indicates cold and seasonal sea ice conditions (Mudie et al., 1984; Polyak and Solheim, 1994). *I. norcrossi* prefers relatively high and stable bottom water salinity (Korsun and Hald, 1998). *N. labradorica* depends on organic matter transported from high productive zones (Steinsund, 1994) and its presence indicates the proximity of the Polar Front (Mudie et al., 1984; Steinsund, 1994; Hald and Korsun, 1997; Korsun and Hald, 1998, 2000). *E. excavatum* and *Elphidium* spp. are opportunistic species, confined to ice-marginal conditions with fluctuating temperatures and salinities (Steinsund, 1994) and their occurrence indicates low salinity (Bauch et al., 1996; Polyak et al., 2002). Together these species indicate freshening and cooling of the shelf bottom waters, increased sea ice cover and a gradually decreasing influence of AW. The epifaunal species *C. lobatulus* and *A. gallowayi* often occur together in areas of coarse sediments. They are indicators of an enhanced bottom current regime resulting in winnowing of shallow shelf areas (Sejrup et al., 1981; Mudie et al., 1984; Mackensen et al., 1985; Korsun and Polyak, 1989; Polyak and Solheim, 1994; Wollenburg and Mackensen, 1998; Polyak et al., 2002; Jennings et al., 2004). *M. barleeanus* is an indicator of a



**Fig. 5.** Foraminifera abundance: (a) to (i) Abundance of benthic species; (j) Planktic and benthic foraminifera flux with calibrated age (red numbers) and uncalibrated/infinite  $^{14}\text{C}$  age in ka (black numbers). The grey curve in panels (c) and (g) shows combined abundance of benthic species *C. lobatulus* with *A. gallowayi* and *E. excavatum* with *Elphidium* spp., respectively.

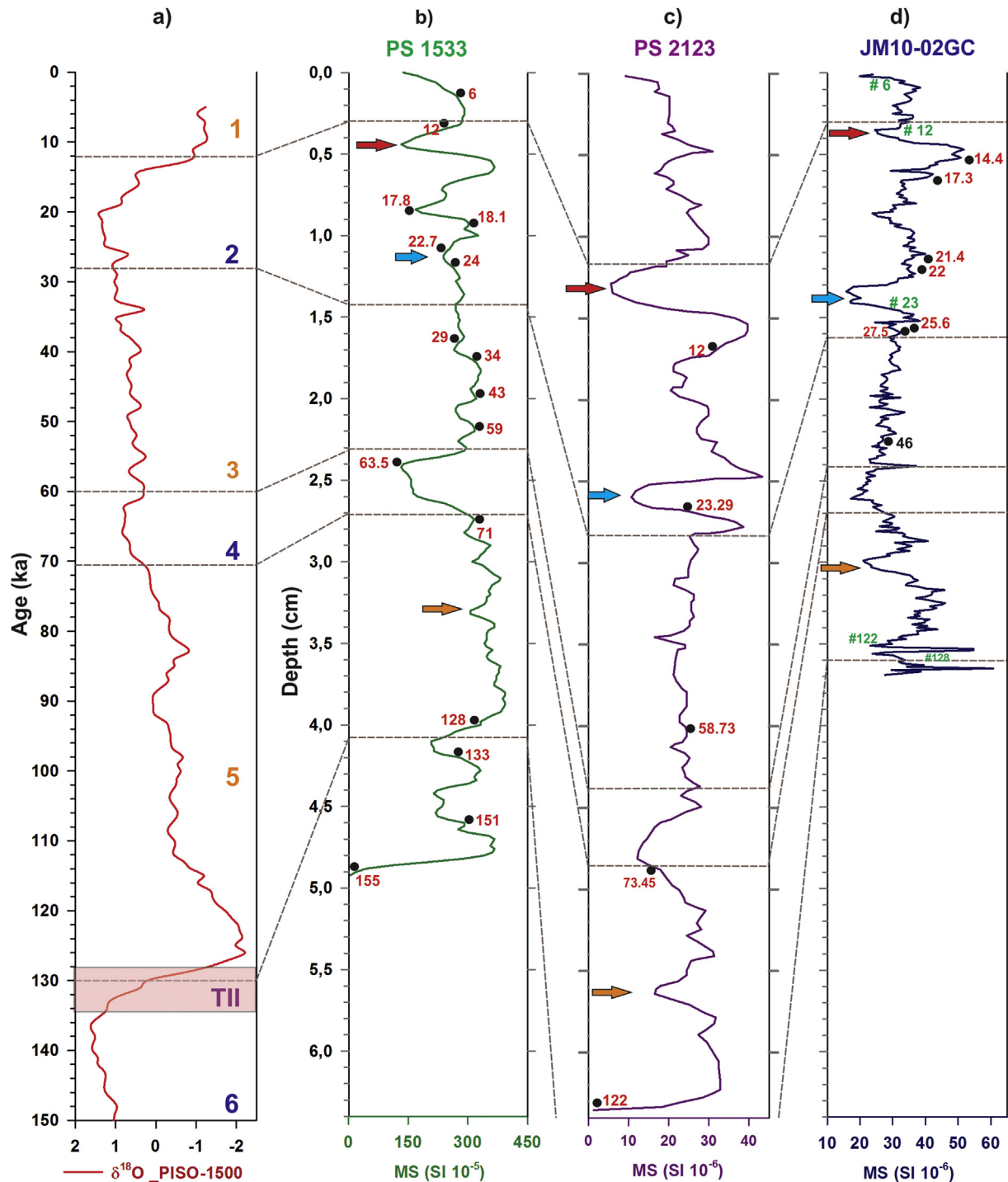


**Fig. 6.** Correlation of magnetic susceptibility (MS) records: (a) The PISO-1500  $\delta^{18}\text{O}$  stack (Channell et al., 2009) provides an age reference for the MS curves. The numbers in orange and blue show MIS stages and TII indicates the Termination II in PISO-1500 stack; MS of the cores (b) PS1533 (Nowaczyk et al., 1994); (c) PS2123 (Vogt et al., 2001) and (d) JM10-02GC (this study). Black dots with red numbers in MS curves show age in ka BP. Black dot with black number in JM10-02GC at 225 cm is an uncalibrated age. The red, blue and orange arrows show respective tie points and the green numbers show tentative ages based on these tie points.

steady supply of partially degraded organic matter to the sea floor and is often connected with the presence of AW (Caralp, 1989; Korsun and Polyak, 1989; Steinsund, 1994; Polyak et al., 2002; Jennings et al., 2004). The benthic species *P. bulloides* is considered as the stratigraphic biomarker for MIS 5e and 5a (Haake and Pflaumann, 1989; Bauch et al., 1996; Fronval and Jansen, 1997; Rasmussen et al., 1999) and it prefers a narrow salinity interval close to 35‰ and temperature between 2 and 4 °C. The planktic

species *N. pachyderma*s reflect the presence of Polar Surface Waters (Bauch et al., 2001).

#### 4. Age model of the core

The age model for the 225–50 cm interval was established using seven AMS- $^{14}\text{C}$  ages from planktic foraminifera (Table 1). Six calibrated radiocarbon ages between 27 and 14 ka BP and one

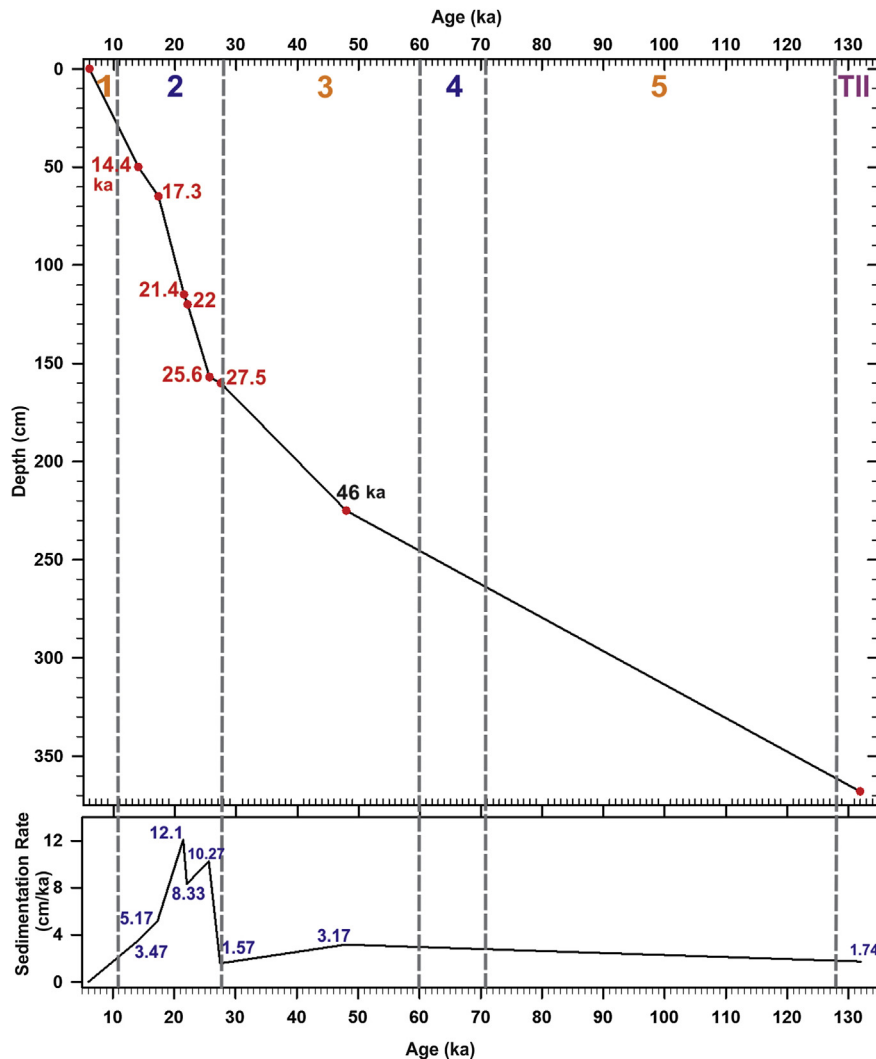


Fig. 7. Age–depth model and sedimentation rates for the core JM10-02GC. Numbers in red and black indicate calibrated and uncalibrated  $^{14}\text{C}$  ages in ka, respectively. The blue numbers in the bottom panel indicate sedimentation rate in cm/ka. Blue and orange numbers show MIS and TII marks Termination II. (For interpretation of the references to colour in this figure legend, the reader is referred to the web version of this article.)

uncalibrated age of 46  $^{14}\text{C}$  ka BP suggest that this section of the core was deposited during the mid-Late Weichselian. The chronology for other sections of the core is based primarily on changes in benthic foraminifera assemblages supported by correlation of magnetic susceptibility values between 50 and 0 cm and  $\delta^{18}\text{O}$  isotope values between 368 and 225 cm.

The planktic oxygen and carbon isotope record from the core has several gaps due to the sections barren of planktic foraminifera (Fig. 2e). This is often the case in Arctic Ocean sediment cores and can cause difficulties in the recognition of Oxygen Isotope Stages (Spielhagen et al., 2004). Therefore, the age model is also based on the correlation of stable isotope and magnetic susceptibility records with those from a well dated core PS1533 on the south-eastern YP (Nowaczyk et al., 1994; Spielhagen et al., 2004) and nearby core PS2123 (Vogt et al., 2001) (Figs. 1, 2 and 6). Furthermore, the benthic and planktic oxygen isotope data is correlated with the two global oxygen isotope curves, the SPECMAP (Martinson et al., 1987) and LR-04 benthic stack (Lisiecki and Raymo, 2005) and the insolation curve at  $80^\circ\text{N}$  (Berger, 1978) (Fig. 3j). The magnetic susceptibility record of the cores PS1533, PS2123 and JM10-02GC has been linked to the  $\delta^{18}\text{O}$  PISO-1500 stack (Channell et al., 2009) (Fig. 6). Stratigraphic biomarker species, *P. bulloides*, characteristic for MIS

5a and the Eemian is also used in the correlation (Haake and Pflaumann, 1989; Bauch et al., 1996; Fronval and Jansen, 1997) (Fig. 2b).

Based on radiocarbon dates, benthic foraminifera assemblage and the above mentioned correlations, the core JM10-02GC covers the time interval from the Termination II (132–128 ka) to the early Holocene (Figs. 2 and 6). The discussion in Chapter 5 is structured according to this robust age model, considering the variations in lithology, isotope records and the geophysical properties of the sediments. Using the basal age of the core c. 132 ka BP and the  $^{14}\text{C}$  ages, the age–depth model is generated by linear interpolation (Fig. 7).

## 5. Paleoceanographic reconstruction

### 5.1. Termination II to Late MIS 5e (core interval 368–340 cm)

#### 5.1.1. Description

The sediment between 368 and 360 cm is grey silt and clay (Fig. 3b). The IRD content is moderate to low whereas the magnetic susceptibility record shows a prominent peak at c. 362 cm (60 SI  $10^{-6}$ ) (Fig. 3f–h). The interval between 360 and 352 cm features the



dark-grey to black laminated layer, rich in fine to medium sand. It is characterised by a peak in the fine IRD (0.150–0.500 mm) and low magnetic susceptibility (c. 20 SI  $10^{-6}$ ) with shell and coal fragments at 350 cm (Fig. 3b, c, f–h). A fine sand unit with high magnetic susceptibility (c. 50 SI  $10^{-6}$ ) and a peak in the coarse IRD fraction is found between 350 and 340 cm. The shear strength has an average value of 40 kPa throughout this interval. There is a decrease of 1‰ and 2.64‰ in planktic  $\delta^{18}\text{O}$  values at 367 cm and 355 cm, respectively and a decrease in benthic  $\delta^{18}\text{O}$  values by 1.58‰ at 352 cm (Fig. 2c, e).

### 5.1.2. Interpretation and implications

**5.1.2.1. Termination II.** The bottom interval of the core between 368 and 360 cm shows high abundance of the benthic species *C. reniforme*, *I. norcrossi* and *C. neoteretis* (Fig. 5a, e, f). In modern conditions, these benthic species are common in areas distal to glaciers with very weak influence of subsurface AW (Polyak et al., 2002). Their presence suggests that the open water conditions existed at the core site with weak sway of AW. Spielhagen et al. (2004) also suggest that there was a period of weak inflow of AW to the Fram Strait from c. 135 ka BP between two meltwater events in late MIS 6. The reduction in planktic  $\delta^{18}\text{O}$  values is probably an indication of fresh and cold meltwater at the sea surface (Fig. 2e). Similar trend of two-step decline in oxygen isotope values close to the MIS 6/5e boundary during TII (134–128 ka BP) is observed in the global SPECMAP  $\delta^{18}\text{O}$  and LR-04 benthic  $\delta^{18}\text{O}$  stack (Martinson et al., 1987; Lisiecki and Raymo, 2005), and regionally on the Vøring Plateau (Haake and Pflaumann, 1989) and on the eastern YP (Spielhagen et al., 2004) (Fig. 2a). This is further supported by Risebrobakken et al. (2006) who suggested that two major meltwater events occurred with an intermediate deglacial period (c. 132–131 ka BP) during TII (134–128 ka BP) in the Nordic Seas. The deglacial period in the Nordic Seas was characterised by northward heat transport by an Atlantic Meridional Overturning Circulation (AMOC) resulting in abundant IRD input yielding high magnetic susceptibility values. In contrast, the benthic foraminifera assemblage, low IRD content and low sedimentation rate during the MIS 6/5e transition in core JM10-02GC indicate that the influence of the northern limb of AMOC was weak on southern YP compared to the eastern part of the Nordic Seas (Figs. 3, 5 and 7). This is supported by the presence of large iceberg ploughmarks of Saalian age across the YP and along the northern Svalbard margin (Dowdeswell et al., 2010; Jakobsson et al., 2010; Noormets et al., 2010).

**5.1.2.2. The Eemian Interglacial.** Above the MIS 6/5e boundary (130 ka BP) at c. 360 cm, there is a gradual decrease in the planktic species *N. pachyderma* s, and the benthic species *C. neoteretis* and *C. reniforme* (Figs. 2b, 5a and f). This implies reduced influence of subsurface AW. The high abundance of benthic species *P. bulloides*, which is the biomarker for MIS 5e (Lloyd et al., 1996; Rasmussen et al., 1999), suggests the presence of relatively warmer surface water with variable salinity during this interval (Fig. 5i).

The relative abundance of fine IRD in the dark laminated layer at 360–355 cm implies a relatively distant IRD source. Low planktic  $\delta^{18}\text{O}$  values of 2.27‰ at 355 cm indicate the influence of freshwater at the surface suggesting a meltwater event around this time (Fig. 2e). The increased input of meltwater could be linked with the inflow of relatively warm water during the Eemian. The  $\delta^{18}\text{O}$  values of benthic foraminifera are less affected by the changes in surface meltwater properties (e.g. temperature, salinity) than the  $\delta^{18}\text{O}$  values of planktic species and carry therefore comparatively stronger signal related to changes in the ice volume. Hence, the decrease in benthic  $\delta^{18}\text{O}$  values probably indicates reduced ice volume (Fig. 2c). Rasmussen and Thomsen (2008) interpreted a similar setting in the Nordic Seas where the increase in water

temperature destabilises marine ice shelves leading to iceberg calving and high meltwater discharge. Risebrobakken et al. (2006) have also reported a major meltwater event between c. 130.5–126 ka BP from the western Svalbard margin and Spielhagen et al. (2004) suggested an outflow of freshwater from large ice dammed lakes at c. 130 ka BP from the Barents and Kara Sea ice sheet. Therefore, the coal fragments in this interval could have an easterly source in the eastern Arctic Ocean, as this would be consistent with the ice drift reconstructions made by Bischof et al. (1990) from Arctic Ocean, Fram Strait and Norwegian–Greenland Sea (Fig. 3f). They demonstrate that the coal fragments were transported by icebergs or sea ice in MIS 5–1. Moreover, the shell fragments overlying the laminated layer imply relatively improved ecological conditions at the sea floor (Fig. 3b).

Following the meltwater event the benthic foraminiferal assemblage was dominated by *E. excavatum* with *Elphidium* spp., *I. norcrossi* and *Buccella* spp. (c. 20–40%) (Fig. 5d, e, g). This assemblage is usually associated with cold conditions and seasonal sea ice cover. Rasmussen and Thomsen (2008) suggested that at the culmination of the meltwater event the ocean water stratifies and the convection breaks, facilitating the formation of sea ice. The benthic species *M. barleeanus*, *C. lobatulus* and *A. gallowayi* also appear as subordinate species, which implies weak influence of AW with a high energy environment and steady food supply in the bottom waters (Fig. 5b, c). This is consistent with the studies from the Nordic Seas suggesting that the period after 127 ka BP was characterised with continental type climate followed by cold climate in its latter phase (Rasmussen et al., 2003).

## 5.2. MIS 5d–5a (core interval 340–270 cm)

### 5.2.1. Description

The sediment in the interval of 340–300 cm consists of fine sand followed by silt and clay with drop stones and peaks in medium-sized IRD between 300 and 285 cm (Fig. 3b, g). The magnetic susceptibility is relatively low (20 SI  $10^{-6}$ ) (Fig. 3c). Between 285 and 270 cm there is a laminated layer of silt and fine sand overlain by a layer of shell fragments (Fig. 3b). The water content reaches a minimum of c. <20% in the fine grain size interval between 335 and 330 cm (Fig. 3e). The maximum shear strength (>60 kPa) and a peak in medium size IRD were recorded between 330 and 320 cm (Fig. 3c).

### 5.2.2. Interpretation and implications

A 5 cm section barren of planktic and benthic foraminifera and containing little IRD between 340 and 335 cm is associated with the end of the Eemian interglacial when the sea ice margin was proximal to the core site (Figs. 3f–h, 5). The lack of foraminifera could indicate, for instance, perennial sea ice that was unsuited for planktic and benthic foraminifera growth or post-depositional dissolution of calcium carbonate and/or a combination of these factors. The low water content between c. 335–330 cm implies somewhat over-consolidated sediments, probably due to ice grounding.

The planktic species *N. pachyderma* s reappears at 330 cm (c. 20%) and the concentration gradually increases up to c. 40% at 320 cm (Fig. 2b). The dominant benthic species were *Buccella* spp. and *I. norcrossi*, which feed on the sea ice margin algal blooms and are therefore indicative of the presence of seasonal sea ice (Fig. 5d, e). The benthic species *C. neoteretis* was less abundant compared to *N. pachyderma* s in this interval suggesting weak influence of AW. The higher planktic  $\delta^{18}\text{O}$  values above 330 cm can be linked to the cold temperature of Polar Surface Water and to the presence of seasonal sea ice (Fig. 2e). The higher benthic  $\delta^{18}\text{O}$  values probably also point toward increased glacier ice volume (Fig. 2c). Therefore, this interval

is characterised by seasonally open water and weak influence of AW and probably represents MIS 5c. However, due to the gap in the oxygen isotope records, a precise correlation is not possible.

The advent of the benthic species *P. bulloides*, which prefer narrow salinity interval of c. 35‰, and temperature between 2 and 4 °C, marks the return of favourable conditions at c. 295 cm core-depth (Fig. 5i). This benthic species is also the biomarker species for MIS 5a (Haake and Pflaumann, 1989). Along with *P. bulloides*, a distinct peak in relative abundance of *M. barleeanus* is observed at 295 cm (Fig. 5b). Both species follow the same food strategy of feeding on partially degraded organic matter supplied to the sea floor (Corliss, 1991). The reappearance of *C. neoteretis*, although in low numbers, indicates a short period of subsurface AW inflow (Fig. 5a). The sedimentological studies from northern Svalbard margin (Knies et al., 2001, 2000) and Central Arctic Ocean (Spielhagen et al., 2004) also point to the advection of AW during MIS 5a. Due to this advection, the sea ice margin moved north of the core site leading to open water conditions.

The occurrence of drop stones between 300 and 285 cm and the accompanying high IRD content indicate increased iceberg rafting during MIS 5a. Based on clay mineralogical studies on the core PS2123, Vogt et al. (2001) suggested the SBIS advance during MIS 5a (Fig. 1B). The planktic  $\delta^{18}\text{O}$  record from JM10-02GC is somewhat ambiguous in this interval due to the lack of planktic foraminifera. However, the general trend of the planktic  $\delta^{18}\text{O}$  curve toward lower values suggests the presence of less saline/fresh surface waters (Fig. 2e). The layer of shell fragments at 270 cm also lends support to the improved environmental conditions at the sea floor (Fig. 3b). Thus, the thick laminated layer with bivalves in its upper part suggests an increased meltwater influence, which probably occurred due to advection of subsurface AW and high insolation during this period (Fig. 3b). This interpretation is supported by the results from the eastern YP, also suggesting a freshwater pulse during MIS 5a (Knies and Vogt, 2003).

### 5.3. MIS 4 (core interval 270–240 cm)

#### 5.3.1. Description

This interval consists of silt and clay with presence of drop stones and a sandy lens at 240 cm (Fig. 3b). The IRD record shows a prominent peak between 245 and 240 cm and the presence of coal fragments just on top of this interval (Fig. 3f–h). At 260 cm and 240 cm the magnetic susceptibility values show considerable decrease ( $<20 \text{ SI } 10^{-6}$ ) and increase (c.  $40 \text{ SI } 10^{-6}$ ), respectively (Fig. 3c).

#### 5.3.2. Interpretation and implications

The reappearance of the planktic species *N. pachyderma* s and high planktic  $\delta^{18}\text{O}$  values (3.68‰) suggests the presence of cold Polar Water at the surface (Fig. 2b, e). The abundance of the benthic species *C. neoteretis* and *C. reniforme*, that are indicative of chilled AW, indicate open water conditions at the core site (Fig. 5a, f). This assemblage suggests that a High Productivity (HP) environment existed after the meltwater event during MIS 5a. Hald et al. (2001) and Hebbeln et al. (1994) suggested that open water conditions in the Nordic Seas and the associated moisture supply could have contributed to the growth of the SBIS. Above the HP zone, the number of benthic species *I. norcrossi* and *N. labradorica* increased (Fig. 5e, h). This faunal assemblage suggests that the sea ice margin and the Polar Front were in the vicinity of the core site. The significant peak in relative abundance of the opportunistic species *Elphidium* spp. and *E. excavatum* (80%) at 260–255 cm core-depth, indicates the onset of fluctuating temperature and salinity conditions (Fig. 5g). This most likely marks the return of polar conditions

with freshening and cooling of shelf bottom waters and increased sea ice cover.

At 255–245 cm core-depth, the distinct peak in abundance of *C. neoteretis* and *C. lobatulus* together with *A. gallowayi* reflects the restoration of AW and strong bottom current activity (Fig. 5a, c). The IRD peak at this interval suggests enhanced iceberg calving, most likely due to the retreat of the SBIS from the continental shelf. Hebbeln and Wefer (1997) suggest that in MIS 4 chilled AW advected northwards into the Fram Strait. Vogt et al. (2001) have also reported strong advection of AW during MIS 4/3 transition in the core PS2123 from YP (Fig. 1B). The retreat of ice sheets on Spitsbergen during MIS 4 was probably controlled by the increased insolation (Mangerud and Svendsen, 1992). The isotope record shows the low planktic  $\delta^{13}\text{C}$  and  $\delta^{18}\text{O}$  values that are most likely caused by the input of fresh surface water from melting glacier ice and icebergs (Fig. 2e). Although there was a distinct influence of AW, the overall flux of benthic and planktic species decreases significantly (Fig. 5j). The high IRD input from melting icebergs leads to mixing of surface water and the increase in suspended sediments decreases the penetration of sunlight and the biological productivity.

### 5.4. MIS 3 (core interval 240–162 cm)

#### 5.4.1. Description

This interval is characterised mainly by silt and clay with some sand lenses containing fine to medium sand. A distinct laminated layer consisting of mud and sand lenses is present between 180 and 165 cm (Fig. 3b). The fine IRD (0.150–0.500 mm) is dominant throughout the interval (Fig. 3h).

#### 5.4.2. Interpretation and implications

Between 240 and 230 cm, the abundant benthic foraminifera species are *M. barleeanus* (c. 55%), *C. lobatulus* with *A. gallowayi* (c.15%) and *Buccella* spp. (c. 30%) (Fig. 5b, c, d). This faunal composition indicates the presence of strong bottom currents, high and steady supply of food and the presence of seasonal sea ice. This environment may be related to the increased discharge from the collapsing SBIS during MIS 4/3 transition. The retreat of the Eurasian Ice Sheet is recorded in the North Atlantic and Arctic Ocean sediment cores with high concentrations of IRD and low concentrations of planktic foraminifera during the early phase of MIS 3 (e.g. Dokken and Hald, 1996; Nørgaard-Pedersen, 1997). The overall fluxes of benthic and planktic foraminifera in the 240–165 cm section are negligible except for two short intervals at 225 and 200 cm (Fig. 5j). The sections barren of foraminifera contain higher amounts of fine IRD (e.g. at 220 cm, 205 cm, 180 cm) (Fig. 3f–h). According to Hebbeln (2000), the high concentration of fine IRD can be associated with sea ice. The benthic species *I. norcrossi*, which reflect cold conditions, is also relatively abundant. Therefore, we infer that the area was covered by seasonal sea ice with the winter sea ice margin situated south of the core site. The observations from the core PS2837 also support the interpretation that the core site was covered by perennial sea ice from 30 ka to 27.5 ka, suggesting severe sea ice conditions on northern YP (Müller et al., 2009) (Fig. 1B).

At 46  $^{14}\text{C}$  ka BP (c. 225 cm), high concentration of planktic (*N. pachyderma* s) and benthic foraminifera (*C. neoteretis* and *C. reniforme*) were recorded, implying a high productivity environment and that the subsurface AW was present throughout the period (cf. Polyak and Mikhailov, 1996) (Figs. 2b, 5a and f). Spielhagen et al. (2004) have reported the influx of AW around 52 ka BP. Therefore, we assume that this core-depth most likely represents approximately the same time interval. Between 240 and 175 cm the foraminifera-rich layers alternate with barren intervals

(Fig. 5). High content of calcium carbonate in the sediment are related to good preservation of foraminifera, whereas the high content of organic matter in the sediment often results in dissolution of calcium carbonate (Archer and Maier-Reimer, 1994; Scott et al., 2008).

Some of our samples contained only benthic foraminifera, whereas planktic species were lacking (Figs. 5 and 2b). Based on this and on the results of several recent studies (see Zamelczyk et al., 2012, 2013) we assume that dissolution of foraminifera tests is the primary reason for the barren intervals. Planktic foraminifera are more susceptible to dissolution than most benthic species (Berger and Killingley, 1977). The reason for this is that dissolution is often associated with formation of seasonal sea ice in the MIZ (Veum et al., 1992; Steinsund and Hald, 1994; Dokken and Hald, 1996; Zamelczyk et al., 2012). The abundance of *C. neoteretis* alternating with the barren intervals is related to the presence of subsurface AW during this stage. As a result, sea floor sediments become organic rich and carbonate poor with a high level of CO<sub>2</sub> in the sediments and pore water (Huber et al., 2000).

It is also possible that this pattern of alternating intervals of productivity and low IRD content versus dissolution and high IRD content reflects the retreat and advance of the SBIS and sea ice. Knies et al. (1998) reported decay of northern SBIS during the MIS 4/3 transition and in late MIS 3 (at 34.9 ka BP) supporting this view. The core PS1533 (Fig. 1B) from the northern YP contains little or no IRD from 50 ka BP up to the last deglaciation (Spielhagen et al., 2004). In contrast, our data show prominent peaks in different size fractions of IRD in MIS 3 and MIS 2. At 175–165 cm, 10 cm of laminated sediment contains low amount of benthic foraminifera and an interval barren of planktic foraminifera (Fig. 3b, i). Spielhagen et al. (2005) suggest that while the benthic species are present, the dissolution of planktic foraminifera could be explained by the variations in salinity. Hence, the interval barren in planktic foraminifera may suggest the increased glacial meltwater input resulting in lower salinity and dissolution.

## 5.5. MIS 2 (core interval 162–32 cm)

### 5.5.1. Description

This interval consists mainly of silt and clay of variable colour between 165 cm and 65 cm (Fig. 3b). A banded sediment unit at 140–130 cm comprising dark coloured layer rich in medium sized sand is characterised by low magnetic susceptibility (<20 SI 10<sup>-6</sup>), relatively high shear strength, low water content (c. 24%) and a prominent peak in all three size classes of IRD (Fig. 3c, e, f–h). A layer rich in shell fragments at 100 cm is overlain by laminated sediments of clayey silt between 90 and 80 cm. A sand lens is present at 80 cm. The section from 65 to 32 cm consists of massive clay with an interval of high magnetic susceptibility (c. 50 SI 10<sup>-6</sup>) between 55 and 45 cm (Fig. 3b).

### 5.5.2. Interpretation and implications

The radiocarbon age of 27.5 ka BP at 160 cm marks the MIS 3/2 boundary (Fig. 3a, b). The beginning of the Late Weichselian correlates with low insolation and relatively high abundance and fluxes of planktic and benthic foraminifera (Fig. 3i, j). The abundance of dominant planktic species *N. pachyderma* s varies between 40 and 80% (Fig. 2b). This is within its modern and Holocene variability in the northern Nordic seas indicating cold surface conditions with inflow of AW (Weinelt et al., 1996; Nørgaard-Pedersen et al., 2003; Sarnthein et al., 2003; Rasmussen et al., 2007). *N. pachyderma* s is common in Polar Waters and its association with a high flux of planktic foraminifera reflects increased surface water productivity (Tolderlund, 1971; Johannessen et al., 1994). Among the benthic species *C. neoteretis* dominates and constitutes up to 70% of the fauna (Fig. 5a). Polyak and

Mikhailov (1996) suggest that in modern conditions *C. neoteretis* has similar distribution as planktic foraminifera *N. pachyderma* s (Fig. 2b). Other benthic species *I. norcrossi* and *C. reniforme* constitute up to 20–30% of the assemblage (Fig. 5e, f). This faunal composition indicates that during MIS 2 the inflow of AW was stronger than during MIS 3 resulting in the retreat of sea ice margin to the north. The open water conditions often supply moisture by evaporation facilitating the growth of an ice sheet resulting in ocean water becoming deficient in the lighter isotope. The higher planktic δ<sup>18</sup>O values in this interval are therefore either due to cold Polar Water at the surface or increased ice volume (Fig. 2e). According to Müller et al. (2009) and Nørgaard-Pedersen et al. (2003) the sea ice biomarker IP<sub>25</sub> shows that the position of the stationary sea ice margin was at 81°N on the northern YP during this period (PS2837; Fig. 1B).

Due to strong advection of the AW to the southern YP and the resultant high abundance of foraminifera, a HP period is recorded between 27.5 and 21.4 ka BP with an interruption between 25.6 ka–22 ka BP (Fig. 5j). The planktic δ<sup>18</sup>O values also show gradual decline after 27.5 ka BP indicating warmer climatic conditions (Fig. 2e). Hald et al. (2001) suggested that the combination of low insolation and open water conditions due to the AW inflow provided moisture for the growth of the SBIS. The resulting ice sheet advance produced the banded sediment unit at 140–130 cm and the prominent IRD peak from 25 ka to 22 ka BP (Fig. 3f–h). On the basis of mineralogical studies Vogt et al. (2001) suggested that the advance of SBIS on Spitsbergenbanken was followed by massive iceberg discharge through Storfjorden, potentially transporting the IRD to the southern YP (Fig. 1B).

Evidence for this event is also found in the cores from the western Svalbard margin (Jessen et al., 2010), the northern Svalbard margin (Hebbeln, 1992; Wagner and Henrich, 1994), the eastern YP (Levitan et al., 2002) and the central YP (Howe et al., 2008; Sellén et al., 2010). Vogelsang et al. (2001) and Nørgaard-Pedersen et al. (2003) dated a similar unit in core PS 2837 from the northern YP to 27.8 ka BP (Fig. 1B). The thickness of the unit decreases from south to north and from the shelf edge towards the continental slope. The ice sheet advance between 24 and 22 ka BP produced numerous sediment mass flows along the western Svalbard margin (Elverhøi et al., 1995; Jessen et al., 2010). The age of this event correlates well with the age of the IRD peak in JM10-02GC (25–22 ka BP) (Fig. 3f–h).

It is possible that the previously reported debris-flow units are a mix of the two processes: intense iceberg rafting and the downslope movement of material from the shelf edge and upper slope at the same time. However, the nearly flat topography of the core site makes local mass-transport of sediments highly unlikely on the southern YP. Therefore, we suggest that the IRD on the YP originate from icebergs.

**5.5.2.1. The deglaciation.** At 100 cm core-depth (c. 20 ka BP), a layer rich in shell fragments reflects probably the onset of more favourable environmental conditions at the sea floor. Lower planktic δ<sup>18</sup>O values at c. 90–80 cm are possibly related to a subsequent meltwater inflow. The abundance of planktic and benthic species in the same interval decreased gradually to zero with the deposition of a sand lens at 80 cm (Fig. 3i). Between 85 and 80 cm, the distinct peak in abundance of *C. lobatulus* together with *A. gallowayi*, which often occur in areas of coarse sediments, suggest the inflow of AW and stronger bottom currents (Fig. 5c). This suggests a meltwater inflow on southern YP at 18.8 ka–19.2 ka BP and marks potentially the beginning of the Heinrich event, H1 (Fig. 7).

From 17.3 ka BP to 14.4 ka BP (c. 65–50 cm) there is a distinct peak in foraminifera flux (Fig. 5j). This time interval probably correlates with the second glacial HP period (19.5–14.5 ka BP) proposed by Hebbeln et al. (1994). The gradual decrease in polar



planktic species *N. pachyderma* s and benthic species *C. neoteretis* (Figs. 2b and 5a) point towards the weakening of chilled AW over the core site by 17.3 ka BP, whereas the prominent increase in opportunistic species *E. excavatum* with *Elphidium* spp. and *N. labradorica* (Fig. 5g, h) can be associated with increased surface meltwater. A prominent peak in the coarse IRD fraction along with relatively low planktic  $\delta^{18}\text{O}$  values at c. 15 ka BP (60 cm) implies the retreat of the ice sheet margin through intense calving and meltwater production (Figs. 2e, 3f–h). This is consistent with earlier studies on the northern Barents Sea (Knies and Stein, 1998). The data from the southern YP imply that the deglaciation of the SBIS occurred in two steps, first one between c. 19–18 ka with an early meltwater pulse and a second step after c. 15 ka BP.

The onset of the Bølling–Allerød (B–A) Interstadials at 14.4 ka BP (50 cm) was characterised by high abundances of benthic species *C. lobatulus* and *A. gallowayi* (Fig. 5c). This, together with the high  $\delta^{13}\text{C}$  values measured in the epifaunal benthic species *C. lobatulus* at 55–40 cm suggest strong bottom water ventilation on the southern YP between c. 14.4–11.5 ka BP (cf. Duplessy et al., 1988; Veum et al., 1992; Rasmussen et al., 2012) (Fig. 2d). Also studies by Birgel and Hass (2004) from the Yermak slope and Ślubowska-Woldengen et al. (2007) from the northern Svalbard margin propose increased inflow of AW at the beginning of the B–A Interstadials. However, the minimal abundance of *C. neoteretis* and *I. norcrossi* and relatively higher abundance of *E. excavatum* with *Elphidium* spp. indicate moderate flow of chilled subsurface AW at the beginning of the B–A Interstadials (Fig. 5a, e, g).

There is a pronounced increase in the abundance of the benthic species *N. labradorica* from 65 cm to 32 cm (c. 14.4–11.5 ka BP), followed by a gradual decrease in abundance above 32 cm (Fig. 5h). This is a clear indicator for the position of the Polar Front at the core site between B–A Interstadials and Younger Dryas/Holocene transition (cf. Koç et al., 2002). The coarse to medium IRD peaks between 55 and 35 cm are probably related to the melting of icebergs during the B–A Interstadials and at the Younger Dryas/Holocene transition (Fig. 3f–h).

## 5.6. MIS 1 (core interval 32–0 cm)

### 5.6.1. Description

The sediment type is dominantly fine sand with presence of drop stones (Fig. 3b). The water content varies from 40% at 32 cm to 24% at 12 cm (Fig. 3e). Distinct peaks in IRD occur throughout this interval and coal fragments are present intermittently (Fig. 3f–h).

### 5.6.2. Interpretation and implications

On the basis of the MS correlation with cores PS1533 and PS2123, we infer the Younger Dryas/Holocene boundary at 32 cm core-depth, which according to Walker et al. (2009) corresponds to c. 11.7 ka BP (Fig. 6). The high concentration of the benthic species *P. bulloides* at this boundary implies improved living environment at the onset of Holocene (Fig. 5i). Other benthic species *C. neoteretis* and *C. reniforme* indicate the advection of AW during that time (Fig. 5a, f). The signature of strong AW advection during this period is also recorded in the nearby core PS2123 (Vogt et al., 2001) (Fig. 1B). The planktic species *N. pachyderma* s was not present in the Holocene section of the core. After 10.8 ka BP (c. 30 cm, Fig. 7), the increase in the abundance of benthic species *N. labradorica* and *I. norcrossi* indicates the presence of seasonal sea ice and the proximity of Polar Front (Fig. 5e, h). Similar conditions were prevailing on the northern YP (Müller et al., 2009). At 20 cm core-depth, there is a prominent peak in the abundance of *Buccella* spp. and a high abundance of *M. barleeanus* (Fig. 5b, d). These species indicate that there was increased supply of organic matter to the sea floor, most likely due to the proximity of sea ice margin to the core site. The top 15 cm of the

core is barren of foraminifera and has a relatively high IRD content (Fig. 3f–h). The interval barren of foraminifera could be the result of dissolution of calcium carbonate due to high input of organic matter, similar to MIS 5 and MIS 3.

Therefore, we suggest that the strong IRD signal indicates the retreat of SBIS with seasonal sea ice conditions during the early Holocene. Based on the magnetic susceptibility correlation with the adjacent cores PS1533 and PS2123, we presume that the sediments younger than 6 ka BP are probably not present in core JM10-02GC (Fig. 6). Low mid-Holocene to modern accumulation rates at the core site (e.g. Dowdeswell et al., 2010) could result from the strong bottom currents due to the reinforcement of the Svalbard Branch of the WSC between 6 ka and the present.

## 6. Summary and conclusion: variations in AW inflow and movement of sea ice margin on the southern YP

Based on the benthic foraminifera assemblages and correlation of isotopic and MS records, the core contains sediments from c. 132 ka BP representing TII to early Holocene (c. 6 ka BP) (Fig. 8). During TII, the northward heat flux in the eastern Nordic Seas did not reach the core site, probably due to cold water temperature and deeper halocline facilitating transport of mega icebergs across the YP. However, there was weak influence of AW on southern YP resulting in open water conditions.

The biomarker species *P. bulloides* marks the Eemian Interglacial. The presence of freshwater at the surface and low insolation during late Eemian resulted in expansion of sea ice onto the southern YP. The meltwater inflow during Eemian can be associated with relatively high ambient water temperature and insolation. MIS 5c was characterised by seasonal sea ice conditions. The AW inflow was weak during MIS 5d–5b. MIS 5a is mainly identified by the presence of *P. bulloides* and was characterised by inflow of AW resulting in meltwater production and melting of icebergs. The advection of subsurface AW that continued at the MIS 5a/4 transition resulted in high productivity (HP event).

During MIS 4, the cold conditions prevailed with the Polar Front and sea ice margin at the core site. Towards the end of MIS 4, the sea ice margin receded due to the revival of AW. Throughout MIS 3, the area was covered with seasonal sea ice (Fig. 8). Periods with increased productivity of planktic and benthic foraminifera are alternating with intervals barren of foraminifera. The bio-productivity is associated with open water conditions due to thinning of sea ice and relatively strong influence of subsurface AW. The barren intervals occur most likely due to carbonate dissolution, which is associated with the formation of seasonal sea ice of the MIZ. There are two short intervals showing increase in foraminifera flux associated probably with strengthening of subsurface AW inflow. The termination of MIS 3 is characterised by laminated sediments resulting most likely from a meltwater event.

MIS 2 began with strong advection of subsurface AW resulting in retreat of the sea ice margin and formation of open-water conditions (Fig. 8). The HP period was recorded between 27 ka and 21 ka BP. This HP period was interrupted by an event of intense iceberg rafting (25–22 ka BP) most likely associated with the advance of the SBIS. The deglaciation after LGM occurred in two phases on the southern YP. The first phase took place between c. 19 ka–18 ka BP and second phase at c. 15 ka BP. During B–A Interstadial strong ventilation of bottom water masses occurred. The Polar Front was in the vicinity of the core site from B–A Interstadials until Younger Dryas/Holocene transition.

The Holocene started with warm waters dominated by the advection of AW and favoured by *P. bulloides*. The presence of seasonal sea ice during the early Holocene on southern YP resulted in calcium carbonate dissolution, most likely due to supply of high organic matter by sea ice margin algal blooms. Correlation with

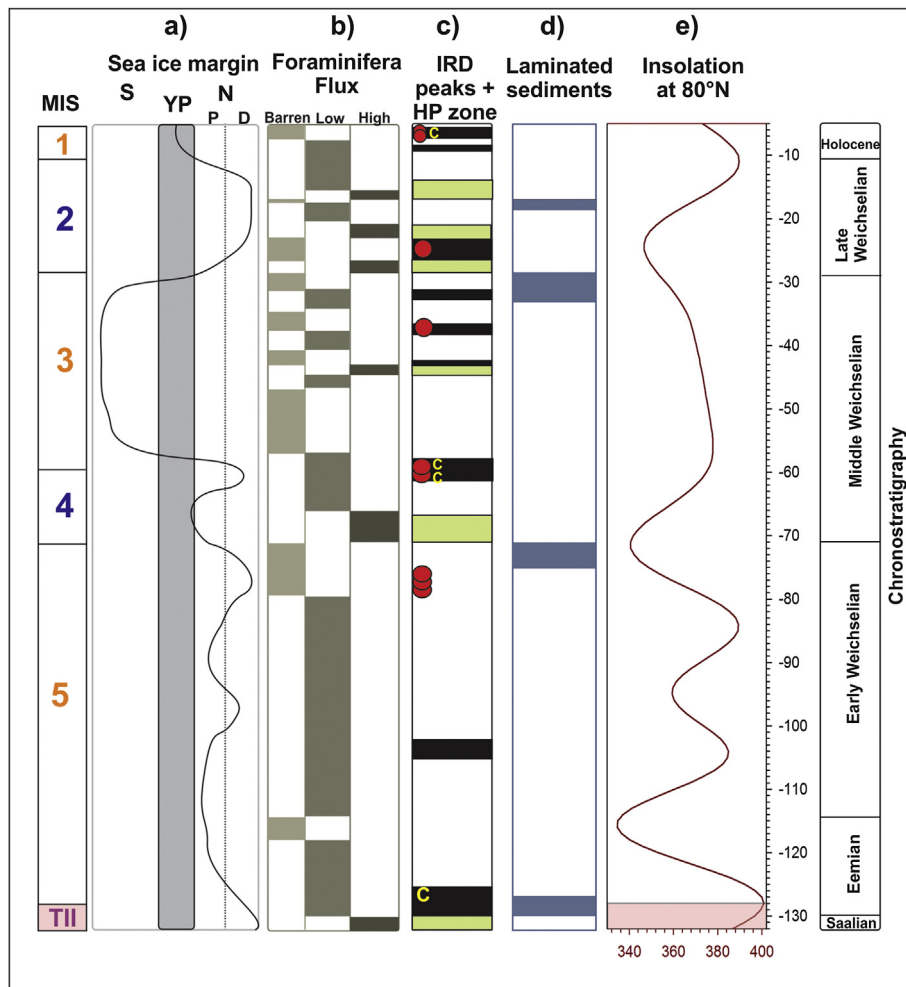


**Fig. 8.** Summary. A diagram summarizing the key results (Not to scale) (a) The interpreted position of the sea ice margin, abbreviations: YP – Yermak Plateau implies to the core site, S – south of YP, N – north of YP, P – proximal, D – distal; (b) Foraminifera flux; (c) IRD peaks (black) and High Productivity (HP) zones (green), red dots signify the occurrence of drop stones, C – coal fragments in IRD; (d) Occurrence of laminated sediments; (e) Insolation at 80°N is according to Berger (1978).

nearby cores suggests the top of the core to be c. 6 ka BP. We assume that the strengthening of the Svalbard Branch between 6 ka and the present resulted in erosion or non-accumulation of younger sediments.

### Acknowledgement

The Research Council of Norway funded this study through a grant to T. Chauhan. Heike Siegmund is acknowledged for performing stable isotope analysis on samples at the Stable Isotope Laboratory, Stockholm. Radiocarbon Laboratory, Uppsala and <sup>14</sup>CHRONO Centre for Climate, Environment and Chronology, Belfast, UK are acknowledged for C-14 analysis. We thank the Captain and crew of *R/V Jan Mayen* (presently *Helmer Hanssen*) for helping in data collection during the cruise in 2010.

### Appendix A. Supplementary data

Supplementary data related to this article can be found at <http://dx.doi.org/10.1016/j.quascirev.2013.10.023>.

### References

Archer, D., Maier-Reimer, E., 1994. Effect of deep-sea sedimentary calcite preservation on atmospheric CO<sub>2</sub> concentration. *Nature* 367, 260–263.

- Bauch, H.A., Erlenkeuser, H., Grootes, P.M., Jouzel, J., 1996. Implications of stratigraphic and paleoclimatic records of the Last Interglaciation from the Nordic Seas. *Quat. Res.* 46, 260–269.
- Bauch, H.A., Erlenkeuser, H., Spielhagen, R.F., Struck, U., Matthiessen, J., Thiede, J., Heinemeier, J., 2001. A multiproxy reconstruction of the evolution of deep and surface waters in the subarctic Nordic seas over the last 30,000 yr. *Quat. Sci. Rev.* 20, 659–678.
- Berger, A., 1978. Long-term variations of caloric insolation resulting from the Earth's orbital elements. *Quat. Res.* 9, 139–167.
- Berger, W.H., Killingley, J.S., 1977. Glacial Holocene transition in deep-sea carbonates: selective dissolution and the stable isotope signal. *Science (New York, NY)* 197, 563.
- Bergsten, H., 1994. Recent benthic foraminifera of a transect from the North Pole to the Yermak Plateau, eastern central Arctic Ocean. *Mar. Geol.* 119, 251–267.
- Birgel, D., Hass, H.C., 2004. Oceanic and atmospheric variations during the last deglaciation in the Fram Strait (Arctic Ocean): a coupled high-resolution organic–geochemical and sedimentological study. *Quat. Sci. Rev.* 23, 29–47.
- Bischof, J., Koch, J., Kubisch, M., Spielhagen, R.F., Thiede, J., 1990. Nordic Seas Surface Ice Drift Reconstructions: Evidence from Ice Rafted Coal Fragments During Oxygen Isotope Stage 6. In: Geological Society, London, Special Publications 53, pp. 235–251.
- Bourke, R.H., Weigel, A.M., Paquette, R.G., 1988. The Westward turning branch of the West Spitsbergen Current. *J. Geophys. Res.* 93, 14065–14077.
- Caralp, M., 1989. Abundance of *Bulimina exilis* and *Melonis barleeaanum*: relationship to the quality of marine organic matter. *Geo-Mar. Lett.* 9, 37–43.
- Channell, J.E.T., Xuan, C., Hodell, D.A., 2009. Stacking paleointensity and oxygen isotope data for the last 1.5 Myr (PISO-1500). *Earth Planet. Sci. Lett.* 283, 14–23.
- Corliss, B.H., 1991. Morphology and microhabitat preferences of benthic foraminifera from the northwest Atlantic Ocean. *Mar. Micropaleontol.* 17, 195–236.
- Dokken, T.M., Hald, M., 1996. Rapid climatic shifts during isotope stages 2–4 in the Polar North Atlantic. *Geology* 24, 599–602.

- Dowdeswell, J., Jakobsson, M., Hogan, K., O'Regan, M., Backman, J., Evans, J., Hell, B., Löwemark, L., Marcussen, C., Noormets, R., 2010. High-resolution geophysical observations of the Yermak Plateau and northern Svalbard margin: implications for ice-sheet grounding and deep-keeled icebergs. *Quat. Sci. Rev.* 29, 3518–3531.
- Duplessy, J.-C., Moyes, J., Pujol, C., 1980. Deep Water Formation in the North Atlantic Ocean during the Last Ice Age. *Nature* 286, 479–482.
- Duplessy, J., Shackleton, N., Fairbanks, R., Labeyrie, L., Oppo, D., Kallel, N., 1988. Deepwater source variations during the last climatic cycle and their impact on the global deepwater circulation. *Paleoceanography* 3, 343–360.
- Elverhøi, A., Andersen, E.S., Dokken, T., Hebbeln, D., Spielhagen, R., Svendsen, J.I., Sørfalten, M., Rørnes, A., Hald, M., Forsberg, C.F., 1995. The growth and decay of the Late Weichselian Ice Sheet in Western Svalbard and adjacent areas based on Provenance studies of marine sediments. *Quat. Res.* 44, 303–316.
- Fairbanks, R.G., Mortlock, R.A., Chiu, T.-C., Cao, L., Kaplan, A., Guilderson, T.P., Fairbanks, T.W., Bloom, A.L., Grootes, P.M., Nadeau, M.-J., 2005. Radiocarbon calibration curve spanning 0 to 50,000 years BP based on paired  $^{230}\text{Th}/^{234}\text{U}$  and  $^{14}\text{C}$  dates on pristine corals. *Quat. Sci. Rev.* 24, 1781–1796.
- Fronval, T., Jansen, E., 1997. Eemian and Early Weichselian (140–60 ka) paleoceanography and paleoclimate in the Nordic Seas with comparisons to Holocene conditions. *Paleoceanography* 12, 443–462.
- Guest, P.S., Davidson, K.L., Overland, J.E., Frederickson, P.A., 1995. Atmospheric–Ocean interactions in the Marginal Ice Zones of the Nordic Seas. In: Smith Jr., Walker O., Grebmeier Jr., M. (Eds.), *Arctic Oceanography: Marginal Ice Zones and Continental Shelves*. American Geophysical Union, Washington DC.
- Haake, F.-W., Pflaumann, U.W.E., 1989. Late Pleistocene foraminiferal stratigraphy on the Vøring Plateau, Norwegian Sea. *Boreas* 18, 343–356.
- Hald, M., Korsun, S., 1997. Distribution of modern benthic foraminifera from fjords of Svalbard, European Arctic. *J. Foraminif. Res.* 27, 101–122.
- Hald, M., Dokken, T., Mikalsen, G., 2001. Abrupt climatic change during the last interglacial–glacial cycle in the polar North Atlantic. *Mar. Geol.* 176, 121–137.
- Hansbo, S., 1957. A New Approach to the Determination of the Shear Strength of Clay by the Fall-cone Test. Royal Swedish Geotechnical Institute.
- Hebbeln, D., 1992. Weichselian glacial history of the Svalbard area: correlating the marine and terrestrial records. *Boreas* 21, 295–302.
- Hebbeln, D., 2000. Flux of ice-rafted detritus from sea ice in the Fram Strait. *Deep Sea Res. II Top. Stud. Oceanogr.* 47, 1773–1790.
- Hebbeln, D., Wefer, G., 1997. Late Quaternary Paleocyanography in the Fram Strait. *Paleoceanography* 12, 65–78.
- Hebbeln, D., Dokken, T., Andersen, E.S., Hald, M., Elverhøi, A., 1994. Moisture supply for northern ice-sheet growth during the Last Glacial Maximum. *Nature* 370, 357–360.
- Howe, J.A., Shimmield, T.M., Harland, R.E.X., Eyles, N., 2008. Late Quaternary contourites and glaciomarine sedimentation in the Fram Strait. *Sedimentology* 55, 179–200.
- Huber, R., Meggers, H., Baumann, K.H., Henrich, R., 2000. Recent and Pleistocene carbonate dissolution in sediments of the Norwegian–Greenland Sea. *Mar. Geol.* 165, 123–136.
- Jakobsson, M., Mayer, L., Coakley, B., Dowdeswell, J.A., Forbes, S., Fridman, B., Hodnesdal, H., Noormets, R., Pedersen, R., Rebesco, M., Schenke, H.W., Zarayskaya, Y., Accettella, D., Armstrong, A., Anderson, R.M., Bienhoff, P., Camerlingh, A., Church, I., Edwards, M., Gardner, J.V., Hall, J.K., Hell, B., Hestvik, O., Kristoffersen, Y., Marcussen, C., Mohammad, R., Mosher, D., Nghiem, S.V., Pedrosa, M.T., Travaglini, P.G., Weatherall, P., 2012. The International Bathymetric Chart of the Arctic Ocean (IBCAO) version 3.0. *Geophys. Res. Lett.* 39, L12609.
- Jakobsson, M., Nilsson, J., O'Regan, M., Backman, J., Löwemark, L., Dowdeswell, J.A., Mayer, L., Polyak, L., Colleoni, F., Anderson, L.G., Björk, G., Darby, D., Eriksson, B., Hanslik, D., Hell, B., Marcussen, C., Sellén, E., Wallin, A., 2010. An Arctic Ocean ice shelf during MIS 6 constrained by new geophysical and geological data. *Quat. Sci. Rev.* 29, 3505–3517.
- Jennings, A.E., Helgadottir, G., 1994. Foraminiferal assemblages from the fjords and shelf of eastern Greenland. *J. Foraminif. Res.* 24, 123–144.
- Jennings, A.E., Weiner, N.J., Helgadottir, G., Andrews, J.T., 2004. Modern foraminiferal faunas of the southwestern to northern Icelandic shelf: oceanographic and environmental controls. *J. Foraminif. Res.* 34, 180–207.
- Jessen, S.P., Rasmussen, T.L., Nielsen, T., Solheim, A., 2010. A new Late Weichselian and Holocene marine chronology for the western Svalbard slope 30,000–0 cal years BP. *Quat. Sci. Rev.* 29, 1301–1312.
- Johannessen, O.M., 1986. Brief overview of the physical oceanography. In: Hurdle, B.G. (Ed.), *The Nordic Seas*. Springer, New York, pp. 103–127.
- Johannessen, T., Jansen, E., Flatøy, A., Ravelo, A.C., 1994. The Relationship between Surface Water Masses, Oceanographic Fronts and Paleoclimatic Proxies in Surface Sediments of the Greenland, Iceland, Norwegian Seas. In: *Carbon Cycling in the Glacial Ocean: Constraints on the Ocean's Role in Global Change*, pp. 61–85.
- Knies, J., Stein, R., 1998. New aspects of organic carbon deposition and its paleoceanographic implications along the Northern Barents Sea Margin during the last 30,000 years. *Paleoceanography* 13, 384–394.
- Knies, J., Vogt, C., 2003. Freshwater pulses in the eastern Arctic Ocean during Saalian and Early Weichselian ice-sheet collapse. *Quat. Res.* 60, 243–251.
- Knies, J., Vogt, C., Stein, R., 1998. Late Quaternary growth and decay of the Svalbard/Barents Sea ice sheet and paleoceanographic evolution in the adjacent Arctic Ocean. *Geo-Mar. Lett.* 18, 195–202.
- Knies, J., Nowaczyk, N., Müller, C., Vogt, C., Stein, R., 2000. A multiproxy approach to reconstruct the environmental changes along the Eurasian continental margin over the last 150,000 years. *Mar. Geol.* 163, 317–344.
- Knies, J., Kleiber, H.-P., Matthiessen, J., Müller, C., Nowaczyk, N., 2001. Marine ice-rafted debris records constrain maximum extent of Saalian and Weichselian ice-sheets along the northern Eurasian margin. *Glob. Planet. Change* 31, 45–64.
- Korsun, S., Hald, M., 1998. Modern benthic foraminifera off Novaya Zemlya Tidewater glaciers, Russian Arctic. *Arct. Alp. Res.* 30, 61–77.
- Korsun, S., Hald, M., 2000. Seasonal dynamics of benthic foraminifera in a glacially fed fjord of Svalbard, European Arctic. *J. Foraminif. Res.* 30, 251–271.
- Korsun, S., Polyak, L., 1989. Distribution of benthic foraminiferal morphogroups in the Barents Sea. *Oceanology* 29, 838–844.
- Koç, N., Klitgaard-Kristensen, D., Hasle, K., Forsberg, C.F., Solheim, A., 2002. Late glacial paleoceanography of Hinlopen Strait, northern Svalbard. *Polar Res.* 21, 307–314.
- Levitani, M.A., Musatov, E.E., Burtman, M.V., 2002. History of sedimentation on the Yermak Plateau during the recent 190 ka: communication 1. Lithology and mineralogy of Middle Pleistocene–Holocene sediments. *Lithol. Mineral. Resour.* 37, 481–492.
- Lisiecki, L.E., Raymo, M.E., 2005. A Pliocene–Pleistocene stack of 57 globally distributed benthic  $\delta^{18}\text{O}$  records. *Paleoceanography* 20, PA1003.
- Lloyd, J.M., Kroon, D., Boulton, G.S., Laban, C., Fallick, A., 1996. Ice rafting history from the Spitsbergen ice cap over the last 200 kyr. *Mar. Geol.* 131, 103–121.
- Lubinski, D.J., Polyak, L., Forman, S.L., 2001. Freshwater and Atlantic water inflows to the deep northern Barents and Kara seas since ca 13  $^{14}\text{C}$  ka: foraminifera and stable isotopes. *Quat. Sci. Rev.* 20, 1851–1879.
- Mackensen, A., Sejrup, H.P., Jansen, E., 1985. The distribution of living benthic foraminifera on the continental slope and rise off southwest Norway. *Mar. Micropaleontol.* 9, 275–306.
- Mangerud, J., Svendsen, J.I., 1992. The last interglacial–glacial period on Spitsbergen, Svalbard. *Quat. Sci. Rev.* 11, 633–664.
- Mangerud, J., Bondevik, S., Gulliksen, S., Karin Hufthammer, A., Høisæter, T., 2006. Marine  $^{14}\text{C}$  reservoir ages for 19th century whales and molluscs from the North Atlantic. *Quat. Sci. Rev.* 25, 3228–3245.
- Martinson, D.G., Pisias, N.G., Hays, J.D., Imbrie, J., Moore, T.C., Shackleton, N.J., 1987. Age dating and the orbital theory of the ice ages – development of a high-resolution 0 to 300,000-year chronostratigraphy. *Quat. Res.* 27, 1–29.
- Mudie, P.J., Keen, C.E., Hardy, I.A., Vilks, G., 1984. Multivariate analysis and quantitative paleoecology of benthic foraminifera in surface and Late Quaternary shelf sediments, northern Canada. *Mar. Micropaleontol.* 8, 283–313.
- Müller, J., Massé, G., Stein, R., Belt, S.T., 2009. Variability of sea-ice conditions in the Fram Strait over the past 30,000 years. *Nat. Geosci.* 2, 772–776.
- Noormets, R., Dowdeswell, J.A., Jakobsson, M., O'Cofoigh, C., 2010. New evidence on past ice flow and iceberg activity on the Southern Yermak Plateau. In: 2010 Fall Meeting, AGU, San Francisco, Calif.
- Nowaczyk, N.R., Frederichs, T.W., Eisenhauer, A., Gard, G., 1994. Magnetostratigraphic Data from Late Quaternary sediments from the Yermak Plateau, Arctic Ocean: evidence for four Geomagnetic Polarity events within the last 170 Ka of the Brunhes Chron. *Geophys. J. Int.* 117, 453–471.
- Nørgaard-Pedersen, N., 1997. Late Quaternary Arctic Ocean Sediment Records: Surface Ocean Conditions and Provenance of Ice Rafted Debris. GEOMAR, Research Centre for Marine Geosciences, Kiel, Germany, Kiel, pp. 1–115.
- Nørgaard-Pedersen, N., Spielhagen, R.F., Erlenkeuser, H., Grootes, P.M., Heinemeier, J., Knies, J., 2003. Arctic Ocean during the Last Glacial Maximum: Atlantic and polar domains of surface water mass distribution and ice cover. *Paleoceanography* 18, 1063.
- Polyak, L., Mikhailov, V., 1996. Post-glacial Environments of the Southeastern Barents Sea: Foraminiferal Evidence. In: Geological Society, London, Special Publications 111, pp. 323–337.
- Polyak, L., Solheim, A., 1994. Late-and postglacial environments in the northern Barents Sea west of Franz Josef Land. *Polar Res.* 13, 197–207.
- Polyak, L., Korsun, S., Febo, L.A., Stanovoy, V., Khusid, T., Hald, M., Paulsen, B.E., Lubinski, D.J., 2002. Benthic foraminiferal assemblages from the southern Kara Sea, a river-influenced Arctic marine environment. *J. Foraminif. Res.* 32, 252–273.
- Rasmussen, T.L., Thomsen, E., 2008. Warm Atlantic surface water inflow to the Nordic seas 34–10 calibrated ka B.P. *Paleoceanography* 23, PA1201.
- Rasmussen, T.L., Thomsen, E., Labeyrie, L., van Weering, T.C.E., 1996a. Circulation changes in the Faeroe-Shetland Channel correlating with cold events during the last glacial period (58–10 ka). *Geology* 24, 937–940.
- Rasmussen, T.L., Thomsen, E., Van Weering, T.C.E., Labeyrie, L., 1996b. Rapid changes in surface and deep water conditions at the Faeroe Margin during the last 58,000 years. *Paleoceanography* 11, 757–771.
- Rasmussen, T.L., Balbon, E., Thomsen, E., Labeyrie, L., Van Weering, T.C.E., 1999. Climate records and changes in deep outflow from the Norwegian Sea ~150–55 ka. *Terra Nova* 11, 61–66.
- Rasmussen, T.L., Thomsen, E., Kuijpers, A., Wastegård, S., 2003. Late warming and early cooling of the sea surface in the Nordic seas during MIS 5e (Eemian Interglacial). *Quat. Sci. Rev.* 22, 809–821.
- Rasmussen, T.L., Thomsen, E., Ślubowska, M.A., Jessen, S., Solheim, A., Koç, N., 2007. Paleocyanographic evolution of the SW Svalbard margin (76°N) since 20,000  $^{14}\text{C}$  yr BP. *Quat. Res.* 67, 100–114.
- Rasmussen, T.L., Forwick, M., Mackensen, A., 2012. Reconstruction of inflow of Atlantic Water to Isfjorden, Svalbard during the Holocene: correlation to climate and seasonality. *Marine Micropaleontology* 94–95, 80–90.
- Risebrobakken, B., Balbon, E., Dokken, T., Jansen, E., Kissel, C., Labeyrie, L., Richter, T., Senneset, L., 2006. The penultimate deglaciation: high-resolution paleocyanographic evidence from a north–south transect along the eastern Nordic seas. *Earth Planet. Sci. Lett.* 241, 505–516.

- Rudels, B., Anderson, L.G., Eriksson, P., Fahrbach, E., Jakobsson, M., Jones, P., Melling, H., Prinsenberg, S., Shauer, U., Yao, T., 2011. Observations in the Ocean. Springer, Berlin.
- Rytter, F., Knudsen, K.L., Seidenkrantz, M.S., Eiriksson, J., 2002. Modern distribution of benthic foraminifera on the North Icelandic shelf and slope. *J. Foraminiferal Res.* 32, 217–244.
- Sarnthein, M., Pflaumann, U., Weinelt, M., 2003. Past extent of sea ice in the northern North Atlantic inferred from foraminiferal paleotemperature estimates. *Paleoceanography* 18, 1047.
- Scott, D.B., Schell, T., Rochon, A., Blasco, S., 2008. Modern benthic foraminifera in the surface sediments of the Beaufort Shelf, Slope and Mackenzie Trough, Beaufort Sea, Canada: taxonomy and summary of surficial distribution. *J. Foraminiferal Res.* 38, 228–250.
- Sejrup, H.P., Fjaeran, T., Hald, M., Beck, L., Hagen, J., Miljeteig, I., Morvik, I., Norvik, O., 1981. Benthonic foraminifera in surface samples from the Norwegian continental margin between 62 degrees N and 65 degrees N. *J. Foraminiferal Res.* 11, 277–295.
- Sellén, E., O'Regan, M., Jakobsson, M., 2010. Spatial and temporal Arctic Ocean depositional regimes: a key to the evolution of ice drift and current patterns. *Quat. Sci. Rev.* 29, 3644–3664.
- Ślubowska-Woldengen, M., Rasmussen, T.L., Koç, N., Klitgaard-Kristensen, D., Nilsen, F., Solheim, A., 2007. Advection of Atlantic Water to the western and northern Svalbard shelf since 17,500 cal yr BP. *Quat. Sci. Rev.* 26, 463–478.
- Spielhagen, R.F., Baumann, K.-H., Erlenkeuser, H., Nowaczyk, N.R., Nørgaard-Pedersen, N., Vogt, C., Weiel, D., 2004. Arctic Ocean deep-sea record of northern Eurasian ice sheet history. *Quat. Sci. Rev.* 23, 1455–1483.
- Spielhagen, R.F., Erlenkeuser, H., Siegert, C., 2005. History of freshwater runoff across the Laptev Sea (Arctic) during the last deglaciation. *Glob. Planet. Change* 48, 187–207.
- Steinsund, P.I., 1994. Benthic Foraminifera in Surface Sediments of the Barents and Kara Seas: Modern and Late Quaternary Applications. University of Tromsø, Tromsø, Norway, p. 111.
- Steinsund, P.I., Hald, M., 1994. Recent calcium carbonate dissolution in the Barents Sea: paleoceanographic applications. *Mar. Geol.* 117, 303–316.
- Swift, J.H., 1986. The Arctic waters. In: Hurdle, B.G. (Ed.), *The Nordic Seas*. Springer, New York, pp. 129–153.
- Tolderlund, D., 1971. Distribution and ecology of living planktonic foraminifera in surface waters of the Atlantic and Indian Oceans. *Micropaleontol. Oceans*, 105–149.
- Veum, T., Jansen, E., Arnold, M., Beyer, I., Duplessy, J.-C., 1992. Water mass exchange between the North Atlantic and the Norwegian Sea during the past 28,000 years. *Nature* 356, 783–785.
- Vogelsang, E., Sarnthein, M., Pflaumann, U., 2001.  $\delta^{18}\text{O}$  Stratigraphy, Chronology and Sea Surface Temperatures of Atlantic Sediment Records (GLAMAP-2000 Kiel). Institut für Geowissenschaften, Universität Kiel.
- Vogt, C., Knies, J., Spielhagen, R.F., Stein, R., 2001. Detailed mineralogical evidence for two nearly identical glacial/deglaial cycles and Atlantic water advection to the Arctic Ocean during the last 90,000 years. *Glob. Planet. Change* 31, 23–44.
- Wagner, T., Henrich, R., 1994. Organo- and lithofacies of glacial–interglacial deposits in the Norwegian–Greenland Sea: responses to paleoceanographic and paleoclimatic changes. *Mar. Geol.* 120, 335–364.
- Walker, M., Johnsen, S., Rasmussen, S.O., Popp, T., Steffensen, J.P., Gibbard, P., Hoek, W., Lowe, J., Andrews, J., Björck, S., 2009. Formal definition and dating of the GSSP (Global Stratotype Section and Point) for the base of the Holocene using the Greenland NGRIP ice core, and selected auxiliary records. *J. Quat. Sci.* 24, 3–17.
- Weinelt, M., Sarnthein, M., Pflaumann, U., Schulz, H., Jung, S., 1996. Ice-free Nordic Seas during the Last Glacial Maximum: potential sites of deepwater formation. *Paleoclim. Data Modell.* 1, 283–309.
- Wollenburg, J.E., Mackensen, A., 1998. Living benthic foraminifera from the central Arctic Ocean: faunal composition, standing stock and diversity. *Mar. Micropaleontol.* 34, 153–185.
- Zamelczyk, K., Rasmussen, T.L., Husum, K., Hafliðason, H., de Vernal, A., Ravna, E.K., Hald, M., Hillaire-Marcel, C., 2012. Paleoceanographic changes and calcium carbonate dissolution in the central Fram Strait during the last 20 ka. *Quat. Res.* 78, 405–416.
- Zamelczyk, K., Rasmussen, T.L., Husum, K., Hald, M., 2013. Marine calcium carbonate preservation vs. climate change over the last two millennia in the Fram Strait: implications for planktic foraminiferal paleostudies. *Mar. Micropaleontol.* 98, 14–27.





Teena Chauhan, Tine L Rasmussen and Riko Noormets. **Paleoceanography of the Barents Sea continental margin, north of Nordaustlandet, Svalbard during the last 74 ka.**

*Accepted for publication in Boreas*



Teena Chauhan, Riko Noormets and Tine L Rasmussen. **Glaciomarine sedimentation and bottom current activity along the north-western and northern continental margin of Svalbard during the late Quaternary**

*Submitted to Geo-Marine Letters*



## APPENDIX A

List of planktic and benthic species identified in cores JM10-02GC and HH11-09GC and taxonomy

Foraminifera species and taxonomy	JM10-02GC	HH11-09GC
<b>Planktic species</b>		
<i>Neogloboquadrina pachyderma</i> (Ehrenberg, 1861)	x	x
<i>Turborotalita quinqueloba</i> (Natland, 1938)		x
<b>Benthic species</b>		
<i>Anomalinoides minimus</i> (Forster, 1892)		x
<i>Astrononion gallowayi</i> Loeblich & Tappan, 1953	x	x
<i>Bolivina</i> d'Orbigny, 1839	x	
<i>Buccella</i> spp.	x	x
<i>Bulimina marginata</i> d'Orbigny, 1826	x	
<i>Bulimina aculeata</i> d'Orbigny, 1826		x
<i>Buliminella hensoni</i> Lagoe, 1977		x
<i>Cassidulina reniforme</i> Nørvang, 1945	x	x
<i>Cassidulina neoteretis</i> Seidenkrantz, 1995	x	x
<i>Centropyxis arenatus</i> (Cushman)		x
<i>Cibicides lobatulus</i> (Walker and Jacob, 1798)	x	x
<i>Cibicides pachyderma</i> (Rzehak, 1886)	x	
<i>Cibicides wuellerstorfi</i> (Schwager, 1866)	x	x
<i>Cornuloculina inconstans</i> (Brady, 1879)		x
<i>Cornuspira distincta</i> (Cole & Scott, 2008)	x	x
<i>Cornuspira involvens</i> (Reuss, 1850)		x
<i>Dentalina</i> spp.	x	x
<i>Eggerella bradyi</i> (Cushman, 1911)		x
<i>Elphidium excavatum</i> (Terquem, 1875)	x	x
<i>Elphidium tumidum</i> Natland, 1938	x	x
<i>Elphidium hallandense</i> Brotzen, 1943	x	
<i>Elphidium</i> spp.	x	x
<i>Epistominella exigua</i> (Brady, 1884)	x	x
<i>Epistominella arctica</i> Green, 1959	x	x
<i>Eilohedra vitrea</i> (Parker, 1953)	x	x
<i>Eilohedra nipponica</i> Kuwano, 1962	x	x
<i>Favulina hexagona</i> (Williamson, 1848)	x	x
<i>Fissurina laevigata</i> Reuss, 1850	x	x
<i>Glabratella</i> Dorreen, 1948		x
<i>Globobulimina auriculata</i> (Bailey, 1894)	x	x
<i>Guttulina</i> d'Orbigny, 1839		x
<i>Gyroidina umbonata</i> (Silvestri, 1898)	x	
<i>Hyalinea balthica</i> (Schröter, 1783)	x	

<i>Ioanella tumidula</i> (Brady, 1884)		X
<i>Islandiella islandica</i> (Nørvang, 1945)	X	X
<i>Islandiella norcrossi</i> (Cushman, 1933)	X	X
<i>Labrospira crassimargo</i> (Norman, 1892)		X
<i>Lagenammina difflugiformis</i> (Brady, 1879)		X
<i>Lagenammina micacea</i> (Cushman, 1918)		X
<i>Lepidodeuterammina ochracea</i> (Williamson, 1858)		X
<i>Marginulinopsis costata</i> (Batsch, 1791)		X
<i>Marsupulina schultzei</i> Rhumbler, 1904	X	
<i>Melonis barleeanus</i> (Williamson, 1858)	X	X
<i>Milionella</i> spp.	X	X
<i>Nodosaria</i> Lamarck, 1816	X	X
<i>Nonionoides turgida</i> (Williamson, 1858)		X
<i>Nonionellina labradorica</i> (Dawson, 1860)	X	X
<i>Oridorsalis tenerus</i> (Brady, 1884)	X	
<i>Oridorsalis umbonatus</i> (Reuss, 1851)		X
<i>Parafissurina lateralis</i> (Cushman 1913)	X	X
<i>Patellina corrugata</i> Williamson, 1858		X
<i>Polymorphinidae</i> d'Orbigny, 1839	X	
<i>Procerolagena gracilis</i> (Williamson, 1848)	X	X
<i>Pullenia bulloides</i> (d'Orbigny, 1826)	X	X
<i>Pullenia osloensis</i> Feyling-Hanssen, 1954	X	X
<i>Pullenia subcarinata</i> (d'Orbigny, 1839)	X	X
<i>Pyrgo</i> sp.	X	X
<i>Pyrgoella irregularis</i> (d'Orbigny, 1839)	X	X
<i>Pyrgo williamsoni</i> (Silvestri, 1923)		X
<i>Quinquoloculina</i> spp.	X	X
<i>Rhabdammina</i> sp.		X
<i>Rhabdammina abyssorum</i> M. Sars, 1869		X
<i>Rheophax</i> sp.		X
<i>Rhizammina algaeformis</i> Brady, 1879	X	
<i>Rupertina stabilis</i> (Wallich, 1877)		X
<i>Robertinoides charlottensis</i> (Cushman, 1925)	X	X
<i>Sagrina subspinescens</i> (Cushman, 1936)	X	X
<i>Sphaeroidina bulloides</i> d'Orbigny, 1826		X
<i>Stainforthia loeblichii</i> Feyling-Hanssen, 1954	X	X
<i>Stainforthia concava</i> (Höglund, 1947)	X	X
<i>Stainforthia fusiformis</i> (Williamson, 1848)		X
<i>Testulosiphon indivisus</i> (Brady, 1884)		X
<i>Trifarina fluens</i> (Todd, 1948)	X	X
<i>Trifarina angulosa</i> (Williamson, 1858)		
<i>Triloculina oblonga</i> (Montagu, 1803)		X
<i>Triloculina trihedra</i> Loeblich & Tappan, 1953	X	X
<i>Trochammina</i> sp.		X
<i>Usbekistania charoides</i> (Jones & Parker, 1860)		X
<i>Valvulineria arctica</i> Green, 1959		X

---

## APPENDIX B

Summary in Hindi

### सारांश

यह शोध सागर के इतिहास के पुनर्निर्माण पर केंद्रित है। इसमें, आर्कटिक सागर में अटलांटिक जल प्रवाह की विविधता और उसका स्वालबार्ड-बरेट्स समुद्र में बर्फ की चादर, बर्फ की परत, तलहटी में प्रवाह शक्ति और अवसादन पर्यावरण (डेपोसिशनल एनवायरनमेंट) पर हुए प्रभाव का अध्ययन किया गया है। इस पुनर्निर्माण के लिए समुद्री तलछट में संरक्षित सूक्ष्म-जीवाश्म (फोरामिनीफेरा), जैविक कार्बन एवं तलछट के कणों के आकार (विशेषकर १० से ६३ माइक्रोन आकार की सिल्ट) की जांच की गयी। नतीजे बताते हैं कि उपसतह अटलांटिक जल प्रवाह की अस्थिरता एवं सौर-ऊर्जा के वितरण (आतपन) का, बर्फ की चादर और परत के विस्तार एवं सीमा पर १३२,००० वर्षों से प्रभाव रहा। इसके आलावा, ग्लेशियरों के पिघलने की अवधि (डिग्लेसिएशन) के दौरान, जैसे ६०,००० वर्षों पहले एवं १९,००० से ११,५०० वर्षों के बीच, ताजा जल के प्रवाह में वृद्धि ने भी सागर संचलन पर विशेष प्रभाव डाला। ताजे जल की परत ने ऊपरी पानी स्तम्भ (अपर वाटर कॉलम) में स्तरीकरण उत्पन्न किया जिससे सागर संचलन कमजोर हुआ। कमजोर संचलन के कारण सागर की तलहटी में वायुसंचार (वेंटिलेशन) कमजोर हुआ और सागर की सतह पर बर्फ की परत का विस्तार हुआ। यह अध्ययन दर्शाता है कि इन "जलवायु चालकों" (अर्थात्, सौर-ऊर्जा, गर्म अटलांटिक जल, ताजा जल) एवं उनकी प्रतिक्रिया तंत्र का प्रभाव स्थानीय अवसादन एवं सागरीय पर्यावरण पर काफी विविध रहा। यह परिणाम इस बिंदु पर जोर देता है कि पिछले जलवायु के पुनर्निर्माण में क्षेत्रीय मानकों एवं उनके प्रतिक्रिया तंत्र पर विचार करना महत्वपूर्ण है।







Dette studiet fokuserer på rekonstruksjon av fortidens variabilitet i innstrømningen av Atlanterhavsvann til Polhavet og dennes påvirkning på Svalbard-Barentshavet iskappen (SBIS), sjøisdekket, variasjoner i styrken på bunnstrømmer og avsetningsmiljøet. For rekonstruksjonen, distribueringsmønsteret til planktonisk og bentisk foraminifera, stabile oksygen og karbon isotoper i planktonisk og bentisk foraminifera, isfjell og sjøis fraktet material (ice-rafted debris), sedimentenes kornstørrelse hovedsak silt av 10–63 micron størrelse (sortable silt) og innholdet av organisk karbon i sedimentene har blitt undersøkt. Resultatene viser at den varierende styrken til Atlanterhavsvannet sammen med solinnstråling har påvirket utbredelsen av sjøisdekket og stabiliteten til SBIS i de siste 132000 år (Termination II). I tillegg har økt ferskvannstilstrømning fra bresmelting under avisingsperioder (deglaciation) for ca. 60000 år siden (MIS 4/3) og mellom 19000 og 11500 år siden (MIS 2/1) hatt en signifikant påvirkning på de oseanografiske forhold gjennom stratifisering av de øvre vannmasser og en svekkelse av havsirkulasjonen. Dette førte til dårligere ventilering av havbunnen og utvidelse av sjøisdekket på overflaten. Effekten av disse “klimapådrivene” på de lokale sedimentene og det oseanografiske miljøet varierte betydelig, noe som understreker betydningen av å ta hensyn til regionale miljøparametere og tilbakekoblingsmekanismer når tidligere klima skal rekonstrueres.